PA DEP FINAL REPORT

WETLAND PROGRAM DEVELOPMENT IN SUPPORT OF PENNSYLVANIA'S AQUATIC RESOURCE PROTECTION AND MANAGEMENT ACTION PLAN, PROGRAM FOCUS AREA 3: HEADWATER AQUATIC RESOURCE RESTORATION MONITORING

Drexel University Master Agreement
Contract No. 4400007960

2017

Project Investigators:

Dr. Robert Walter, Franklin & Marshall College
Dr. Dorothy Merritts, Franklin & Marshall College
Dr. Marina Potapova, Academy of Natural Sciences, Drexel University
Dr. William Hilgartner, The Johns Hopkins University
Dr. David Bowne, Elizabethtown College
Telemonitor, Inc., Robert Johnson and Jim Moore

Deliverables:

Deliverable 1: A written report that analyzes diatom communities and determines changes that may have resulted from aquatic ecosystem restoration at BSR. (Potapova)

Deliverable 2: A database of water quality records along with a description of the sampling and analysis procedures and protocols. A written report that analyzes trends over time by comparing pre-restoration and post-restoration water quality parameters and results of the 2D flow models. (Merritts/Walter, USGS)

Deliverable 3: A written report and database with records for biological components that compare post-restoration and pre-restoration conditions. (Hilgartner/ Bowne)

Deliverable 4: A written report providing analysis of changes in sediment sources and fluxes over time by comparing pre-restoration and post-restoration conditions. (Merritts/Walter)

Deliverable 5: A digital image database and data representing fixed interval time-lapsed site photography. (Telemonitor, Inc.)

OUTLINE

A. Executive Summary

B. Deliverable 1: A written report that analyzes diatom communities and determines changes that may have resulted from aquatic ecosystem restoration at BSR.

C. Deliverable 2: A database of water quality records along with a description of the sampling and analysis procedures and protocols. A written report that analyzes trends over time by comparing pre-restoration and post-restoration water quality parameters and results of the 2D flow models.

D. Deliverable 3: A written report and database with records for biological components that compare post-restoration and pre-restoration conditions.

E. Deliverable 4: A written report providing analysis of changes in sediment sources and fluxes over time by comparing pre-restoration and post-restoration conditions.

F. Deliverable 5: A digital image database and data representing fixed interval time-lapsed site photography.

A. Executive Summary

Deliverable 1: A written report that analyzes diatom communities and determines changes that may have resulted from aquatic ecosystem restoration at BSR.

- Diatom assemblages of Big Spring Run are typical for small hard-water and nutrient-rich streams of Lancaster County. They are dominated by eutraphentic cosmopolitan diatoms mostly from genera *Navicula, Nitzschia, Achnanthidium, Planothidium* and *Eolimna*. Diatom assemblages of this type formed in Lancaster county streams after European settlement. Our investigation of diatom communities taken from a bank section shows that before 1700s Big Spring Runwas inhabited by different diatom communities reflecting entirely different stream geomorphology and nutrient regimes. Big Spring Run likely is representative of the diatom community changes in other streams of the region.
- Diatom diversity increased after restoration based on mean species richness (rarefied down to 400 individuals) in the restored reach that increased from 31.5 in 2011 to 44.2 in 2015 samples. The increase in species richness may be attributed to enhanced habitat complexity that now provides a greater diversity of substrates and flow conditions.
- The values of diatom nutrient metrics declined after the restoration thus showing that assemblages had fewer diatoms associated with hyper- and eutrophic conditions and more of those indicative of low nutrients.
- Although the restoration led to a reduction of nutrient concentrations in stream water, nutrients are still high because of their input from upstream reaches. Therefore, post-restoration diatoms assemblages continue to be dominated by eutraphentic species. Our investigation of Great Marsh wetland showed what type of diatom assemblage could be expected if a stream in an agricultural landscape would retain its valley bottom wetland. While eutraphentic diatoms are still present in Great Marsh, the diversity of these assemblages is rather high with a considerable contribution of low-nutrient indicating and native species. It would be unrealistic to expect the biota to revert to its pre-1700s condition, but increased diversity and higher proportion of oligotraphentic species should be considered as positive effect of the restoration.
- Post-restoration analysis was based on samples collected in 2015, and that there might well be further improvements now, as of 2017, which would warrant a continued study of BSR diatoms periodically over the next decade or so.

Deliverable 2: A database of water quality records along with a description of the sampling and analysis procedures and protocols. A written report that analyzes

trends over time by comparing pre-restoration and post-restoration water quality parameters and results of the 2D flow models.

- See USGS report (Langland et al, 2017) for summary of annual sediment loads at the three gage stations.
- 2D flow modeling indicates a substantial reduction in bed shear stresses throughout the restored wetland floodplain from pre- to post-restoration conditions for a modeled high flow event.
- Sampling of bedload from a high flow event at multiple locations throughout the restoration reach and several hundred feet downstream in the unrestored reach, near the downstream gage, agrees with modeling results of low bed shear stresses throughout the restoration reach.

Deliverable 3: A written report and database with records for biological components that compare post-restoration and pre-restoration conditions.

- Analysis of vegetation transects before and after restoration at Big Spring Run reveals a major ecological change after legacy sediment was removed. Vegetation shifted from a dry, upland pasture environment to a hydric, wet meadow. that is still undergoing succession as vegetation stabilizes within the hydrologic regime.
- The wetland has expanded from essentially a 5-meter area around a single channel meander before 2011 Wetland areas increased from small isolated wetland pockets predominantly located along the valley margins and totaling less than 1 acres to a 40-50-meter-wide and contiguous 4.6 acre wetland with hydric plant dominance persisting since being established in 2012.
- A strictly sedge dominated wet meadow, similar to that which existed for thousands of years prior to burial by legacy sediment, has not been established; instead a species-rich wet meadow plant community dominated rice cutgrass, jewelweed, and cattail, with scattered flowering composites and sedge dominated patches. This plant community providesdiverse wetland habitat that is comparable to the sedge dominated paleo plant community from an ecological standpoint.
- Since wetland restoration, *E. bislineata* (northern two-lined salamander) has consistently increased in the restored stretches while its captures in the unrestored stretches have fluctuated. The main stem, in particular, is good habitat for this species.
- The quality of the western branch for *E. bislineata* is more questionable as captures in this branch decreased in 2015 and 2016 from the post-restoration peak in 2014.

- All captures in the restored areas have been of larvae *E. bislineata*, indicating that this species is not only present but is reproducing in the restored wetland. This is an excellent sign for the future of this species in the Big Spring Run wetland.
- Neither *Lithobates clamitans* (green frog) or *Lithobates catesbeianus* (bullfrog) was detected via an analysis of the recordings taken from 2010 to 2016. We visually confirmed an adult *L. clamitans* in May 2013, heard one in May 2014, and saw eggs and then a tadpole in 2015 in the west branch. In May 2016, we found a second *L. clamitans* tadpole in the same area of the west branch.
- An exciting development for the herpetological fauna at Big Spring Run is the confirmation of breeding *Lithobates clamitans* in the restored west branch. This species breeds in standing water and the shifting channels in the west branch have allowed for the development of former channels with stream flow only under very wet conditions. Thus, breeding habitat for frogs is created where it did not exist prior to the restoration. While *L. clamitans* is a nationally common frog species, it now residing and breeding at Big Spring Run despite the surrounding agricultural matrix is a positive statement of the success of the Big Spring Run restoration.

Deliverable 4: A written report providing analysis of changes in sediment sources and fluxes over time by comparing pre-restoration and post-restoration conditions.

- Monitoring changes in sediment erosion and storage indicate that the unrestored reaches of the eastern and western tributaries and the main stem between the gage stations and the restored reach are net sources of 23 to 55 tons of sediment per year.
- Annual sediment loads on the two tributaries entering the restoration area are 70 and 28 tons/yr, and an additional 13 to 30 tons/yr is eroded from unrestored reaches of these tributaries upstream of the restored area, giving a total incoming annual load of 111 to 128 tons/yr to the restored area.
- Monitoring net change with repeat RTK GPS surveying in the restored area indicates that it is net depositional, accumulating about 0.06 ± 0.03 ft/yr of sediment.
- Monitoring deposition with tile pads in the restored area indicates that it is net depositional, accumulating about 0.03 ± 0.04 ft/yr. This is about half the estimate from RTK GPS surveying.
- A sediment budget for all measured fluxes in the restoration area can be balanced using tile pad data, and is consistent with net deposition in the restoration area.

- An inventory of fallout ^{137}Cs activity from two hill slope transects adjacent to Big Spring Run yields average modern upland erosion rates of 1.2 t ac^{-1} yr^{-1} and 2.3 t ac^{-1} yr^{-1}.
- A mass balance calculation of ^{137}Cs data indicates that 85-100% of the pre-restoration (<November 2011) suspended sediment storm load in Big Spring Run can be accounted for by stream bank sources.
- Mass balance calculations from the post-restoration period (>November 2011) indicates that 93-100% of the sediment on tile pads is from stream bank sources.
- From these ^{137}C data, it is clear that upland farm slopes contribute little, if any, soil to the suspended sediment load within our study area at Big Spring Run.

Deliverable 5: A digital image database and data representing fixed interval time-lapsed site photography.

- Time-lapse photos were taken from sunrise to sunset at one minute intervals from two web cameras set up on towers at the downstream and upstream (western tributary) ends of the restoration area at Big Spring Run from 2011-2015, including the time during restoration construction. These are available on line.

B. Deliverable 1: Diatom community analysis and response to restoration

Contact Person: Marina Potapova, Drexel University

Tasks: Analyze diatom communities from samples collected prior to restoration. Collect and analyze diatom communities from post restoration samples. Hypothesis: as diatoms are known to be sensitive indicators of aquatic ecosystem characteristics and their communities reflect water quality characteristics, their response to change resulting from restoration may be rapid, and diatoms may be an early and reliable biological indicator of progress towards restoring natural aquatic ecosystem functions and services. Compare diatom communities with natural aquatic ecosystems of exceptional quality (e.g., Great Marsh, French Creek).

Deliverables: A written report that analyzes diatom communities and determines changes that may have resulted from aquatic ecosystem restoration at BSR.

B. 1. Introduction.

Together with fish and aquatic macroinvertebrates, diatom algae are widely used to monitor rivers and streams (Stevenson et al. 2010). In contrast to aquatic animals that are good indicators of water oxygen content and general quality of the habitat, diatoms are especially sensitive to concentrations of the dissolved and suspended solids, pH, and organic and inorganic nutrients in water (van Dam et al. 1994, Hering et al. 2006). Diatoms are ubiquitous and abundant in benthic freshwater habitats and their communities are usually species-rich, thus providing ample information on water quality. As other microscopic organisms, diatoms reproduce fast and species composition of their assemblages quickly tracks water quality changes. A multitude of diatom metrics and indices have been developed starting from the saprobic indices designed to monitor organic pollution (e.g., Pantle & Buck 1955, Sládeček 1986) to metrics focused on nutrients (Kelly 1995, Potapova & Charles 2007), other specific stressors (Van Dam 1994, Potapova & Charles 2003) or general stream degradation (e.g., Lowe 1974). Many of these metrics and indices are successfully used by environmental agencies, while the current trend has been to construct metrics for specific geographic regions and environmental settings (Potapova & Carlisle 2011).

The use of diatoms for monitoring stream water quality in the United States was pioneered by Dr. Ruth Patrick who conducted the first biological river survey in 1948 in the

Conestoga River Basin mostly located in Lancaster County of Pennsylvania (Patrick & Roberts 1949, Figure 1.1). By 1948 most of the land in the Lancaster County was already developed and used for agriculture and industrial purposes. The streams studied in the course of the survey ranged from moderately to severely polluted with biological communities being especially impoverished in waters receiving toxic industrial waste. The observations of diatom assemblages made in Conestoga River survey led Patrick to develop her ideas about the biological diversity being an important indicator of river health (Patrick 1949, 1959, 1953, 1956).

As has been shown by Walter & Merritts (2008) and Merritts et al. (2011, 2013), most streams of mid-Atlantic Piedmont have been drastically transformed by European settlers not just by chemical pollution, but also by damming that caused the accumulation of fine-grained sediment in valley bottomsand channel incision into this legacy sediment after dam breaching. The Big Spring Run restoration project in Lancaster County, PA, aims at reconstructing a natural valley bottom environment by removing the legacy sediment. The anticipated outcome of removing legacy sediment, is restoring valley and stream morphologies that consist of an anastomosing channel flowing through a palustrine emergent marsh. In turn, this physical transformation and aquatic ecosystem development is anticipated to decrease sediment and nutrient loading to the stream.

Diatoms, alongside other aquatic and riparian biota, may track environmental changes brought by the restoration. In particular, diatom assemblages may respond to changes in physical and chemical characteristics of their habitat, such as decreased flow velocities, depth, siltation and sediment scouring, increased complexity and diversity of the habitats and decrease in nutrient concentrations. The goal of this study was to evaluate changes in diatom assemblages following the BSR restoration using such attributes of diatom assemblages as community composition, diversity and diatom metrics developed specifically to monitor biotic responses to river eutrophication.

The diatom collections made on Lancaster county streams in 1948 by Patrick and her collaborators have been housed at the Academy of Natural Sciences of Drexel University and represent an important source of information on the conditions of streams at that time. In this project, we re-evaluated these and other historical diatom samples and compared them with recently sampled diatom assemblages from the BSR. This comparison is important to put the BSR data in a wider regional context and to attach greater significance to observed trends in species composition and diversity.

B. 2. Materials and Methods

The following materials were used to study the effect of legacy sediment removal andaquatic ecosystem restoration on diatom communities at Big Spring Run:

1) Ten benthic stream samples collected from 6 locations in Big Spring Run and its tributaries in July 2011 prior to the restoration. Samples were collected from rocks and fine-grained sediment (silt) by Amy Moser and Candace Grand-Pre.
2) Twenty-two benthic stream samples collected in Big Spring Run and its tributaries in December 2015 after the restoration. Samples were collected from a variety of substrates, including rocks, silt, watercress and green (*Cladophora* and *Zygnema*) or xanthophyte (*Vaucheria*) filamentous algae. Sampling locations are listed below:

Reference sites:

- West Branch, USGS station 015765185, 39.9911 N 76.2640 W
- East Branch, USGS station, 39.9917 N 76.2611 W
- "Houser grid", 39.9961 N 76.2499 W
- Long Rifle Road, 39.9991 N 76.2643 W

Main stem BSR sites affected by restoration:

- Site 1, "Type locality", 39.9931 N 76.2625 W
- Site 2, "Lauren plot", 39.9941 N 76.2631 W
- Site 2, Downstream gage, USGS station 015765195, 39.9959 N 76.2641 W

3) Eighty permanent diatom slides representing benthic stream samples collected in 1948 from streams of the Lancaster County (mostly Conestoga River Basin) by the ANS staff and housed at the ANS Diatom Herbarium. Sampling locations are shown on a map from the Conestoga River report (Figure 1.1).
4) Forty-five diatom counts representing benthic samples from French Creek and its tributaries (Chester County) and various rivers and streams of Lancaster and Chester Counties from 1993 to 2015. The counts have been generated by the ANS staff and stored in ANS databases.
5) Seven diatom samples collected from Marsh Creek and Great Marsh wetland on April 30, 2016. Great Marsh site is a palustrine wetland that formed about 10,000 years ago (Martin 1958, Grand Pre et al. 2012) and never accumulated considerable legacy sediment because the stream was never dammed (Walter et al 2013).
6) Six sediment samples from a bank section of Big Spring Run collected by R. Walter and D. Merritts and previously dated by ^{14}C method and analyzed for presence of plant fossils.

The full list of studied materials is in the Appendix I.

Diatom samples were boiled in 50% nitric acid for 40 minutes and then rinsed several times with distilled water until neutral pH was attained. The bank section samples were enriched for diatoms with centrifugation in CdI_2/KI "heavy liquid". Aliquots of the slurries were strewn onto glass coverslips and allowed to evaporate at room temperature. Coverslips were then mounted onto microscope slides with Naphrax. For each sample, a minimum of 400 diatom valves were identified and enumerated using a Zeiss AxioImager microscope fitted with x100, 1.4 N.A. oil immersion lens and differential interference contrast optics. Diatoms were documented by capturing images with an AxioScope MRm digital camera. For SEM examination diatom slurries were dried on aluminum stubs, sputter-coated with Pt-Pd and observed with Zeiss Supra 50 scanning electron microscope under 10 kV accelerating voltage.

Identifications were made to the lowest taxonomic level using numerous taxonomic sources (Hofmann et al. 2013, Krammer 1997a, b, 2000, Krammer & Lange-Bertalot 1986, 1988, 1991, 2004, Patrick & Reimer 1966, 1975; Spaulding et al. 2010). To create a taxonomically consistent dataset, the counts obtained from the databases were checked and selected slides were examined to establish correspondence between taxa names used currently an in the past. A minimum of 400 diatom valves were identified from each examined slide, except for 4 samples that were extremely sparse.

To evaluate trends in diatom species diversity, the raw species richness numbers were rarefied down to 400 individuals using R script available in the VEGAN package of R (Oksanen et al. 2016).

To assess trends in diatom species composition relative to nutrient status, several diatom metrics developed by Potapova & Charles (2007) were calculated for all examined diatom samples. These metrics have been designed to monitor diatom assemblages that are indicative of concentrations of total nitrogen and total phosphorus in US rivers and streams. Since diatom species responses to nutrients may vary depending on the regional settings, both nation-wide and region-specific metrics were calculated.

To explore general patterns of variation of diatom assemblages and to elucidate the most important environmental factors influencing their structure, several multivariate techniques were implemented using the CANOCO v.5 program (ter Braak & Smilauer 2013)

B. 3. Diatom communities of Big Spring Run before and after the restoration.

The dataset of 32 samples collected in Big Spring Run and its tributaries before (2011) and after (2015) the restoration contained 152 diatom taxa (Figure 1.2, Appendix B.I). The most abundant diatoms were *Achnanthidium minustissimum, Amphora pediculus, Eolimna minima, Navicula gregaria, N. reichardtiana, Nitzschia palea* and *Planothidium frequentissimum*. These species are among the most common river diatoms in moderately to heavily polluted rivers in temperate zone, including the US (Hofmann 2013, Spaulding et al. 2010).

Only 9 samples collected in 2011 were available for numerical analyses because a sample from the East Branch location had too few diatoms. This low number of samples collected prior to restoration considerably limited the power of statistical tests. Diatom metrics indicated the prevalence of nutrient-tolerant species in the majority of samples (Table B.1). The paired samples T-test demonstrated the lack of difference between 2011 and 2015 values of nutrient metrics for samples collected at the reference sites ($n=16$, $p=0.97$), but significant decline in the metrics' values from 2011 to 2015 for samples from the restored portion of the main stem ($n=16$, $p=0.03$). This result demonstrates a shift towards diatoms indicative of lower nutrient concentrations in the restored portion of the stream.

Comparison of diatom assemblages before and after the restoration showed an increase in diatom diversity in the restored BSR reach, which we explain as a consequence of enhanced microhabitat diversity. The average species richness of diatom assemblages (values rarefied down to 400 individuals per sample) increased after the restoration from 31.5 to 44.2 species per sample, although the paired t-test did not have sufficient power to confirm significant difference because of the low number of observations. The difference in species richness before and after the restoration evaluated by the unpaired t-test with rarefied data (four 2011 samples vs. eleven 2015 samples) was statistically significant at p-level of 0.02.

Table B.1. Diatom metrics calculated for 31 diatom samples collected before and after the BSR restoration. N all – Total Nitrogen nation-wide, P all – Total Phosphorus nation-wide, N east – Total Nitrogen eastern plains, P east - Total Phosphorus eastern plains metric. Metric values range from 0 indicating the lowest concentrations of nutrients to 10 indicating concentrations (for further explanations see Potapova & Charles 2007).

Site	**Substrate**	**Metric**							
		N all		P all		N east		P east	
		2011	2015	2011	2015	2011	2015	2011	2015
Reference sites									
West Branch	rocks	4.0	3.0	3.6	1.9	2.9	1.7	3.5	1.6
	silt	6.5	7.2	6.2	6.8	4.1	6.3	5.8	6.2
	watercress		5.3		4.0		4.1		3.3
Spring near West Branch	watercress		9.0		8.2		7.8		8.5
East Branch	silt		1.6		0.7		0.8		0.7
	watercress		4.2		3.7		3.0		3.8
	moss		2.6		1.2		1.4		1.8
	rocks		7.1		6.5		6.6		3.9
"Houser grid"	rocks	9.6	5.2	9.5	6.3	8.9	6.3	9.5	6.3
Long Rifle Road	rocks	5.6		4.8		2.8		4.4	
	silt	7.4		6.7		6.3		5.6	
	Vaucheria on rocks		9.2		9.1		8.7		8.5
	Cladophora on rocks		8.7		8.1		8.3		6.2
Main stem restored portion									
Site 1 ("type locality")	rocks	8.8	6.1	8.5	5.2	8.8	5.3	8.2	3.5
	silt	9.1	9.7	8.9	9.9	7.8	9.9	8.8	9.8
	Cladophora		4.3		3.5		2.9		2.5
	watercress		6.1		4.7		4.7		4.4
	Zygnema		4.5		4.4		3.9		3.2
Site 2 ("Lauren plot")			7.1		6.9		6.4		5.7
	Cladophora on rocks		7.2		7.2		7.2		5.5
	watercress		4.7		4.1		3.6		3.1
Site 3 ("Downstream gage")	rocks	5.6		5.3		2.2		5.1	
	silt	9.6	8.5	9.5	8.4	9.6	7.3	9.6	7.4
	Cladophora on rocks		3.8		3.3		2.8		2.4
	Vaucheria on rocks		5.4		5.0		4.9		3.4

An unconstrained ordination reveals major patterns in the variation of diatom assemblage composition in BSR (Figures 1.3 and 1.4). The species and samples plots show a considerable among-site differences with samples from East Branch and Houser Grid sites being rather dissimilar from the rest. This among-site variability together with low number of observations prior to restoration make it impossible to use a BACI (Before-After-Control-Impact) analysis for diatom data. The ordination demonstrates, however that post-restoration samples had higher proportion of species characteristic for less polluted waters (such as monoraphid diatoms from the genera *Achnanthidium, Cocconeis* and *Planothidium*) than before-restoration samples which had higher numbers of notoriously nutrient-tolerant representatives of the genera *Navicula, Nitzschia* and *Cyclotella.* At the same time, the sample plot reveals a tendency for all sites, not just sites of the restored reach to have less pollution-tolerant taxa in 2015 compared to 2011. Although this trend is not significant, it shows that further observations are necessary to confirm the effect of restoration on diatoms.

B. 4. Historical trends in water quality of Lancaster County streams inferred from diatoms.

To evaluate ecological status of diatom assemblages from the restored reach of the Big Spring Run we also analyzed several additional sets of samples.

We identified and enumerated diatoms from the bank section samples dating back to the time prior to European settlement. At the base of this section (160-163 cm and 154-156 cm depth intervals, Table B.2), diatom assemblages were dominated by several large-celled species of *Pinnularia* (such as *P. viridiformis var. minor, P. neomajor. Var. inflate* and *P. mesogongyla*) characteristic for unpolluted wetlands, bogs and marshes (Krammer 2002). Other abundant diatoms in these samples were a few *Stauroneis* species (*S. acuta*, *S*. cf. *phoenicentron*, and *S. reichardtii*) also typical for wetlands, and several species of *Hanthzschia* and *Luticola* mostly found in aerophytic habitats, such as marshes and wet soils. This assemblage indicated a shallow valley bottom wetland throughout the late Holocene until the 1700s; this is consistent with previous stratigraphic and sub-fossil seed evidence.

Historic sediment immediately overlying this wetland soil (134-136 cm, 124-136 cm and 114-116 cm intervals) marks a transition from wetland to mud flat. The large-celled and other wetland diatoms disappear and the assemblage is dominated by *Gomphonema drutelingense*, a diatom that has been insufficiently characterized ecologically, but that is apparently typical for springs in watersheds underlain by calcareous bedrock (Reichardt

1999). The search of the ANS databases for the occurrences of this diatom in the US revealed that it has been most often recorded in Alaska thus pointing at its low temperature preference. This species has been also sometimes recorded in recent collections from the Lancaster county streams, especially in the headwaters and less polluted sites. The sharp transition from the *Pinnularia*- to *Gomphonema*-dominated assemblage is a strong evidence of a modification of the valley bottom wetland by European settlers. The upper interval (56-58 cm) had very sparse diatoms, which may be caused by the high sediment accumulation rate in the post-European settlement times. The most abundant species are aerophytic species, which points at the possibility of these diatoms being washed into the impoundment from the watershed soils.

Table B.2. The most abundant diatoms in the BSR bank section.

Depth (cm)	*Pinnularia* spp.	*Stauroneis* spp. (large-celled species)	*Gomphonema drutelingense*	*Hantzschia amphioxys*	*Luticola mutica*
56-58	6.7	0.0	2.4	20.0	16.7
114-116	0.5	2.3	87.0	0.0	0.0
124-126	18.8	2.2	37.2	0.0	0.4
134-136	7.6	1.0	60.2	0.0	3.1
154-156	32.9	3.3	1.3	5.3	2.6
160-163	40.0	10.0	5.7	2.9	0.0

Great Marsh wetland may be considered as reference site in relation to streams that experienced damming and legacy sediment accumulation. Besides being diverse, diatom assemblages from Great Marsh (sampled in 2016) had some similarity to BSR bank section samples from the deepest intervals representing pre-European settlement wetland. The species identity was not the same between these two sample sets, but Great Marsh samples also had some large-celled species of *Pinnularia* and *Stauroneis* and some other large-celled diatoms (Figure 1.5) that are not normally found in agricultural streams of southeastern Pennsylvania. Some difference between Great Marsh and Lancaster County streams may be attributed to different bedrock composition with Marsh Creek having somewhat softer water compared to hard-water streams near Lancaster. This is reflected by diatom assemblages that have a higher proportion of *Eunotia* species and other diatoms, such as *Nitzschia acidoclinata* associated with relatively soft waters. Unlike pre-European settlement BSR samples, many diatoms in Great Marsh are eutraphentic cosmopolitan

species, indicating moderate to high nutrient concentrations. At the same time, the high diversity of the assemblages together with presence of rare native species, such as *Sellaphora alastos* and typical wetland diatoms indicate a unique environment that still bears some resemblance to now-extirpated ecosystems of valley bottom marshes.

Diatom slides housed at the ANS Diatom Herbarium and representing collections made in Lancaster County in 1948 had to be re-examined and enumerated because the original diatom counts could not be located and only a few dominant diatom species were listed in the original Conestoga report (Patrick & Roberts 1949). In addition, diatom taxonomy and microscopy evolved so much in the past ~70 years that the modern counts would be hardly comparable to the old ones. The investigation of these historic diatom slides showed that in 1948 many streams were dominated by eutraphentic and sediment-tolerant *Navicula, Nitzschia, Mayamaea, Eolimna, Melosira* and *Fistulifera* species. These diatoms clearly indicate strong nutrient pollution, while low species diversity at some sites also points at toxic effects probably due to industrial waste. For example, the average rarefied species richness for Lititz Run 1948 samples was 10.9, while it was as high as 41.4 in samples from Cocalico Creek that was relatively weakly polluted in 1948. The average species richness (rarefied) in Great Marsh wetland 2016 samples was 38.5 and in the restored portion of Big Spring Run it was 44.2. Patrick (1949) concluded that extremely low diatom diversity in Lititz Run was caused by severe pollution and went on to recommend using biotic diversity as a general measure of river health. Subsequent studies showed that relationships between diatom diversity and pollution are not that straightforward (Stevenson et al. 2010, Sullivan 1986) and that relatively clean streams may have low-diversity diatom assemblages because of the nutrient and/or light limitation (Liess et al. 2012). At the same time the combination of low diversity and dominance of pollution-tolerant taxa is a strong indication of stream pollution. Thus, increased diversity in restored reaches of streams in agricultural landscapes, such as BSR is a positive sign of increased complexity of biological communities and ecosystem stability.

In order to elucidate major patterns in the composition of diatom assemblages in streams of Lancaster County and adjacent areas, we constructed a combined dataset consisting of 2011 and 2015 BSR samples, 1948 Patrick's samples, 1993-2015 diatom counts from ANS databases, and seven 2016 Marsh Creek samples. Figures 1.6-1.8 show the result of an unconstrained ordination (DCA) of this dataset. The nutrient diatom metrics calculated for each sample and year of sampling were added as passive environmental variables and the direction of the arrows corresponding to these variables shows that diatoms in older samples on average indicated higher nutrients than in more recent collections (see Figure 1.6). Since there was no repeated sampling of the same sites across years, it is impossible to

tell whether this is a real temporal trend or the consequence of targeting more polluted sites in the past. Ruth Patrick's team obviously focused on several streams that were heavily polluted by untreated industrial sewage, such as Lititz Run and a section of Mill Creek near New Holland. Richardson et al. (1996) reported that point-source pollution has been drastically reduced in Lancaster County already starting from 1970s, and both Lititz Run and Mill Creek experienced notable increase in water quality as evidenced by the return of aquatic animals and diminished proportions of the pollution-tolerant species in diatom assemblages. There was no evidence, however, of any decrease of the non-point source pollution in Lancaster County, especially nutrient input from fertilizers either in 1990s (Richardson et al. 1996) or later. BSR samples are positioned towards the lower part of the DCA plot (see Figure 1.6) and thus appear to reflect less nutrient-enriched environment than most sites sampled in 1948, at least as inferred from diatoms. The environmental gradient underlying variation of diatom assemblages along the second DCA axis may also include siltation. Diatom species positioned at the high end of ordination, such as *Diatoma vulgaris, Melosira varians, Navicula capitatoradiata* and *N*. *tripunctata* are known to prefer fine-grained sediments, while diatoms in the lower part of the plot are monoraphids *Achnanthidium minutissimum, Planothidium lanceolatum* and *P*. *frequentissimum* that live attached to silt-free surfaces.

The first DCA axis is likely reflecting the variation of diatom assemblages along the gradient of water mineral content: the samples from French Creek that has lower conductivity than most Lancaster County streams are positioned on the far right of the ordination, while of the far left there are 1948 samples from extremely polluted portion of Lititz Run, which is a hard-water stream. The expanded portion of the DCA samples plot shown in Figure 1.7 demonstrates that BSR samples are quite similar in their diatom species composition to headwater portions of other streams of Lancaster and County, such as Hammer Creek, Lititz Run, and Cocalico Creek and that diatom assemblages in this area have not experienced considerable change in the last 70 years. Post-restoration BSR samples in Figures 1.6 and 1.7 are positioned below pre-restoration samples, which confirms their shift towards fewer eutraphentic species.

B. 5. Conclusions

The investigation of bank section samples confirmed that prior to European settlement BSR site supported a shallow wetland inhabited by diatoms that are known to prefer slow-moving clean waters with abundant vegetation (large-celled *Pinnularia* and *Stauroneis* species). Abrupt changes in diatom assemblages in the sediments overlaying buried hydrosol indicate drastic modifications of stream channel by European settlers that led to disappearance of valley bottom wetland.

Examination of diatom collections made by Ruth Patrick in 1948 showed that almost no diatom species that were present in the 1700s remained in the streams of the Conestoga River basin by 1948. At that time, the assemblages were dominated by hyper- and eutraphentic and sediment-tolerant cosmopolitan *Navicula, Nitzschia, Maamaea, Eolimna,* and *Fistulifera* species.

Diatom assemblages of Big Spring Run are typical for small hard-water nutrient-rich Lancaster County streams. The overall diatom species composition in the restored BSR reach did not considerably change by December 2015 compared to pre-restoration, which could be expected considering still relatively high water nutrient concentration in the stream. Some positive trends were, however, observed. First, the assemblages became more diverse. The increase in species richness could be attributed to the enhanced complexity of the habitat which now provides a greater diversity of substrates and flow conditions. Second, diatom nutrient metrics indicated that post-restoration assemblages had fewer diatoms associated with high nutrients and more of those indicative of low nutrients.

Although the restoration led to a reduction of nutrient concentrations in stream water, nutrients are still high because of their input from upstream reaches. Therefore, diatoms assemblages are still dominated by eutraphentic species. Our investigation of the Great Marsh wetland showed what type of diatom assemblage could be expected if a stream in an agricultural landscape would retain its valley bottom wetland. While eutraphentic diatoms are still present in Great Marsh, the diversity of these assemblages is rather high with a considerable contribution of low-nutrient indicating and native species. It would be unrealistic to expect the biota to revert to its pre-1700s condition, but increased diversity and higher proportion of oligotraphentic species should be considered as positive effect of the restoration.

We conclude by noting that this post-restoration analysis was based on samples collected in 2015, and that there might well be further improvements now, as of 2017. This could warrant a continued study of BSR diatoms periodically over the next decade or so in order to determine whether there is additional improvement.

B. 6. Data files.

1) List of sampling locations and diatom samples. Excel file.
2) Diatom count data. Excel file.

B. 7. References

Grand Pre, C. A., Walter, R.C., Merritts, D.J., Moser, A.C., Bernhardt, C., Potapova, M. & Hilgartner, W.B. 2012. A High-Resolution Multi-proxy Record of Late Pleistocene and Holocene Climate Change from Great Marsh, Southeastern PA. In 2012 GSA Annual Meeting in Charlotte. North Carolina.

Hering, D., Johnson, R. K., Kramm, S., Schmutz, S., Szoszkiewicz, K. & Verdonschot, P. F. M. 2006. Assessment of European streams with diatoms, macrophytes, macroinvertebrates and fish: a comparative metric-based analysis of organism response due to stress. Freshwater Biology 51:1757–1785.

Hofmann, G., Lange-Bertalot, H., & Werum, M. 2013. Diatomeen im Süßwasser-Benthos von Mitteleuropa: 2 Corrected Edition. Koeltz Scientific Books, Königstein, 908 pp.

Kelly, M.C. & Whitton, I.A. 1995. The trophic diatom index: a new index for monitoring eutrophication in rivers. Journal of Applied Phycology 7: 433-444.

Krammer, K. 1997a. Die cymbelloiden Diatomeen. Eine Monographie der weltweit bekannten Taxa. Teil 1. Allgemeines und *Encyonema*. Bibliotheca Diatomologica 36: 1-382.

Krammer, K. 1997b. Die cymbelloiden Diatomeen. Eine Monographie der weltweit bekannten Taxa. Teil 2. *Encyonema* part., *Encyonopsis* and *Cymbellopsis*. Bibliotheca Diatomologica 37:1-469.

Krammer, K. 2000. The genus *Pinnularia*. The Diatoms of Europe. Diatoms of Inland Waters and Comparable Habitats 1: 1-703.

Krammer, K. & Lange-Bertalot, H. 1986. Bacillariophyceae. 1. Teil: Naviculaceae. In: Ettl, H., J. Gerloff, H. Heynig and D. Mollenhauer (eds.) Süsswasserflora von Mitteleuropa, Band 2/1. Gustav Fisher Verlag, Jena. 876 pp.

Krammer, K. & Lange-Bertalot, H. 1988. Bacillariophyceae. 2. Teil: Bacillariaceae, Epithemiaceae, Surirellaceae. In: Ettl, H., J. Gerloff, H. Heynig and D. Mollenhauer (eds.) Susswasserflora von Mitteleuropa, Band 2/2. Gustav Fisher Verlag, Jena.

Krammer, K. & Lange-Bertalot, H. 1991. Bacillariophyceae. 3. Teil: Centrales, Fragilariaceae, Eunotiaceae. In Ettl, H., Gerloff, J., Heynig, H. & Mollenhauer, D. (Eds.). Süsswasserflora von Mitteleuropa. 2(3): 1-576. Gustav Fisher Verlag, Stuttgart, Germany.

Krammer, K. & Lange-Bertalot, H. 2004. Bacillariophyceae 4. Teil: Achnanthaceae, Kritische Erganzungen zu *Navicula* (Lineolatae), *Gomphonema* Gesamtliteraturverzeichnis. Teil 1-4 [second revised edition]. In: H. Ettl et al., Suesswasserflora von Mitteleuropa. Spektrum Akademischer Verlad Heidelberg, 468 pp.

Liess, A., Le Gros, A., Wagenhoff, A., Townsend, C.R. & Matthaei, C.D. 2012. Landuse intensity in stream catchments affects the benthic food web: consequences for nutrient supply, periphyton C:nutrient ratios, and invertebrate richness and abundance. Freshwater Science 31 (3): 813-824.

Lowe, R.L. 1974. Environmental requirements and pollution tolerance of freshwater diatoms. US Environmental Monitoring Series. EPA 670/4--74--005, 1-334.

Martin, P.S. 1958. Taiga-Tundra and the Full-Glacial Period in Chester County, Pennsylvania. American Journal of Science 256 (7): 470–502.

Merritts, D., Walter, R., Rahnis, M., Hartranft, J., Cox, S., Gellis, A., Potter, N., Hilgartner, W., Langland, M. & Manion, L. 2011. Anthropocene Streams and Base-Level Controls from Historic Dams in the Unglaciated Mid-Atlantic Region, USA. Philosophical Transactions of the RoyalSociety A: Mathematical, Physical and Engineering Sciences 369 (1938): 976–1009.

Merritts, D., Walter, R., Rahnis, M., Cox, S., Hartranft, J., Scheid, C., Potter, et al. 2013. The rise and fall of Mid-Atlantic streams: Millpond sedimentation, milldam breaching, channel incision, and stream bank erosion. Reviews in Engineering Geology 21: 183-203.

Oksanen, J., Blanchet, G. F., Kindt, R., Legendre, P., Minchin, P.R., O'Hara, R. B. Simpson, G. L., Solymos, P., Stevens, M. H. H. & Wagner, H. 2016. R package version 2.3-5. http://CRAN.R-project.org/package=vegan.

Pantle, R. & Buck, H. 1955. Die biologische Überwachung der Gewasser und die Darstellung der Ergebnisse. Gas und Wasserfach 96: 604-624.

Patrick, R. 1949. A proposed biological measure of stream conditions based on a survey of Conestoga Basin, Lancaster County, Pennsylvania. Proceedings of the Academy of Natural Sciences of Philadelphia 101: 277-341.

Patrick, R. 1950. Biological measure of stream conditions. Sewage and Industrial Wastes 22(7): 926-938.

Patrick, R. 1953. Biological phases of stream pollution. Proceedings of the Pennsylvania Academy of Sciences 27: 33-36.

Patrick, R. 1954. Diatoms as an indicator of river change. Proceedings of the 9th Industrial Waste Conference, Purdue University Engin. Bulletin 87: 325-330.

Patrick, R. 1956. Diatoms as indicators of changes in environmental conditions. In: C.M. Tarzwell (Ed.), Biological Problems in Water Pollution. Robert A. Taft Sanitary Engineering Center; Cincinnati, Ohio, pp. 71-83.

Patrick, R., & C.W. Reimer. 1966. Diatoms of the United States. Vol. I. Monograph 13, Acad. Nat. Sci. Philadelphia.

Patrick, R., & C.W. Reimer. 1975. Diatoms of the United States. Volume II, Part 1. Monograph 13, Acad. Nat. Sci. Philadelphia.

Patrick, R., & Roberts, H.R. 1949. Biological survey of the Conestoga Creek Basin and observations on the West Branch Barndywine Creek. A report to the Sanitary Water Board, Comonwealth of Pennsylvania by the Academy of Natural Sciences of Philadelphia.

Petranka, J. 1988. Salamanders of the United States and Canada. Smithsonian Institution Press.

Potapova, M. & Carlisle D.M. 2011. Development and application of indices to assess the condition of benthic algal communities in U.S. streams and rivers. U.S. Geological Survey Open File Report 2011-1126.

Potapova, M. & Charles, D.F. 2003. Distribution of benthic diatoms in U.S. rivers in relation to conductivity and ionic composition. Freshwater Biology 48: 1311-1328.

Potapova, M. & Charles, D.F. 2007. Diatom metrics for monitoring eutrophication in rivers of the United States. Ecological Indicators 7:48-70.

Reichardt, E. 1999. Zur Revision der Gattung *Gomphonema*: Die Arten um *G. affine/insigne, G. angustatum/micropus, G. acuminatum* sowie gomphonemoide Diatomeen aus dem Oberoligozän in Böhmen. Annotated Diatom Micrographs. Edited by Horst Lange-Bertalot. Iconographia Diatomologica, Volume 8, A.R.G. Gantner.

Richardson, J.L., Mody, N.S. & Stacey, M.E. 1996. Diatoms and water quality in Lancaster County (PA) streams: a 45-year perspective. Journal of the Pennsylvania Academy of Science 70(1): 30-39.

Sládeček, V. 1986. Diatoms as Indicators of Organic Pollution. Acta Hydrochimica et Hydrobiologica 14(5): 555-566.

Spaulding, S.A., Lubinski, D.J. & Potapova, M. 2010. Diatoms of the United States. http://westerndiatoms.colorado.edu.

Stevenson, R. J., Pan, Y. & van Dam, H. 2010. Assessing ecological conditions in rivers and streams with diatoms. In Stoermer, E. F. & Smol, J. P. [Eds.] The Diatoms: Applications to the Environmental and Earth Sciences. 2nd edn. Cambridge University Press, Cambridge, pp. 57–85.

Sullivan, M.J. 1986. Mathematical expression of diatom results: are these pollution indices valid and useful? In M. Ricard (ed.) Proceedings of the 8th International Diatom Symposium, Koeltz Scientific Books, Kenigstein, p. 772-775.

Ter Braak, C.J.F. & Smilauer, P. 2012. CANOCO reference manual and user's guide: software for ordination, version 5.0. Microcomputer Power. 496 pp.

van Dam, H., Mertens, A. & Sinkeldam, J. 1994. A coded checklist and ecological indicator values of freshwater diatoms from The Netherlands. Netherlands Journal of Aquatic Ecology 28: 117-133.

Walter, R. C., & Merritts, D.J. 2008. Natural Streams and the Legacy of Water-Powered Mills." *Science* 319 (5861): 299–304.

Walter, R., Merritts, D., Rahnis, M., Langland, M., Galeone, D., Gellis, A., Hilgartner, E=W., Bowne, D., Wallace, J., Mayer, P. & Forshay, K. 2013. Big Spring Run natural floodplain, stream, and riparian wetland - aquatic resource restoration project monitoring. PA DEP final report.

C. Deliverable 2: Analysis and interpretation of surface water and ground water quality parameters at the BSR restoration site for two years, and comparison with 2D flow modeling for pre- and post-restoration conditions.

Contact person: Dorothy Merritts (flow modeling), Franklin and Marshall College, Art Parola (flow modeling), University of Louisville, and Michael Langland (surface and ground water quality), USGS

Tasks: Assist in the collection, processing, and analysis of groundwater and surface water parameters necessary to interpret change over time. Compile and provide a database of post-restoration water quality parameters that corresponds with pre-restoration water quality parameters. Analyze water quality trends over time by comparing pre-restoration and post-restoration water quality parameters.

Deliverables: A database of water quality records along with a description of the sampling and analysis procedures and protocols. A written report that analyzes trends over time by comparing pre-restoration and post-restoration water quality parameters.

C.1. Surface and ground water quality: See separate report from Langland et al, 2017, to PA DEP.

C.2. 2D-Flow Modeling for Pre- and Post-Restoration Conditions

C.2. 1. Introduction

We used a 2D hydrodynamic model to evaluate pre- and post-restoration flow and shear stresses on the channels and floodplain between the three gage stations at Big Spring Run, including the restoration area. Input for the model was as follows:

1) Pre-restoration channel breaklines from a 2010 pre-restoration design, aerial survey contours (3D, NAVD88 ft) at 1 foot interval, existing bank edge and thalweg (2D, all elevations zero), and design bank edge and thalweg (2D, all elevations zero).

2) Post-restoration channel breaklines from an as-built survey, with surveyed points and contours (3D, NAVD88 ft) and bank top edge and bank toe (3D).

3) Dimensions and elevations (upstream and downstream) for a culvert that existed pre-restoration in the western tributary upstream of its confluence with the eastern tributary.

4) Locations with elevations of the sensors at all three stream gages.

5) A 15-minute time series for stage and discharge of a high flow event (October 15, 2014) for all three gages.

6) Time series for stage and discharge of a high flow event (October 15, 2014at the two upstream gauges (Figure C.2.1). The simulation starts at 10:00 AM EDT on October 15, 2014, and continues ~12 hours, through 10 PM EDT.

7) Locations of debris and logs placed along the main channel during restoration construction.

Additional data for the third of these is provided here:

USGS 01576516 -- Eastern tributary

Big Spring Run Tributary near Willow Street, PA

http://waterdata.usgs.gov/usa/nwis/uv?01576516

Latitude 39°59'29.56", Longitude 76°15'39.35" NAD83
Lancaster County, Pennsylvania, Hydrologic Unit 02050306
Drainage area: 0.36 square miles
Datum of gage: 315 feet above NGVD29.
Also referred to as # 015765159.

USGS 015765185 -- Western tributary

Unnamed Tributary to Big Spring Run near Willow Street PA

http://waterdata.usgs.gov/usa/nwis/uv?015765185

Latitude 39°59'28.29", Longitude 76°15'50.23" NAD83
Lancaster County, Pennsylvania, Hydrologic Unit 02050306
Drainage area: 1.05 square miles
Datum of gage: 325 feet above NGVD29.
Also referred to as #015765184.

USGS 015765195-- Big Spring Run near Mylin Corners, PA

Main stem of Big Spring Run near Mylin Corners, PA

https://waterdata.usgs.gov/pa/nwis/uv?site_no=015765195

Lat 39`59'45.37", long 76`15'50.54" NAD83

Lancaster County, Pennsylvania, Hydrologic Unit 02050306
Drainage area: 1.68 square miles
Datum of gage: 305 feet above NGVD of 1988, from Lidar.

C.2. 2. Flow Modeling

The bed stress is computed by the following equation in the 2D TUFLOW model:

$$\tau_{bed} = \frac{\rho g V^2 n^2}{2.208\, y^{\frac{1}{3}}}$$

in which ρ is density, g is gravity, V is velocity, n is Manning's roughness coefficient, and y is water depth. Velocity is the local total velocity comprised of the two horizontal component velocities.

C.2. 2. Results

For the pre-restoration conditions, bed shear stresses for the modeled flow event exceed 2 psf at multiple times and locations during the simulation (Figure C.2.2). For the post-restoration conditions, bed shear stresses never exceed 0.5 psf within the restored area, but still exceed 2 psf in the unrestored parts of the channel (Figure C.2.3).

Note that highest shear stresses within the restored area occur at the upstream end along the western tributary where the unrestored channel with high banks enters the restored reach. Bed shear stresses diminish downstream in this reach. The slope along this portion is higher than elsewhere within the restoration, and since restoration this area has experienced some deposition of sand and gravel during high flow events (see XS 3 and 4 in Figure 4.5 in part D of report).

Given that higher bed shear stresses are capable of transporting larger size sediment, it is possible to evaluate the spatial variability in bed shear stresses by sampling gravel that was transported during a high flow event. In May 2016, we sampled 11 recent gravel deposits (25 to 150 grams per sample) along the margins of channels throughout the restoration area and downstream in the unrestored reach, near the gage station (Figure C.2.4). We did not find any recent gravel deposits in the lower half of the restoration area, where the floodplain is widest and valley slope lowest. We used a Ro-Tap sieve to determine particle size distribution for each sample.

The median grain sizes (D_{50}) of these samples decrease from up to downstream in the restored reach, diminishing to sand size (<2 mm) within several hundred feet of the upper end of the restoration area (see Figure C.2.4). Downstream of the restoration reach, near

the gage station, the median grain size (16 mm) increases to a size similar to samples at the uppermost end (southwestern) of the restoration reach.

D. Deliverable 3: Post-restoration biological indicators of ecosystem conditions at BSR and analysis of ecosystem changes over time by comparing pre-restoration and post-restoration biological parameters.

Contact person: Dr. William Hilgartner, The Johns Hopkins University; Dr. David Bowne, Elizabethtown College:

Tasks: Analyze post-construction biological parameters at the BSR restoration site. Compile the data into appropriate databases and analyze trends over time by comparing the pre-restoration with post-restoration biological components of the ecosystem.

Deliverables: A written report and database with records for biological ecosystem components that compare post-restoration and pre-restoration conditions.

D. 1. Vegetation Analysis: Introduction

This report focuses on plant species diversity within the upper Big Spring Run valley before and after the Big Spring Run Restoration that occurred between September and November, 2011. Results of transect analysis during the summer of 2016 are first summarized and then data from the same transect is compared for 2010, 2011, 2012, 2015 and 2016.

D. 2. Vegetation Analysis: Summer, 2016

Vegetation transect analysis was conducted at a permanent transect site at Big Spring Run Restoration (BSR) in early September, 2016 and a brief survey was conducted in early July, 2016. The purpose of the transect analysis was to record plant species that dominate in late summer at one of the permanent transect lines established in 2010, in order to compare plants that bloom in late summer at the same transect within the same time period.

Species composition and percent cover (abundance) in 14 quadrats along Transect 6 (TR 6) was conducted by Hilgartner (Table D.1). Transect analysis was conducted in the following way: In the field percent cover (%C) was estimated for each species identified and recorded for each of 14 quadrats. In the lab, the *Total percent cover (Total % C)* for each species in 14 quadrats was determined by summing %C for each species. *Relative percent cover* (*Rel. %C)* for each species was determined by summing the Total %C (Sum Total %C) for all species and dividing the Total % C of each species by the Sum Total %C. *Frequency (Freq.)* of each species along the transect was determined by dividing the number of quadrats in which a

species occurred out of 14 quadrats. All frequencies were summed (Sum Freq.) and each species' Freq. was divided by the Sum Freq. to provide *Relative Frequency (Rel. Freq.).* Finally, *Importance Value (I.V.)* was determined by adding Rel.%C + Rel. Freq. The Importance Value is actually a frequency based on 200% (100% for Rel.%C and 100% Rel. Freq.). This approach used consistently with transect analysis over the past 6 years can show whether a species has increased, decreased or remained steady in importance.

Seventeen wetland species occurred within the 35-meter wetland section of the transect, while 14 upland species occurred within 20 meters of TR 6 on the hills at the east and west edge of the wetland (see Table D.1). The most importat species (marked in bold, I.V. > 0.10, see Table D.1) within the wetland portion of the restoration along TR 6 include *Leersia oryzoides* (rice cutgrass), *Impatiens capensis* (jewelweed), *Typha latifolia* (broad-leaved cattail) and *Nasturgium officinale* (watercress). *Leersia, Typha* and *Nastugium* fall within the wetland status of OBL, while *Impatiens* is FACW. The most important species along the periphery of the wetland on the valley hillsides were spring blooming grasses, including *Poa pratensis, Festuca elatior, Agropyron repens, Setaria glauca, Dactylus glomerata, Lolium perenne* and *Secale cerale,* as well as the Canada thistle *Cirsium arvense*. These species are overwhelmingly typical of fields, dry meadows, pastures and waste places, and all of these dominants except *Setaria* have a wetland indicator status of FACU.

D. 3. Vegetation Analysis: Sedges (Cyperaceae)

There has been interest in sedges (Cyperaceae) and related species at BSR, because of the importance of the Cyperaceae in the pre-settlement wetland based on fossil seeds. A brief survey was conducted on 5 July 2016 by Hilgartner. The following sedges and rushes were observed growing in various areas of the restored wetland: *Carex stricta* (tussock sedge), *C. vulpinoidea* (foxtail sedge), *C. lurida, (*lurid sedge), *Schoenoplectus tabernaemontana* (soft-stem bulrush), *S. cyperinus* (woolgrass), *S. atrovirens* (dark green bulrush), *Juncus effusus* (soft rush), and *J. bufonius* (toad rush). All of these species were either seeded or planted following legacy sediment removal during the restoration in 2011 except. *J. bufonius,* first observed in 2014, which has moved into the wetland voluntarily. Sedges occurring along TR 6 in 2016 included *Schoenoplectus tabernaemontana* (I.V. = 0.05), and *Carex lurida* and *C. vulpinoidea*, (both I.V. = 0.02). J.Hartranft of the Pennsylvania Department of the Environment has confirmed the identifications of these species during the past 5 years. As of June, 2015 Hartranft and Hilgartner had recorded the following sedges: *Carex crinita, C. comosa, C. frankii, C. lurida, C. scoparia, C. stipata, C. stricta, C. vulpinoidea, Cyperus sp., Eleocharis sp., Rhyncospora sp.*, *Schoenoplectus americanus (= Scirpus pungens), Schoenoplectus tabernaemontana, Scirpus atrovirens, S. cyperinus.* Rushes included *Juncus bufonius* and *J.effusus.*

D. 4. Vegetation Analysis: Summary of Pre- and Post-Restoration Vegetation (2010 to 2016)

Methodology

A set of 6 permanent transects were established at BSR spanning the river channel at upstream and downstream locations by Jeff Hartranft in 2010 (Figure 3.1). Quadrats spaced 5 meters apart along each transect permitted determination of percent cover, frequency and importance value of plant species within the quadrats. The transect lines were established before the restoration in order to establish a baseline of existing pre-restoration vegetation. Monitoring from year to year following the restoration (since September, 2011) has been conducted in order to compare the newly established plant species immediately after the restoration, as well as changes in plant species presence and abundance in succeeding years.

All six transects have been examined at points during the growing season (June – September), by B. Hilgartner, Jeff Hartranft, and students and staff from Franklin and Marshall College. These include (among others) the following dates and transects:

Pre-Restoration: TR 1, TR 4 and TR 6 on 8/17/2010; TR 4, TR 6 on 6/17/2011.

Post-Restoration: TR 6 on 8/24/2012; TR 1 on 6/14/2013; TR 5 and TR 6 on 6/24/2015; TR 3 and TR 6 on 9/6/2015; TR 6 on 9/3/2016.

Results (Transect 6, 2010-2016)

For this report only Transect 6 data (TR 6) has been analyzed for simplicity in understanding species trends in wetland development in late summer (late August, early September) at a central location within the wetland. Most of the species found at TR 6 also occur in the other BSR transects. TR 6 was monitored over a 6-year span by Bill Hilgartner and Jeff Hartranft in 2010, 2011, 2012, 2015 and 2016 (Table D.2). Seventy-seven species have been recorded at TR 6, which is 50% of all species found throughout the BSR valley before and after restoration. The importance value (IV) determined from data gathered on 5 dates provides a vegetation comparison within the 6-yr period. Importance value is determined by adding the relative percent cover and relative frequency of species along the transect.

Pre-Restoration (Before September 2011)

Before the restoration in September, 2011, the transect vegetation was dominated by upland species, primarily 10 grass species. The most important species were the grasses *Poa pratensis, Festuca elatior, Agropyron repens, Setaria glauca, Dactylus glomerata, Lolium*

perenne and *Secale cerale,* collectively referred to as "upland grasses", and the Canada thistle *Cirsium arvense*. The importance of these species declined sharply after 2011 as they were confined to the upper edges of the restored wetland. These species are typical of fields, dry meadows, pastures and waste places, and all of these dominants except *Setaria* have a wetland indicator status of FACU. Of the 37 upland species with UPL, FACU and nl (not listed) in Table D.2 all but 4 species occurred only in 2010 and June, 2011 prior to restoration. In other transects and in locations between or beyond transects, upland species such as poison hemlock *Conium maculatum* was also common.

Wetland species before restoration were dominated by Reed Canary Grass *Phalaris arundinacea* (IV= 0.33-0.39) with lesser occurrence of Jewelweed *Impatiens capensis* (IV= 0.04-0.05) (Table D.2). *Impatiens* was situated at or within the banks of the channel, at each transect, while *Phalaris* grew further away from the channel banks in dominant patches. The wetland portion of the transect where *Impatiens* occurred was essentially only 5 meters wide, while the *Phalaris* zone was as much as 20 meters.

Post-Restoration (after November 2011)

Several important changes in plant dominance occurred after the restoration, which involved removal of over a meter of legacy sediment to expose a lowered ground layer near the ground water table. The upland grasses declined from IV values of 1.06 and 1.0 before restoration in September 2011, to 0.14, 0.30 and 0.24 after the restoration, where these species are confined to the periphery of the wetland. *Cirsium* IV dropped from 0.15 to 0.02 and 0.05. Other pasture or dry field species declined or occurred in low numbers. An exception is *Solidago canadensis* (Canada goldenrod) which has increased within the hill slope periphery with IV values of 0.03 or 0.02 before restoration to 0.06 after restoration.

Wetland species (FACW and OBL) underwent a significant increase, both in diversity and importance. Many species were planted or seeded following the legacy sediment removal but a number of species have moved in while others that were established in the first year have declined or disappeared as succession progresses. For example, in August of 2012 *Panicum rigidulum* was the most important species along with the codominant *Leersia oryzoides* along Transect 6, while in the summer of 2015 and 2016 *Panicum rigidulum* was not found. *Phalaris arundinacea* also underwent a decline and does not occur in TR 6 in 2015 and 2016, although it occurs in patches elsewhere. An increasing number of sedges have become established and are scattered throughout the wetland in patches, some which are "caught" within the transect and some found outside the transect line. For example, in June 2015 fifteen species of sedges and two species of rush were identified by Hilgartner and Hartranft. While most were part of the original planting in late 2011, 5 species were new volunteers to the wetland (*Carex scoparia, Scirpus americanus, Cyperus* sp., *Eleocharis*

sp. and possibly *Rhyncospora* sp.), showing that succession is progressing with new arrivals and the disappearance of original species as the wetland adjusts to the current hydrologic regime.

Leersia oryzoides has become the most important species in TR 6 (and through much of the wetland) since the restoration with IV values increasing from 0.19 in 2012 to 0.37 in 2015 and 0.41 in 2016.The other important dominant is *Impatiens capensis* with IV values increasing from 0.05 before the restoration to 0.23 after restoration. A new volunteer species which is increasing and becoming more important is broad-leaved cattail *Typha latifolia*, not appearing until 2015 with an IV of 0.05 and increasing to 0.16 in 2016. *Nasturgium* has become the dominant within the shallow, slow-moving channels in the restored wetland. Other notable species include the composites beggar ticks *Bidens frondosa*, nodding bur marigold *B. cernua*, (both IV = 0.02) and boneset *Eupatorium perfoliatum,* IV = 0.06. All together since the restoration 40 wetland species (OBL, FACW) have been identified along TR 6 compared with only 2 FACW species and 2 FAC species before the restoration, *showing a tenfold increase in FACW and OBL species.*

D. 5. Vegetation Analysis: Conclusions

Transect vegetation before and after the wetland design/restoration of Big Spring Run reveals a major ecological change was created when legacy sediment was removed. Vegetation shifted from a dry, upland pasture environment to a low, hydric wet meadow that is still undergoing succession as vegetation stabilizes within the hydrologic regime. Before 2011 a single stream channel with 1 m high banks meandering through a cow pasture dominated by non-native agricultural grasses and the native Canada thistle. The area contained only a handful of hydric species around the channel margins and a few scattered patches of other wetland species near a spring.

After restoration, a diverse wetland system dominated by rice cutgrass, jewelweed, cattail, and numerous sedges and composites became established. Comparing the data from TR 6 with other transects, as well as regular surveys, it is evident that the “new” wetland is settling into a kind of wet meadow with scattered patches of sedge meadow. The wetland has expanded from essentially a 5-meter area around a single channel meander before 2011 to a 40-50-meter-wide wetland with considerable increase in hydric plant diversity since 2012.

The fossil seed record from the buried hydric layer at the bottom of the channel bank studied before 2011 has been described in other reports (Neugebauer 2011; Hilgartner et al. 2010; Voli et al. 2009). ^{14}C and pollen-dating revealed a nearly 3000-year-old stable, sedge meadow persisted prior to the early 1700s. Members of the Cyperaceae (sedge

family) were the dominant species growing in a surface ground water table, indicating that a water table near ground surface level provided stability within the BSR valley. Beginning around 1730 burial of the prehistoric wetland began to occur as back water from a downstream dam trapped eroding sediment from nearby deforestation and farming.

Part of the underlying goal of the BSR restoration, along with stated goals of sediment, nutrient and flood control and enhancement of wetland biodiversity and stability, was to see if the original sedge meadow would return if the gradient level of the valley were properly established near the ground water table. This would have the added bonus of providing the specific habitat of the endangered bog turtle, a specialist of tussock sedge and sedge meadow wetlands. Many sedge species were planted or seeded soon after legacy sediment had been removed in late 2011 and 2012. Most of these sedges remain or have expanded within the wetland occurring in patches, while rice cutgrass, jewelweed, cattail and patches of composites have predominated more widely. Thus, a strictly sedge meadow has not yet been established; instead a species-rich "wet meadow" has emerged with rice cutgrass, jewelweed, cattail, scattered flowering composites and sedge dominated patches providing a diverse wetland habitat that has the potential to be "equally as valuable" from an ecological and plant diversity standpoint.

D. 6. Amphibian surveys: Introduction

Amphibian surveys were conducted by David Bowne with assistance from Elizabethtown College students Alyssa Taylor and Jennah Krause (2015, 2016) and Alexandra Charnigo (2016).

Our contribution to the Big Spring Run restoration project was to determine the response of amphibians to the restoration. We designed the surveys for salamanders to focus on relative abundance of larval stages at the restored branches of Big Spring Run (West and Main), the unrestored branch of Big Spring Run (East), and an upstream reference location (Kennel Branch). The cryptic nature and small size of salamanders make them difficult to study. We used a variety of techniques to increase the detection probability. These techniques included litter bags, kick nets, and dip nets. Litter bags create a site of suitable habitat for salamanders to colonize while not restricting their movements. Each litter bag was a 0 .7 X 0.7 m piece of plastic netting with a mesh size of 1.75 cm filled with rocks and leaf litter and bundled with a plastic twist tie. The large mesh size allowed for unobstructed access by salamanders to the interior of each bag. We placed fifteen litter bags into each branch each season. The kick net technique consisted of disturbing approximately 1.0 m^2 of upstream substrate for one minute while catching the disturbed

material in a fine mesh net. We performed 30 kick nets per stream branch, with one upstream and one downstream sample around each litter bag. We also used a D-frame dip net to haphazardly sample the aquatic environment. We performed 10 dips upstream and 10 dips downstream of each litter bag for a total of 300 dips per branch. These three techniques were employed in May/June every year from 2011 to 2016. Within each year, we expended the same capture effort in each branch.

D. 7. Amphibian surveys: Methods

This report focuses on the data collected only during the duration of the subcontract, 2015 and 2016.

Our survey for anurans was based on vocalizations and opportunistic sightings. We installed a Song Meter (Wildlife Acoustics, Cambridge, MA) near the confluence at Big Spring Run and programmed it to record for 30 minutes at sunset each night from mid-March to late July in 2010 to 2016. We then used the program Song Scope (Wildlife Acoustics, Cambridge, MA) to analyze the recordings for specific anuran species. We also documented anuran sightings and vocalizations when we were on site during the day.

D. 8. Amphibian surveys: Results

Eurycea bislineata (northern two-lined salamander) was the most common species captured at Big Spring Run. All of the captured *E. bislineata* were larvae, as identified by presence of external gills. In 2015 and 2016, the total number of captures in the restored branches continued to increase following the restoration (Figure 3.2). Captures in Main Branch increase by 400% in 2015 compared to 2014 (Figure 3.3). Main Branch captures in 2016 were almost equal to their 2015 post-restoration high numbers (see Figure 3.3). The captures of *E. bislineata* in the restored West Branch were lower in 2015 and 2016 from its post-restoration peak in 2014. The first third of the length of East Branch was restored and the number of captures of *E. bislineata* in it has increased from one (1) capture in 2011 to 11 captures in 2016. The captures in the unrestored sections of East Branch have remained fairly constant (~24 captures per season) since increasing dramatically in the year immediately following the restoration. Captures in the control stream of Kennel Run were reduced by over a half since the restoration. As Kennel Run is upstream of the West branch it should be unaffected by the restoration at Big Spring Run.

Pseudotriton ruber (northern red salamander) was detected at Big Spring Run but not at Kennel Run. In 2015, a larval specimen was captured in an unrestored area of East Branch and a second one captured in West Branch. A dead adult was found in East branch in 2016 but no live individuals were detected.

We have conducted analyses of the audio recordings for two common anuran species, the *Lithobates clamitans* (green frog) and *Lithobates catesbeianus* (bullfrog). Neither species has been detected via an analysis of the recordings taken from 2010 to 2016. We did visually confirm an adult *L. clamitans* in May 2013, heard one in May 2014, and saw eggs and then a tadpole in 2015 in the West branch. In May 2016, we did find a second *L. clamitans* tadpole in the same area of West Branch. We did not hear or see any anurans in our pre-restoration work.

D. 9. Amphibian surveys: Discussion

Prior to restoration, the amphibian community at Big Spring Run appeared to be restricted to *E. bislineata* and *P. ruber*. *Eurycea bislineata* was most abundant in the Main and West branches. The frequency of capture of immature individuals suggests local recruitment was occurring. In the first field season following the restoration, *E. bislineata* was still detected at Big Spring Run but its numbers had decreased. Captures in Main and West branches were very low but captures increased in East branch.

Our finding that captures increased in the East Branch after the restoration suggested this branch served as refugia for *E. bislineata*. The immediate impact of the restoration was evidenced by the lack of change in *E. bislineata* captures in Kennel Run. Given the restoration was a major disruption to the system, it was expected that captures of *E. bislineata* would decrease in the restored Main and West branches in the short-term.

In the years following the wetland restoration, *E. bislineata* has consistently increased in the restored stretches while its captures in the unrestored stretches have fluctuated. The Main Branch in particular is revealing itself to be good habitat for this species. The quality of West Branch for this species is more questionable as captures in this branch have decreased in 2015 and 2016 from the post-restoration peak in 2014. Considering that all captures in the restored areas have been of larvae *E. bislineata*, this species is not only present but is reproducing in the restored wetland. This is an excellent sign for the future of this species in the Big Spring Run wetland.

Pseudotriton ruber is persisting at Big Spring Run, albeit at low numbers. This species is more difficult to detect with captures only coming from the litter bag method so it may be more common than our capture numbers indicate. As this species prefers slow-moving water and abundant wetland vegetation (Petranka 1988), we do expect it to increase in number as the wetland community continues to develop.

An exciting development for the herpetological fauna at Big Spring Run is the confirmation of breeding *Lithobates clamitans* in the restored West Branch. This species breeds in

standing water and the shifting channels in the West Branch have allowed for the development of former channels with stream flow only under very wet conditions. Thus, breeding habitat for frogs is created where it did not exist prior to the restoration. While *L. clamitans* is a nationally common frog species, it now residing and breeding at Big Spring Run despite the surrounding agricultural matrix is a positive statement of the success of the Big Spring Run restoration.

E. Deliverable 4: Post restoration sediment sources and fluxes at the BSR restoration site.

Contact persons:

Sediment Fluxes: Dorothy Merritts, Michael Rahnis, Allen Gellis, Michael Myers, Aaron Blair, Kayla Schulte, Evan Lewis

Sediment Sources: Robert Walter, Eric Schwarz, Allen Gellis, Karen Mertzman, Alexandra Sullivan, Douglas Smith, Stacey Sosenko Daniels, Zachary Stein, Eric Ohlson, Danielle Verna, Erin Peck, Amber Carter, Yuning Bai

Tasks: Collect sediment samples and perform laboratory analyses. Compare pre-restoration and post-restoration data and provide analyses of changes over time.

Deliverables: A written report providing analysis of changes in sediment sources and fluxes over time by comparing pre-restoration and post-restoration conditions.

E.1. 1. Sediment Fluxes: Introduction

At least 4 fluxes must be quantified to evaluate the annual contribution of valley bottom change (erosion – deposition) to total suspended sediment load in a sediment budget analysis for the restoration reach at BSR:

1) Total annual suspended sediment load entering the study area (i.e., *Flux In*);

2) Total annual suspended sediment load exiting the area (i.e., *Flux Out*);

3) Annual rate of stream bank, bed, and bar erosion within the study reach; and

4) Annual rate of deposition (storage) within the study reach.

One other source that might provide sediment to a valley bottom is upland hillslopes adjacent to the study area. Common processes that move sediment from uplands to the valley bottom include slope wash, rilling, and gullying. No rills or gullies on vegetated slopes adjacent to the study area were observed in the Big Spring Run study area during the monitoring period[1], but small, short rills occur on some dirt roads. Although rills and

[1] During the period of restoration in the fall of 2011, when the ground was bare, small rills developed on short slopes immediately adjacent to the restored wetland. These were mitigated with planting during the spring of 2012.

gullies can be observed on historic aerial photos of the area prior to the 1970s, since then the use of numerous best management practices for agriculture has reduced upland soil erosion.

E.1. 2. Sediment Fluxes: Flux in and flux out at USGS gage stations

The first two fluxes in the above list—total suspended sediment load entering and exiting the study area--were measured at three USGS stream gage stations located upstream and downstream of the restoration reach (Langland et al, 2017). The locations of each station with respect to the restoration reach are shown in Figure 4.1, and the USGS station identifiers in Figure 4.2. No tributaries enter the reach between these gage stations.

Flux in for each of two tributaries of Big Spring Run was measured at gage stations located 131 feet and 1017 feet, respectively, upstream of the restoration area (white polyline in Figure 4.1). F*lux out* was measured at a gage station 558 ft downstream of the restoration reach. Because the gage stations are not located precisely at the upper and lower ends of the restoration reach, the channels and floodplains between each gage station and the restored area are potential sources or sinks for sediment. In total, the distances between the three gages and the restored area sum to 1706 feet (see Figure 4.2). In contrast, the overall length of the restoration reach along a mid-line down the center of the valley bottom is less than that, only 1509 ft. The length of the restoration reach (not the length of channel within the reach) is less than the total length of all three channels between the restoration reach and the three gage stations. For these reasons, we refer to the valley bottom area bracketed by the three gage stations as the "reach between the gages", and the smaller restoration area as the "restoration reach".

Flux in and Flux out—Pre- and Post-Restoration Annual Loads: In order to estimate the flux of suspended sediment at each of the gages the USGS collected continuous data on turbidity from October 2008 to present, and sampled stream water during base flow and some storm flows for the same time period (Langland et al, 2017). The USGS used two approaches to model annual sediment loads based on turbidity data and samples of stream water. To date the USGS has modeled annual loads for water years 2009 through 2015 (see middle, Figure 4.2).

The three-year period from 2009 to 2011 was the pre-restoration period and the four-year period from 2011 to 2015 was the post-restoration period. The 2011 water year ended on September 30, 2011, about one month after restoration work began. Construction for restoration ended about November, 2011, but the ground was bare until plantings were done in May 2012, so at least the first half of the initial water year after restoration was characterized by bare ground conditions.

Using the GCLAS model, the average annual sediment load contributed from the reach between the gages was 173 tons for three years prior to restoration and 105 tons for four years after restoration. Using sediment transport and regression equations, the average sediment load contributed from the reach between the gages was 159 tons for three years prior to restoration and 112 tons for four years after restoration.

Average annual load data for the eastern and western tributaries are combined in Figure 4.2 to estimate load entering (i.e., *flux in*) the restoration reach. This total incoming load is subtracted from the load out (i.e., *flux out*) at the downstream gage in order to estimate how much sediment must be contributed from (or stored in) the reach between the gages. Using GLCLAS for 2015, for example, the flux out at the downstream gage was 108 tons and the flux in from the eastern and western tributaries was 68 tons. The difference between these two (i.e., Out – In), 40 tons, is the amount of sediment estimated to be derived from the reach between the gages.

Thus far, the pre- to post-restoration reduction in contribution of average annual sediment load from the reach between the gages is 39% and 30%, respectively, for the two USGS approaches to estimating loads. Of note is that the ratio of (flux in) to (flux out) increased all four years since restoration, from 0.43 to 0.63, with greatest increase in 2015 (see middle and bottom panels, Figure 4.2). For the three years that were monitored prior to restoration, this ratio varied from 0.37 to 0.46. When this value is below 1, the reach between the gages is a source of sediment; if greater than 1, the reach between the gages would be a net sink for sediment. With additional years of monitoring and load analysis, it would be possible to test the hypothesis that the restoration area will store an increasing proportion of incoming sediment with time.

E.1. 3. Sediment Fluxes: Fluxes within the reach: Erosion and deposition from repeat RTK-GPS surveys

The third and fourth contributors to the sediment budget, erosion and deposition with the study reach, were determined by repeat topographic surveying over a 1.3- to 4.07-year duration, from 2013 to 2017 (Figures 4.3 and 4.4). Prior to restoration, we did a similar analysis with repeat topographic surveying from 2004-2010 (see Walter et al, 2013). In 2004, twelve cross sections perpendicular to channel flow were installed and surveyed along the study reach with a total geodetic station. These were surveyed with a total geodetic station again in 2006, 2008, and 2009. Three additional cross sections, XS's 13-15, were installed with a laser level by A. Gellis, D. Merritts, and M. Rahnis in 2008. All cross sections were surveyed again with a real-time kinematic (RTK) GPS survey unit in 2010. We estimate the vertical survey error as ± 1.0 cm (0.33 ft) across the length of each

cross section. The propagated uncertainty is ± 1.4 cm (0.047 feet) when estimating the difference between two repeat surveys of a given cross section.

All but one of the 15 cross sections continue to be re-surveyed to monitor post-restoration change (see Figures E16-22 in Walter et al, 2013). Cross sections 8 and 9 were closely spaced and redundant, so we discontinued XS 9 (see black line near XS-8 in Figure 4.3). Since 2010, surveys have been done with RTK GPS. All but XS's 1 and 2, which are in the area that was not restored, were extended after restoration. Coordinate points for all surveys, including end points, are provided at an on-line repository:

https://github.com/mrahnis/orangery

In this report, we focus on surveys of seven of these original cross sections done between 2013 and 2017 (see Figure 4.5). We selected those cross-sections that spanned the wetland area, were nearly perpendicular to the main channel, and had good quality static data at the RTK base station. The duration of time spanned by cross section pairs ranged from 1.31 to 4.07 years and the total length surveyed was 1105 feet.

Along each pair of surveys for a given cross section, we identified polygonal areas of deposition (ground elevation increased) or erosion (ground elevation decreased; see red lines along x-axis in Figure 4.5). Numbers along horizontal axis above red lines indicate polygon numbers. Each polygon is an area of erosion or deposition, with eroded areas shown as hachures and depositional areas shown as shading. We calculated the sum of areas of deposition and erosion for the low-lying core wetland area along each cross-section pair, leaving out the ends of cross sections where located well above the elevation of the wetland on the adjacent hillslopes. For these ends, there was no significant net change.

Proxies for average deposition or erosion rates along a section were obtained by dividing the sum of area for each by the length of the section and by the duration of time between surveys (Figure 4.6). For deposition, these rates ranged from 0.03 to 0.11 ft/yr, with a mean of 0.08 ± 0.03 ft/yr. For erosion, these rates ranged from ~0 to 0.03 ft/yr, with a mean of -0.01 ± 0.01 ft/yr. From up to downstream, cross sections with highest erosion rates are 14 and 8, in the mid-portion of the restoration reach. From up to downstream, cross sections with highest deposition rates are 3, 5, 6, and 8. Of all cross sections, 8 had the highest deposition rate and one of the two highest erosion rates. Cross section 10, the most downstream of all sections, had the lowest deposition rate.

The sums of areas of deposition (positive) and erosion (negative) yield the net changes in vertical (cross-sectional) area for each cross-section survey pair. By dividing the net

change in cross-sectional area by length of section we obtain a net change rate for each cross-section pair. For all 7 cross sections evaluated here, this net change is positive (net deposition), and we refer to it as aggradation. Six shorter cross sections that are not perpendicular to the main channel and not discussed here also experienced net aggradation. The net change rate (aggradation in these cases) ranged from 0.01 to 0.09 ft/yr, with highest values at cross sections 3, 5, 6, and 8, and lowest values at cross sections 14 and 10. Interestingly, cross section 8 had among the highest rates of erosion, deposition, and net change.

Aggradation along a cross section is different than deposition at a point or average deposition for a cross section, in that some parts of cross sections experienced deposition (an increase in ground elevation) and others erosion (a decrease in ground elevation). Adding areas of deposition (+) and erosion (-) to get net change in area and then dividing by length of cross section yields an overall amount of aggradation for the entire section rather than an average rate of deposition for those areas experiencing deposition. Other methods, such as measuring deposition on tile pads (see below), give estimates of true rates of deposition at a point.

E.1. 4. Sediment Fluxes: Fluxes within the reach: Deposition from tile pad measurements

In addition to repeat topographic surveying, tile pads were used to measure deposition at specific points within the restoration reach from 2013 to 2017 (Figure 4.7). Rates of deposition on tile pads can be compared with average deposition and net aggradation rates that are based on repeat surveying along the length of each cross section.

Mike Myers and Allen Gellis of the USGS mounted 130 ceramic tile pads (14.7 cm by 14.7 cm in dimensions) with concrete at the ground surface along 13 of the RTK-GPS surveyed cross sections at Big Spring Run about one year after completion of restoration (December 2012 to January 2013; Figure 4.8). The number of pads on each section ranged from 7 to 18 (spacing about 8 to 18 feet per section). Two of these sections are near the USGS gage station on the eastern tributary, in the unrestored portion of the study area. We do not evaluate them here, but focus instead on pads within the restored reach. Cross section 15, a short section oriented roughly parallel to rather than perpendicular to the valley, is located between sections 6 and 14 and shares one pad with section 14. Of the other 7 pads installed on this section, two were buried by large leaf and debris packs in 2014 and two others were missing in 2016. Thick organic debris packs were common in this area for several years after restoration. For these reasons, in particular that section 15 had few tiles and is located near two other long sections, we do not evaluate he data from its

remaining pads. In sum, we evaluate 108 tile pads within the wetland area on the remaining 10 sections.

All pads on these 10 sections were measured first on May 8, 2014, about 1.3 to 1.4 years after installation. Pads along 9 sections were measured again in April of 2016 and June of 2017, giving a range in duration of monitoring periods of 3.25 to 4.50 years for nine of the 10 sections (see Figure 4.8). Pad deposition, not including overlying vegetation, was measured with a thin metal ruler inserted vertically at three locations on the pad. The average of these three measurements was recorded.

For each pad, amount of deposition and duration of time between the date of installation and most recent measurement are then used to get a deposition rate (Figures 4.9 and 4.10). The majority of deposition rates were less than 0.04 ft/yr. Using the average rate of deposition for two adjacent pads, we weight the values by the spacing between the pads relative to the total length of the cross section. These estimates of weighted average deposition rate range from 0.01 to 0.08 ft/yr. From up to downstream, cross sections with highest average pad deposition rates are 4, 6, and 10. Note that cross section 6, near the mid portion of the restoration reach, also is located immediately upstream of a dirt road crossing which acts as a low, grade control that pools water during higher flow events (see Figure 4.9). The other seven cross sections have similar estimates of pad deposition rates, with most 0.2 to 0.3 ft/yr. The only exception is cross section 5, with an average pad deposition rate of 0.01, the lowest of all cross sections.

Seven of these ten cross sections also were surveyed with RTK GPS to get long-term rates of erosion, deposition, and net change that can be compared with deposition rates for the tile pads (see last column, Figure 4.8). For three sections, the average rates of deposition from surveying are similar to those from tile pads (sections 4, 14, 6, and 10). For the remaining sections evaluated with both approaches, the deposition rates estimated from repeat RTK-GPS surveying are about 4 to 7 times greater than those from tile pads. Accordingly, the average rate of deposition estimated from tile pads for all cross sections (0.03 ± 0.02) is about half that estimated from repeat RTK-GPS surveying (0.06 ± 0.03).

E. 5. Sediment Fluxes: Annual sediment load estimates for the restored reach

With the four fluxes listed above quantified, we can evaluate the annual contribution of valley bottom change (erosion minus deposition) to total suspended sediment load. The USGS flux in and flux out estimates are in units of mass per unit time (tons/year) of suspended sediment; repeat surveys along cross sections yield annual net change in area (ft^2/yr) or ground surface elevation (ft/yr); and tile pads yield annual rates of deposition in ft/yr. Data from cross sections and tile pads can be converted to units of volume by

extrapolating the average rates of change from the pads and section lines to the entire area from which sediment might be derived at those rates. The low area within the elevation range of overbank flooding in the restored wetland floodplain encompasses about 202,600 ft^2 ($\pm$ 5000 ft^2).

Volume estimates can be converted to mass if the dry bulk density and percent organic matter of the soil and sediment are known. We use the dry bulk density (mass/volume) of sediment deposited on tile pads in the restoration area since restoration (Figure 4.11). The average bulk density for 9 samples of sediment from tile pads along cross section 14 and for 11 samples from tile pads along section 5 yield a mean bulk density of 0.99 $\pm$ 0.49 g/cm^3 (n=20). From triplicate loss on ignition analyses for these same soil samples after removal of pieces of vegetation (e.g., roots, twigs, leaves, etc.) the organic matter content is 8.26 $\pm$ 1.78%. As a result, we use a bulk density of 0.91 g/cm^3 (56.81 lbs/ft^3) in order to convert volume of soil to mass of sediment.[2]

Multiplying area by rate of aggradation (net change) from repeat RTK GPS surveying and bulk density, we estimate 351 $\pm$ 104 tons/yr (247 to 455 tons/yr) of deposition within the restored area (see Figure 4.1). Using average rates of tile pad deposition (0.03 $\pm$ 0.02 ft/yr) instead, we estimate 173 $\pm$ 115 tons/yr (~58 to 289 tons/yr) of deposition within the restored area (see Figure 4.1).

E.1. 6. Sediment Fluxes: Annual sediment load estimates for the unrestored reaches between gage stations

As noted above, the three USGS gage stations are not located precisely at the upper and lower ends of the restoration reach, so the channels and floodplains between each gage station and the restored area are potential sources or sinks for sediment. In total, the distances between the three gages and the restored area sum to 1706 feet (see Figure 4.1). These unrestored channels have bare, high, vertical banks (>3 to 4 ft) that consist of historic (legacy) sediment that consist of ~85% fine particles (clay, silt, and fine to medium sand) for which the bulk density is 1.4 g/cm^3 (87.40 lbs/ft^3). They also carry bedload during high flow events and build bars of sand and gravel (10% fine sediment) at meander bends for which the bulk density is 1.6 g/cm^3 (99.88 lbs/ft^3). (See Walter et al,

[2] Now that we have monitored the tile pads for >3 years, we are removing the entire sediment sample on each pad in order to analyze it for bulk density, organic matter content, grain size, and other attributes. Once all grain size analyses are done, we will adjust load estimates to account for the portion of deposition that is fine (clay, silt, and fine to medium sand) sediment versus bed load (i.e., coarse sand and gravel). Cross section 3, for example, has experienced some sand and gravel deposition coming from the unrestored part of the western tributary since restoration.

2013, PA DEP report for data on eroding banks and bars along channels with legacy sediment at Big Spring Run prior to restoration).

We use lidar dem-differencing for airborne lidar data acquired in 2008 and 2014 to estimate how much sediment has been eroded from banks and deposited in bars during the 6.6 years between the lidar surveys (Figures 4.12 and 4.13). In addition, by taking amount of erosion minus amount of deposition of fine sediment for each reach, we estimate how much sediment might leave or remain in these unrestored channel areas. All three reaches are net degradational with respect to fine sediment that can become suspended sediment load downstream (i.e., more fine sediment is eroded from banks than deposited in bars).

We estimate that the net amount of fine sediment eroded from the three reaches is 38.9 ± 15.7 tons/yr (23.2 to 54.6 tons/yr). It is possible that some sediment is deposited atop the high legacy sediment surfaces, but that amount would be hard to detect with lidar dem differencing if it is less than a foot or so of height difference.

E.1. 7. Sediment Fluxes: Annual sediment budget

For the post-restoration period, a sediment budget is constructed for the reach between the gage stations using erosion and deposition measurements in order to estimate a mass and then compare this mass to the difference in suspended sediment load between the up and downstream gage stations, as follows:

$I + \Delta S = O$

I = 1) input of sediment from upstream gages on the two tributaries at Big Spring Run, and 2) input of sediment from channel banks, channel bed, and bars (tons/yr) between the gages and the restoration reach; ΔS is change in sediment storage in channel banks, channel bed, and bars and floodplains in the restoration reach (tons/yr); and O = annual suspended sediment load export at the downstream gage on the main stem at Big Spring Run.

The average annual suspended sediment input from the upstream gages for water years 2012-2015 is 98 tons/yr (70 tons/yr + 28 tons/yr; see USGS report by Langland et al, 2017). Our lidar dem differencing estimate of input of sediment from bank, bed, and bar erosion between the gages and restoration reach is 38.9 ± 15.7 tons/yr. Our estimate of net change within the restoration reach (erosion + deposition) is 351 ± 104 tons/yr. The average annual suspended sediment output from the downstream gage for water years 2012-2015 is 203 tons/yr. We will compare our estimate of output to the USGS average of 203 tons/yr.

The final sediment budget using the equation above and data from repeat RTK GPS surveying of transects for change in storage within the restoration reach is:

(98 tons/yr + 38.9 ± 15.7 tons/yr) (I) - 351 ± 104 tons/yr (ΔS) = -214 ± 120 tons/yr (O)

Using just the left side of the equation to quantify inputs and change in storage, we would predict no annual sediment export at the downstream gage. In fact, we estimate more storage within the restoration reach than enters the reach from upstream tributaries.

The tile pad deposition data indicate that about half as much deposition is occurring as estimated by repeat RTK GPS surveying of transects. A possible cause of this difference is that surveying measures the ground surface, including vegetation (both living and detritus), whereas tile pad deposition measurements are made from the pad to top of soil, not including the vegetation cover. Using the tile pad data, we estimate the following sediment budget:

(98 tons/yr + 38.9 ± 15.7 tons/yr) (I) - 173 ± 115 tons/yr (ΔS) = -36 ± 131 tons/yr (O)

With the tile pad data, we would predict an annual suspended sediment load at the downstream gage that might range from zero (i.e., -167 tons/yr) to 95 tons/yr. The maximum of these estimates is still much less than the average of 203 tons/yr estimated by the USGS. In other words, if we assume that annual loads for all three USGS gage stations and our estimates of change from reaches between the gages and restoration area (from lidar dem differencing) are accurate, then our estimates of deposition within the reach are too high using both repeat RTK GPS surveying and tile pad deposition data. However, the tile pad deposition data yield a much smaller mismatch that at least would support 95 ton/yr of sediment at the downstream gage. A possible explanation is that the contribution of the restored area to downstream sediment loads is diminishing with time, as discussed next.

E.1. 8. Sediment Fluxes: Discussion of mismatch between sediment budget and downstream gage loads

A fundamental mismatch occurs in that USGS estimates of annual loads indicate that net erosion must be occurring between the up and downstream gages (see Figure 4.2), and yet the restoration reach is largely net depositional based on both repeat RTK GPS surveying along 7 transects that total 1105 feet and monitoring of 130 tile pads.

There are several possible explanations for the mismatch:

1) Estimates of annual loads at one or more of the three USGS gage stations are inaccurate.

2) Our estimate of change in storage within the restoration reach is inaccurate.

3) Another source of sediment is unaccounted for in this analysis.

4) The time period of monitoring is insufficient to resolve a sediment budget with confidence; in particular, loads might be changing as a result of wetland development, vegetation growth, and channel adjustments since restoration.

We focus first on the last of these. For water years 2012 to 2015, the USGS GCLAS estimates of erosion (output minus input from the three gages) from the entire reach between the three gage stations are 101, 146, 138, and 40 tons/yr (average = 112 tons/yr). Note that these estimates of erosion have decreased every year since water year 2012 (October 2011 to September 2012), which overlapped construction during restoration from September to November 2011 and initial planting on bare ground in May 2012. The corresponding proportions of sediment loads from the reach between the three gages stations relative to outgoing amounts are 57, 55, 52, and 37 percent from water years 2012 to 2015.

If we were to use only water year 2015 (October 1, 2014 to September 30, 2015) and tile pad data for a sediment budget, there would be little to no mismatch between our quantification of sediment fluxes and the USGS load estimates, as follows:

$$(68 \text{ tons/yr} + 38.9 \pm 15.7 \text{ tons/yr})\ (I) - 173 \pm 115 \text{ tons/yr}\ (\Delta S) = -27 \pm 131 \text{ tons/yr}\ (O)$$

The estimated output, -27 ± 131 tons/yr, would range from -158 to +104 tons/yr. We reject values <0 because suspended sediment is passing the downstream gage station. The high end of this result (104 tons) compares well with the USGS estimated load output of 108 tons at the downstream gage station in 2015. Achieving the high end requires the

highest amount of erosion (± 1 S. D.) from unrestored channel reaches between the gages and the lowest amount of deposition (± 1 S. D.) within the restored reach.

There is merit to considering only the most recent water year analyzed, 2015, for a sediment budget analysis. For five cross sections the most recent surveys were done in 2015. For two others, XS-3 and XS-4, measurements spanned a longer time period, with most recent surveys in 2017. Measurement of deposition on tile pads spanned the period December 2012-January 2013 to May-June 2017, similar to measurements on cross sections 3 and 4. It is possible that deposition rates were higher during the first few years after restoration, as plantings became established and denser with time. Estimates of erosion and deposition from lidar dem differencing span the longest time period, from April 2008 to December 2014 (6.7 yrs), but are only useful for estimating change for the unrestored reaches.[3]

As for the first possible source of mismatch regarding USGS load estimates, it is possible that the interpolation of data during times of missing data might lead to under or over estimates of loads at one or more of the gage stations (see Langland et al, 2017). As for the second possible cause of mismatch regarding our estimates of changes in storage within the restored reach, all monitoring, field work, and analyses indicate measurable deposition throughout much of the wetland-floodplain area. Evidence of net deposition is strong.

On the other hand, the amount of deposition is generally low (see Figure 4.10) and spatially variable in thickness (see Figure 4.9), so that extrapolating an average value across the entire area of 202,600 square feet (4.7 acres) results in relatively large uncertainties. In general, deposition is thinnest along valley margins and thickest adjacent to channels (see Figure 4.5). In addition, our estimates of average floodplain deposition rates at Big Spring Run are similar to those measured with clay pads for floodplains throughout the Piedmont and Coastal Plain in the mid-Atlantic region (Figures 4.14 and 4.15).

The third possible source of mismatch is another source of fine sediment supplied from areas adjacent to the area between the gages. No obvious sources exist, and deposition pads on the toe of slope adjacent to the restored area have little to insignificant erosion or deposition. Adjacent hillslopes are generally low in gradient and vegetated. Nevertheless, we cannot discount the possibility of some sediment from unknown hillslope sources.

[3] In a separate analysis, we are evaluating net change within the restoration reach from 5 different acquisitions of ground based lidar done by UNAVCO between 2013 and 2016, including two done during "leaf-off" conditions in April 2014 and April 2016.

E.1. 9. Sediment Fluxes: Comparison of pre- and post-restoration erosion and deposition

A key finding from our repeat topographic surveying and grain size analysis from 2004 to 2011, prior to restoration, was that ~91 tons/year was eroded from high stream banks that consisted of nearly 100% fine sediment within the reach between the gages (see Walter et al, 2013, report to PA DEP). This result was consistent with USGS gage data, which showed that that 94 tons of fine suspended sediment was contributed from the reach between the three gage stations for 3 years prior to restoration (average annual value for water years 2009, 2010, and 2011). In contrast, a key finding of this report is that net deposition of 173 ± 115 tons/yr is occurring within the restoration reach. In addition, the unrestored portions of channels between the three gages and the restoration reach continue to contribute substantial amounts of sediment via bank erosion.

E.2. Sediment Fluxes and Sources from ^{137}Cs Gamma Spectroscopy

E.2 1. Synopsis

Within Pennsylvania's Chesapeake Bay watershed, Lancaster County stands out as a hotspot for high sediment and nutrient yields. Other high-yield regions also are situated within Pennsylvania's Lower Susquehanna River region, including York, Adams, Cumberland, Dauphin and Lebanon Counties. Combined, this south-central PA region accounts for 40 to 45% of the nutrient and sediment loads delivered to the Bay, despite comprising only 20% of Pennsylvania's Chesapeake Bay watershed. Why low-relief Piedmont terrains should yield such high sediment and nutrient loads is an apparent paradox, which to unravel requires a thorough understanding of possible sources of sediments and nutrients, the processes causing their erosion, and their delivery mechanisms to downstream waterways. Current models for the Lower Susquehanna Watershed suggest that agricultural sources account for nearly 90% of the needed sediment load reductions, despite little experimental evidence to validate these claims.

Here we use a ^{137}Cs inventory to document the relative contributions of sediment from two main landscape sources at Big Spring Run, a small agricultural watershed in southcentral Lancaster County. These two sources are cultivated, upland agricultural slopes and valley bottom stream banks. Big Spring Run was the site of a new restoration experiment, summarized in a 2013 report to PA DEP (Walter et al. 2013), designed to establish a new Best Management Practice for stream restoration.

An inventory of fallout ^{137}Cs activity from two hill slope transects adjacent to Big Spring Run yield average erosion rates of 1.2 t ac^{-1} yr^{-1} and 2.3 t ac^{-1} yr^{-1}. These rates reflect the average

rates between the the early 1960s (the peak of ^{137}Cs production) and 2006 (when these samples were collected), and thus reflect the periods of high rill and sheet erosion before the implementation of conservation farming practices. As of 1982, the state-wide average for cultivated land was 5.3 t ac^{-1} yr^{-1} (United States. Department of Agriculture 1990). The measured ^{137}Cs erosion rates reported here agree with a previous study of the Big Spring Run watershed using the revised universal soil loss equation, GIS interpretation of land use changes from aerial photographs between 1940 and 2005 and land owner interviews. This study indicates a dramatic reduction in soil erosion rates from ca. 25 t ac^{-1} yr^{-1} in 1940 to ca. 5 t ac^{-1} yr^{-1} by 1988, which also agrees with the USDA assessment at that time.

How much of eroded upland soil enters the stream? The average contribution of sediment supplied to Big Spring Run from various sources can be deduced using mass balance calculations of ^{137}Cs data. Our results show that 85-100% of the sediment supplied to this watershed can be accounted for by stream bank sources, with little if any from cultivated upland slopes.

E.2. 2. Introduction

In our 2013 report to PA DEP entitled "Big Spring Run Natural Floodplain, Stream and Riparian Wetland-Aquatic Resource Restoration Monitoring Project" (Walter et al. 2013), we documented pre-restoration sediment sources using trace element fingerprinting techniques. The three key results of that study are:

(1) We conducted a methodological test of our trace element sediment fingerprint procedures through a blind study of samples from the Mill Stream Branch (MSB) in the Maryland Coastal Plain that had been examined previously and independently by an analytical laboratory at the USGS. Our investigation on the same samples that were analyzed by the USGS yielded identical results to those presented in Banks et al 2005 and Massoudieh et al 2012. These results indicate that stream banks contributed ca. 100% of the suspended sediment load to MSB, even though the USGS and F&M labs used different sample preparation methods and analytical methods. This methods test adds a high level of confidence and quality assurance to the trace element fingerprinting methods employed by our group at BSR.

(2) Applying the same analytical procedure and mixing model calculations that we used to demonstrate the similarity between USGS and F&M results for the Mill Stream Branch sediment fingerprint study, we find that 60-70% (average of 63%) of the suspended sediment load sampled at the downstream gage at BSR (located just below the restoration

reach), was derived from stream bank erosion. Conducting the same mixing model calculations for the fluvial sediments collected at the East Branch (Sweeney) and West Branch (Fry) gages at BSR, we estimate that stream banks contributed up to 33% of the East Branch (Sweeney) gage sediments and up to 54% of the West Branch (Fry) gage sediments.

(3) We observe a overall 63% stream bank contribution (i.e., from bank erosion) at the downstream Main Stem (Keener) gage, which indicates from mass balance calculations that bank erosion between the upstream (East and West Branch gages) and the downstream Main Stem gage at BSR must be ca. 80- 90%.

In the present study, we applied ^{137}Cs gamma spectroscopy to complement the trace element fingerprinting study of Walter et al (2013), and to elucidate and quantify sediment fluxes and sources within the Big Spring Run restoration study area.

The unusual circumstance surrounding the production of radioactive ^{137}Cs makes it ideal as an environmental tracer for studying erosion and sedimentation (Ritchie and McHenry 1990). With no natural sources of ^{137}Cs, this isotope is formed only as one of the more common products of nuclear fission – especially of ^{235}U – in nuclear reactors and nuclear weapons. Its presence in the environment today is due solely to above-ground testing of thermonuclear bombs during 1950s-70s and to the catastrophic release from critical breaches of nuclear reactors, such as from Chernobyl (Ukraine) in 1986 and Fukushima (Japan) in 2011 (Wise 1980; Walling, Bradley, and Wilkinson 1986; Imanaka, Hayashi, and Endo 2015). Cesium-137 was first released on a local scale in 1945, coincident with the first, small-magnitude nuclear bomb tests (Carter and Moghissi 1977). Global environmental dispersal of ^{137}Cs began with high-yield thermonuclear tests in 1952 (Perkins and Thomas, 1980). In these tests, ^{137}Cs and other radionuclides were injected into the stratosphere (Longmore 1982), circulated globally and returning to the earth's surface as radioactive fallout. Deposition of ^{137}Cs is strongly influenced by local precipitation patterns and rates (Davis 1963; Longmore 1982), such that regions with higher precipition have higher ^{137}Cs concentrations in surface soils (Matisoff and Whiting 2012).

Cesium-137 has a half-life of 30.17 +/ 0.16 years (NIST). About 94.6 percent decays by beta emission to a metastable nuclear isomer of barium: barium-137m (Ba-137m). The remainder directly populates the ground state of barium-137, which is stable. Ba-137m has a half-life of about 153 seconds, and is responsible for all of the emissions of gamma rays in samples of ^{137}Cs. About 85.1% of metastable barium then decays to ground state by emission of gamma rays having energy 0.6617 MeV, and the main photon peak for gamma spectroscopy of Ba-137m is 662 keV (Unterweger 2002; Unterweger and Fitzgerald 2014).

Because ^{137}Cs is strongly adsorbed to cation exchange sites (Davis 1963; Eyman and Kevern 1975; Ioannides et al. 1996), it's movement is closely aligned with the movement of fine soil particles (clays and silts), and not by chemical or biological processes (Tamura 1964; Sawhiney 1972; Campbell 1983). Physical processes of erosion and tillage are the major pathways for redistribution of ^{137}Cs in soils and for the movement of ^{137}Cs from soils to water (Ritchie and McHenry 1990). Because ^{137}Cs is uniformly distributed across the landscape along precipitation contours, and it is strongly adsorbed on soil particles, it can be used as a tracer for studying the physical processes of erosion and sedimentation. Spatial measurements of ^{137}Cs provide quantitative information on rates and patterns of erosion and sedimentation (Matisoff, Bonniwell, and Whiting 2002a, 2002b).

E.2. 3. Background

In drainage basins with large areas in cultivation, the surfaces of agricultural fields often appear to be the greatest source of sediment to suspended loads of adjacent streams (Nagle and Ritchie 2004). Most erosion research in agricultural areas, such as in the Chesapeake Bay Watershed, has focused on either small plot-based erosion studies and on mathematical models that quantify erosion rates under different cropping practices in large areas (Boomer, Weller, and Jordan 2008; Shenk and Linker 2013), but both are based on plot-scale soil loss equations. Extrapolating plot-scale rates to larger landscapes to predict sediment delivery to streams and stream sediment loads creates substantial problems and can be misleading (Dunne and Dietrich 1982; Walling 1994; Boomer, Weller, and Jordan 2008). Paradoxically, in-stream sediment yields remain high despite successful soil-conservation measures that substantially reduced soil loss from agricultural fields (Trimble 1999; Trimble and Crosson 2000; Pionke, Gburek, and Sharpley 2000). As a result, many soil conservation and sediment management programs in rural agricultural areas still focus on reducing erosion and runoff from cultivated fields (Brakebill, Ator, and Schwarz 2010). It is often assumed that the dominant source of suspended sediment to streams is from agricultural fields (Lowrance et al. 1997; Boesch, Brinsfield, and Magnien 2001; Mellerowicz et al. 1994).

A likely reason for this paradox is that even in areas where cultivation has been practiced for over two centuries, such as in the mid-Atlantic region, with historically high surface erosion from croplands, much of the eroded soil was deposited and stored as colluvium on lower foot slopes and on valley bottom terraces as slack water deposits behind bridges and dams (legacy sediment) where it can remain for centuries before washing into streams (Happ 1945; Knox 1972; Costa 1975; Walter and Merritts 2008). In drainage networks with a large capacity to store sediment, much of the fine suspended sediment in streams is derived from eroding stream banks in riparian areas (Knox 1972; Olley and Prosser 1999; Walter and Merritts 2008).

The objective of this study is to determine the sources of suspended sediment in the Big Spring Run (BSR) watershed of Lancaster County, Pennsylvania, through the use of the ^{137}Cs isotopic tracer. The BSR watershed has been severely altered by agriculture since European settlement, as it was the first watershed settled in Lancaster County in 1710, and it is listed on the EPA 303d list for impaired water bodies due to the "agricultural" pollutants of sediment, phosphorus and nitrogen.

The critical question is how much of the sediment load in BSR during storms is from recently eroded cropland (with relatively high ^{137}Cs s concentrations) and how much is from pre-20th century colluvial sediment remobilized via bank erosion (with low or non-existent ^{137}Cs concentrations) (Merritts et al. 2011, 2013). Also, there are serious questions on the reliability of surface-erosion estimates for the watershed used to model sediment yields (Boomer, Weller, and Jordan 2008). It is widely held that ^{137}Cs and other radio-isotopic tracers have a crucial role to play in overcoming the challenges in model calculations by unequivocally identifying and quantifying sediment sources (Ritchie and McHenry 1990; Walling 1994; Matisoff, Bonniwell, and Whiting 2002a).

Given the uncertainty in modeled surface erosion rates, it is important to have a more reliable measure for net erosion from cropland. By measuring the spatial distribution of ^{137}Cs across landscapes, rates of soil loss and deposition for a field can be quantified (Ritchie and McHenry 1977; Walling and Bradley 1988). Because the method accounts for the redistribution and deposition of soil, the ^{137}Cs technique measures net soil loss at each site, providing a more accurate quantification of erosion and sediment delivery rates than do short-term erosion plot studies that occupy only a small area. The ^{137}Cs method makes possible a detailed analysis of sediment movement on hillsides with different topographic characteristics and patterns of land use (Walling and Quine 1990; Quine and Walling 1993).

E.2. 4. Methods

Analytical Procedures

Cesium-137 analysis is an effective tool for quantifying erosion and determining sediment sources, but is not as widely used as it could or should be because gamma ray detectors are expensive, sampling is laborious, and analyses are long (8-72 hours or greater, depending on sample size and ^{137}Cs activity). Through a National Science Foundation Major Research Instrumentation Grant (NSF-MRI 0923224) our laboratory at Franklin and Marshall College purchased two high-efficiency, Canberra Broad Energy Germanium solid state, lead-shielded gamma ray detectors along with two high-precision multi-channel analyzers and software for analyses and calibration (Apex Gamma and LabSocs). A major part of Deliverable 4 for this grant period was to calibrate these gamma spectrometers, made possible through the purchase of an

Eckert and Ziegler mixed gamma ray source (1 g-cm epoxy matrix in a 1 L Marinelli beaker). This mixed gamma source was internally calibrated by Eckert and Ziegler against National Institute of Standards (NIST) calibration standards (Table E.2.1). Eckert and Ziegler participates in a NIST measurement assurance program to establish and maintain implicit traceability for a number of nuclides, based on the blind assay (and later NIST certification) of Standard Reference Materials (as in NRC Regulatory Guide 4.15). Nuclear data were taken from IAEA-TECDOC-619, 1991, and the overall uncertainty in Eckert and Ziegler's Certificate of Analysis for our mixed gamma standard is calculated at the 99% confidence level as follows:

Once our gamma spectrometers were calibrated, we checked the calibration against a natural sediment standard (NIST-Standard Reference Material 4350B), also purchased through this grant. Our analyses of NIST-SRM 4350B yielded a ^{137}Cs activity of 2.75E-02 Bq g^{-1} for one detector and 2.90e-2 Bq $g^{-1}$for the other detector, which compares favorably with the Certificate of Analyses (COA) for this material of 2.90e-2 Bq g^{-1} (Table E.2.2). Compared to the NIST standard (SRM 4350B), the difference between analyses on our two detectors is 5.2% and 0%, respectively, which are within the analytical error of the measurement (6.3% for both the NIST-SRM and the F&M analyses).

The basis of the ^{137}Cs technique is illustrated in Figure E.2.1. This illustration shows that ^{137}Cs was produced as a by-product of the atmospheric testing of thermonuclear weapons from the 1950s to the 1970s, it was distributed globally in the stratosphere and deposited with precipitation. The regional distribution of ^{137}Cs shows variation is related to annual rainfall, but at the field level deposition appears to have been relatively uniform.

Figure E.2.2 provides a schematic representation of the possible impact of various agricultural activities upon the distribution of ^{137}Cs within the soil. The sharp decline in ^{137}Cs concentration below the soil surface at the grassland site indicates the strong binding of the radionuclide by the fine fraction. In the 62 years since the initial deposition of ^{137}Cs, some downward movement may be expected. The presence of some ^{137}Cs at depth reflects the long period of time over which deposition has occurred, bioturbation, illuviation and/or cultivation.

The relatively level site (Figure E.2.2) has almost the same ^{137}Cs inventory (i.e., the sum of ^{137}Cs concentrations per unit area for a single profile) as the pasture and orchard locations, indicating minimal loss of soil, although the upper half of the profile was likely modified by bioturbation or previous cultivation (Walling and Quine 1990). In contrast, the inventory of the eroded cultivated site has been reduced by almost 40 per cent. At the depositional site, a 40% enrichment is observed. Surface accretion led to the burial of a layer of soil that was previously at the surface and within the plough zone, producing a 'stretched' ^{137}Cs profile. The elevated inventory is significant, reflecting an additional input of ^{137}Cs -bearing soil to a preexisting profile, and demonstrating that this erosion and deposition must be post-1963, considered to

be the peak period of ^{137}Cs deposition. A distinction can be made between eroded, uneroded and depositional sites by inspection of their ^{137}Cs profiles, and also by comparison of the total ^{137}Cs inventories (per unit surface area) at a sample site to the ^{137}Cs inventory at a reference site. This reference inventory is obtained by sampling an area of level, undisturbed grassland in the vicinity of the study site.

A useful attribute of gamma spectroscopy is the simultaneous solution of multiple energy lines from multiple gamma emitting isotopes. For example, ^{210}Pb and ^{226}Ra are naturally occurring radionuclides of the ^{238}U radioactive decay chain, with half-lives (t1/2) of 22.23 and 1,600 years, respectively. In most environmental systems that have remained "closed" for more than about 120 years (five times the half-life of ^{210}Pb), ^{210}Pb is derived from its ^{226}Ra parent radionuclide. Lead-210 and ^{226}Ra are measured simultaneously (along with ^{137}Cs) by gamma-spectroscopy. For ^{210}Pb, the 46.5 keV decay energy of ^{210}Pb is used with high relative efficiency (Zaborska et al. 2007). Ra-226 activity is determined by quantifying intermediate daughter radionuclides ^{214}Pb (at 295 and 352 keV) and ^{214}Bi (at 609 keV) after establishing their radioactive equilibrium with ^{222}Rn (Kirchner and Ehlers 1998; Swarzenski et al. 2006). Determination of ^{226}Ra allows the activities of supported ^{210}Pb to be estimated. These isotopes can provide additional evidence for determining sediment sources.

Sampling Procedures and Preparations

Soil and sediment samples were collected in one of four ways: (1) vertical coring into a soil profile to depth of >40 cm using at 5 cm ID, 1.5 m long PVC tube, beveled at the end to facilitate penetration into the soil. The PVC pipe was driven into the soil using a fence post-driver (Figure E.2.3). Measurements were taken of the depth of the hole and of the thickness of the core to correct for compaction. The core was extruded and soil samples collected in desired increments (generally between 2.0 to 5.0 cm); (2) 1 m^3 soil pits were dug and the upslope side wall was excavated using a metal mason's trowel in the desired increments (generally 5 cm); (3) scraping of the upper 5 cm of a surface soil or an active point bar deposit in the stream channel; or (4) by sampling of a vertical stream bank section by the "channel" method in 5 cm increments (Walter and Merritts 2008).

All field samples were prepared and analyzed according to the procedures outlined in Figure E.2.4. Gamma spectrometric analysis of each sample yields the total activity of the sample (Bq), and the total activity per unit mass (Bq $g^{-}1$). For core and soil pit profiles, samples of the total activity can be converted into an inventory per unit area (Bq cm^{-2}) by dividing by the internal cross-sectional area of the coring tube or the area excavated. The configuration of the F&M gamma spectroscopy laboratory is shown in Figures E.2.5.

Mixing Models and Statistical Methods

To determine net soil loss or gain at each sample point, calculations were made with a mass balance model of Zhang et al. (Zhang, Quine, and Walling 1998).

$$Re = Hv\left\{1 - \left[\frac{X}{Y}\right]^{\frac{1}{N-1963}}\right\} \qquad (1)$$

where:

Re = total soil erosion rate (kgm^{-2} yr-1)

Y = reference 137 Cs inventory from control sites (in Bq m^{-2})

X = 137 Cs inventory (Bq m^{-2}) at sampling point

H = depth of the plow layer (m)

V = specific density of the plow layer (kgm^{-3})

N = year of sampling

Calculations were made for composited samples with ^{137} Cs inventories that differed more than 10 percent from the reference value (term Y in Equation 4) to determine the volumes of erosion and deposition (Loughran and Campbell 1995). This approach accounts for potential natural variability in the deposition of the radionuclide that might confound erosion estimates (Nagle and Ritchie 2004).

To quantify the relative contribution of bank and surface sediment sources the mean values of the sediment tracer properties (i.e., ^{137}Cs) were incorporated into a simple mixing model. Multiple traces could be analyzed in this way (Peart and Walling 1986; Wallbrink et al. 1996):

$$C_s = \frac{Pr - Pb}{Ps - Pb} \times 100 \qquad (2)$$

where:

C_s = contribution from cultivated surface sources (%)

P_r = mean value of property for bottom sediment

P_s = mean value of property for cultivated soil

P_b = mean value of property for bank material

To quantify the potential error in the estimates made with Equation 1 the following calculations were based on this formula presented in (Taylor 1997):

$$\sigma_m = \sigma_s / \sqrt{n} \qquad (3)$$

where:

σ_m = standard error of the mean

n = number of samples

σ_s = standard deviation of the variable

Using this equation, we obtain the relationship between sample variability and the estimates for the contribution of surface sources (the Cs term in Equation 2) (Nagle and Ritchie 2004). This gives the coefficient of variation (CV) of the Cs term which is:

$$CV \text{ of } C_s = \left[\sqrt{\frac{\sigma^2_{m_{Pr}} + \sigma^2_{m_{Pb}}}{Pr - Pb}} + \sqrt{\frac{\sigma^2_{m_{Ps}} + \sigma^2_{m_{Pb}}}{Ps - Pb}} \right]^{0.5} \qquad (4)$$

Sediment Budget Procedures

A method of applying ^{137}Cs measurements to sediment budget studies is shown in Figure E.2.4 (Walling, Bradley, and Wilkinson 1986). To identify sediment sources within the basin, levels of ^{137}Cs can be used to rank soil erosion status. Where the ^{137}Cs levels can be calibrated against measurements of net soil loss, sediment sources may be quantified. At sedimentation sites, ^{137}Cs can provide direct information on rates of accumulation since 1954 and other useful temporal variations linked to the fallout pattern (Campbell, Loughran, and Elliott 1988).

E.2. 5. Results and Discussion

Erosion Rates

Table E.2.3 provides new ^{137}Cs data on upland, stream bank and suspended sediment samples collected from the pre-restoration period (between 2006 and 2011), and from tile pad samples from the restored floodplain (collected in 2015, four years after restoration). All samples were analyzed in the F&M gamma laboratory (Figure E.2.5).

Table E.2.4 summarizes the ^{137}Cs results of two hillslope transects collected in 2006 (Sullivan 2006) and analyzed by Dr. Jerry Ritchie at the NRCS gamma laboratory in Washington, D.C. Complete analytical results for these transects are provided in Appendix 1. Cesium-137 inventories from the two hillslope transects (Figure E.2.6 and 7) were compared to the ^{137}Cs inventory of the reference section. Using Equation 1, amounts of erosion and deposition at each sampling point was quantified (Figure E.2.8), and a total erosion rate was determined for each transect.

Both data sets (Tables E.2.4 and 4) show elevated ^{137}Cs concentrations in the upper ~20 cm of upland soils, ranging from 1.65 e-2 Bq g^{-1} (sample T2B1, Appendix 1) to 2.99e-3 Bq g^{-1} (sample Up3, Table E.2.3). Depth profiles (Figures E.2.6a and 7a), show an enrichment in ^{137}Cs in the upper ca. 25 cm, and a decline to zero below 20-35 cm. In some cases, such as in sample T1D, ^{137}Cs increases slightly below the surface before declining to zero at depth (Table E.2.3). The most common pattern is the one typical of a cultivated field (Figure E.2.2) (Walling and Quine 1990), indicating a mixing and homogenizing of soil within the plow zone. Eroded sites show shallow, truncated ^{137}Cs distributions, ending abruptly at the base of the ca. 20-cm-thick plow zone. Transects showing erosion (T1A-T1D and T2A, T2B and T2E, Figures E.2.6a and 7a) are depleted in ^{137}Cs compared to the reference site. Where deposition occurred, profiles are characterized by a lengthening of the ^{137}Cs profile, due to the burial of a previous plow zone with additional ^{137}Cs-bearing sediment derived from upslope erosion. This creates an enrichment in ^{137}Cs compared to the reference section (T1E, T1F, T2C, T2D and T2F, Figures E.2.6a and 7a).

None of these transect sections display the classic profile for undisturbed deposition (e.g., high ^{137}Cs at the surface rising to a peak at shallow depth, ca 5-10 cm, then declining to zero at ca 25-35 cm depth). Instead, these transect profiles are similar to cultivated field profiles shown in Figure E.2.2. Only three of the twelve profiles achieved zero ^{137}Cs concentration at the profile base, T1B and T1E and the Reference Section (R) (Appendix 1). As a consequence, any erosion or deposition rates calculated from the remaining nine profiles are considered minimum estimates.

Erosion calculations from these ^{137}Cs inventories (Equation 1 and Table E.2.4) show net minimum erosion rates of 2.28 t ac- yr^{-1} for the T1 transect and 1.18 t ac^{-1} yr^{-1} for T2. It is worth emphasizing that these represent average annual erosion rates between ca. 1960, when ^{137}Cs was first deposited globally, and 2006 when these transect samples were collected. Based on aerial photographic analyses from the 1930s to the 2000s, and from farmer interviews, land use history and application of the Revised Universal Soil Loss Equation, Sullivan (2006) determined that soil loss in the Big Spring Run Watershed declined from 67 t ac^{-1} yr^{-1} in 1940 to the 5 t ac^{-1} yr^{-1} by 1988 (Table E.2.5). During this same interval, Sullivan also documented a decline in

straight row plowing, thought to cause rill and gully erosion, commensurate with an increase in contour plowing. Contour plowing is a soil conservation method advocated by the U.S. Soil Conservation Service (now USDA-NRCS) since the 1930s, but it did not become widespread in the Big Spring Run Watershed until the early 1980s, rising from 12% in 1940 to 24% in 1988 and to 37% by 1993 (Sullivan 2006). The calculated ^{137}Cs erosion rates of 1.2 and 2.3 t a- yr^{-1} determined here are consistent with Sullivan's (2006) trend, which show that soil conservation practices since the 1940s, such as contour plowing, was effective in slowing erosion from the agricultural field. Despite this decline in upland erosion rates, Big Spring Run and other streams in the Mill Creek/Conestoga River Watersheds remain on the EPA 303d list for high sediment and nutrient loads (Lancaster County Conservation District 2006).

Sediment Sources

Table E.2.6 lists the results of a mixing model (Equation 2) that quantifies the relative contribution of stream bank and upland (surface) sediments to the suspended sediment load at Big Spring Run. Prior to restoration, the ^{137}Cs data suggests that between 85 and 100% of the suspended sediment load was derived from stream bank erosion. The suspended sediments used in the calculation were collected from the upper surface of active inset point bar deposits (see Figure E.2.8 C), where pools of silt-clay rich water remained after storms. Once desiccated, these samples were collected as proxy suspended sediment samples. The term "proxy" is used to differentiate these point bar deposits from true suspended sediment samples collected at the USGS gage stations. Note that the mass of samples collected from the gage stations were insufficient to be analyzed by gamma spectroscopy, hence the need for the proxy suspended sediment samples described here.

In our 2013 DEP report (Walter et al. 2013) we concluded that 60-70% (average of 63%) of the suspended sediment load sampled at the downstream gage at BSR (located just below the restoration reach), was derived from stream bank erosion based on a multi-element geochemical fingerprint study. We (Walter et al. 2013) also summarized a previous ^{137}Cs data study, stating that between 30-65% of the sediment supplied to the upper BSR watershed prior to restoration can be attributed to bank erosion. We noted that these ^{137}Cs values reflect a minimum estimate of the contributions from bank erosion, since the stream banks themselves contain an appreciable amount of ^{137}Cs in the upper ca. 30 cm of the stream bank section. Furthermore, we determined that 100% of the sediment load within the restoration reach was derived from bank erosion.

In the more refined pre-restoration source analyses presented here (Table E.2.6), we used twelve upland sample sites from the surrounding BSR watershed (Figure E.2.8 B-D), six stream bank samples (Site 1, E.2.8 A) and four suspended sediment samples (Figure E.2.8 C), from which we calculate that 85-100% of the suspended sediment load being transported by Big

Spring Run during a storm prior to restoration was derived from stream bank sediments. The Coefficients of Variation (CV) for these analyses are: (1) Upland = 39% (n=12); (2) Suspended Sediment = 40% (n=5); and Stream Bank = 12% (n=6), indicating that there is moderately broad dispersion within each sample group that is typical and expected for these three environmental settings (Nagle and Ritchie 2004).

Both the dispersion of ^{137}Cs data within each data set and the ability of this method to discriminate among data sets is demonstrated in Figures E.2.9a and b. These binary diagrams show the relationship between ^{137}Cs concentrations and ^{210}Pb(total) and ^{226}Ra, respectively.

In both cases, we observe that the Proxy Suspended Sediment samples and the Tile Pad samples coincide with Stream Bank samples, adding visual credence to our mixing model calculations. In addition, the Upland and Transect samples overlap within a second "Upland" group that is separate and distinct from the "Stream Bank" group. There are two apparent exceptions to these groupings: (1) two of the Transect samples (light blue dots in Figures E.2.9a and b) plot within the Stream Bank group; and (2) two Stream Bank samples (gray dots in Figures E.2.9a and b) plot within the Upland group. On closer inspection (Table E.2.3) we observe that the Stream Bank samples that overlap with the Upland group are the upper 20 cm of the bank and contain appreciable ^{137}Cs, and that the Transect samples that overlap with the Stream Bank group are stratigraphically low in the profile and contain no ^{137}Cs. These observations highlight two main complexities in determining sediment sources from ^{137}Cs data: (1) the upper 20-30 cm of a stream bank section contains appreciable amounts of ^{137}Cs and as a consequence it could be misinterpreted to be an Upland sediment; and (2) rills and gullies that incise more than 35 cm into a cultivated field will transport sediment with no ^{137}Cs, which could be misinterpreted to be from a Stream Bank source.

In our post-restoration mixing calculations, using Tile Pad samples from the restoration reach after November 2011 (Table E.2.7), we calculate that 93% of the suspended sediment load carried by the stream and deposited on tile pads in the restored floodplain is from stream bank sources. This is a minimum estimate because, as discussed, the upper 20-30 cm of stream bank profiles contain appreciable amounts of ^{137}Cs which would otherwise skew the calculation toward more upland sources. A high percentage of stream bank sediment on the modern floodplain indicates that most of the sediment coming into the restoration reach, via the East and West Branch tributaries, are from stream bank sources.

E.2. 6. Conclusions

Calibrating the gamma spectroscopy laboratory at Franklin and Marshall College in order to use its instruments to evaluate sediment fluxes and sources at Big Spring Run was a key outcome of this grant. Funds from this grant enabled the lab to acquire a mixed-gamma standard and to

calibrate its spectrometers. We tested our calibration against a National Institute of Standards Standard Reference Material (SRM 4350B) sediment from the Columbia River in Washington state. Running this SRM as an unknown, our spectrometers matched the ^{137}Cs concentration reported in the Certificate of Analyses for this SRM. This gives us a high level of assurance in the accuracy and precision of our measurements.

Fluxes and sources of suspended sediment to Big Spring Run were quantified and identified by ^{137}Cs analyses. Cesium-137 is ideal for this purpose because: (1) it does not occur naturally; (2) it was produced over three decades and distributed globally as a result of above-ground nuclear bomb tests; (3) it is chemically inert, and is strongly adsorbed to cation-exchange sites on fine (silt and clay) sedimentary particles; and (4) it moves with these sedimentary particles.

An inventory of fallout ^{137}Cs activity from two hill slope transects adjacent to Big Spring Run yield average erosion rates of 1.2 t ac^{-1} yr^{-1} and 2.3 t ac-^{1} yr^{-1}. These rates reflect the average rates between the early 1960s (the peak of ^{137}Cs production) and 2006 (when these samples were collected), and thus reflect the periods of high rill and sheet erosion before the implementation of conservation farming practices. As of 1982, the state-wide average for cultivated land was 5.3 t ac^{-1} yr^{-1} (United States. Department of Agriculture 1990). The measured ^{137}Cs erosion rates reported here agree with a previous study of the Big Spring Run watershed using the revised universal soil loss equation, GIS interpretation of land use changes from aerial photographs between 1940 and 2005 and land owner interviews. This study indicates a dramatic reduction in soil erosion rates from ca. 25 t ac^{-1} yr^{-1} in 1940 to ca. 5 t ac^{-1} yr^{-1} by 1988, which also agrees with the USDA assessment at that time.

The average contribution of sediment supplied to Big Spring Run from various sources also can be deduced using mass balance calculations of ^{137}Cs data. Results of these calculations indicate that 85-100% of the sediment supplied to this watershed can be accounted for by stream bank sources, with little if any from cultivated upland slopes.

E.2. 7. References

Boesch, Donald F., Russell B. Brinsfield, and Robert E. Magnien. 2001. “Chesapeake Bay Eutrophication.” Journal of Environmental Quality 30 (2): 303–20. doi:10.2134/jeq2001.302303x.

Boomer, Kathleen B., Donald E. Weller, and Thomas E. Jordan. 2008. “Empirical Models Based on the Universal Soil Loss Equation Fail to Predict Sediment Discharges from Chesapeake Bay Catchments.” Journal of Environmental Quality 37 (1): 79–89. doi:10.2134/jeq2007.0094.

Brakebill, John W., Scott W. Ator, and Gregory E. Schwarz. 2010. “Sources of Suspended-Sediment Flux in Streams of the Chesapeake Bay Watershed: A Regional Application of the SPARROW Model1.” JAWRA Journal of the American Water Resources Association 46 (4): 757–76. doi:10.1111/j.1752-1688.2010.00450.x.

Campbell, B. L. 1983. “Application of Environmental Caesium-1 3 7 for the Determination of Sedimentation Rates in Reservo Irs and Lakes and Related Catchment Studies in Developing Countries.” Technology Document 298: 7–30.
Campbell, B. L., R. J. Loughran, and G. L. Elliott. 1988. “A Method for Determining Sediment Budgets Using Caesium-137.” Sediment Budgets. IAHS Publication, no. 174.
Carter, Melvin W., and A. Alan Moghissi. 1977. “Three Decades of Nuclear Testing.” Health Physics 33 (1): 55–71.
Costa, John E. 1975. “Effects of Agriculture on Erosion and Sedimentation in the Piedmont Province, Maryland.” Geological Society of America Bulletin 86 (9): 1281–86. doi:10.1130/0016-7606(1975)86<1281:EOAOEA>2.0.CO;2.
Davis, J. J. 1963. “Cesium and Its Relationship to Potassium in Ecology.” Radioecology. Reinhold, New York, 539–556.
Dunne, Thomas, and William Dietrich. 1982. “Sediment Sources in Tropical Drainage Basins.” Soil Erosion and Conservation in the Tropics: 41–55.
Eyman, L. Dean, and Niles R. Kevern. 1975. “Cesium-137 and Stable Cesium in a Hypereutrophic Lake.” Health Physics 28 (5): 549–555.
Happ, Stafford C. 1945. “Sedimentation in South Carolina Piedmont Valleys.” American Journal of Science 243 (3): 113–26. doi:10.2475/ajs.243.3.113.
Imanaka, Tetsuji, Gohei Hayashi, and Satoru Endo. 2015. “Comparison of the Accident Process, Radioactivity Release and Ground Contamination between Chernobyl and Fukushima-1.” Journal of Radiation Research 56 (suppl_1): i56–i61.
Ioannides, K., T. Mertzimekis, D. Karamanis, K. Stamoulis, and I. Kirikopoulos. 1996. “Radiocesium Sorption-Desorption Processes in Lake Sediments.” Journal of Radioanalytical and Nuclear Chemistry 208 (2): 549–557.
Kirchner, G., and H. Ehlers. 1998. “Sediment Geochronology in Changing Coastal Environments: Potentials and Limitations of the 137Cs and 210Pb Methods.” Journal of Coastal Research, 483–492.
Knox, James C. 1972. “Valley Alluviation in Southwestern Wisconsin.” Annals of the Association of American Geographers 62 (3): 401–10. doi:10.1111/j.1467-8306.1972.tb00872.x.
Longmore, M. E. 1982. “The Caesium-137 Dating Technique and Associated Applications in Australia-a Review.” In Archaeometry: An Australasian Perspective. https://inis.iaea.org/search/search.aspx?orig_q=RN:14775549.
Loughran, R. J., and B. L. Campbell. 1995. “The Identification of Catchment Sediment Sources.” In Sediment and Water Quality in River Catchments, edited by I. Foster, A. Gurnell, and B. Webb, 189–205. New York: Wiley. http://ci.nii.ac.jp/naid/10012147305/.
Lowrance, Richard, Lee S. Altier, J. Denis Newbold, Ronald R. Schnabel, Peter M. Groffman, Judith M. Denver, David L. Correll, et al. 1997. “Water Quality Functions of Riparian Forest Buffers in Chesapeake Bay Watersheds.” Environmental Management 21 (5): 687–712. doi:10.1007/s002679900060.
Matisoff, Gerald, Everett C. Bonniwell, and Peter J. Whiting. 2002a. “Radionuclides as Indicators of Sediment Transport in Agricultural Watersheds That Drain to Lake Erie.” Journal of Environmental Quality 31 (1): 62–72.
———. 2002b. “Soil Erosion and Sediment Sources in an Ohio Watershed Using Beryllium-7, Cesium-137, and Lead-210.” Journal of Environmental Quality 31 (1): 54–61.

Matisoff, Gerald, and Peter J. Whiting. 2012. “Measuring Soil Erosion Rates Using Natural (7Be, 210Pb) and Anthropogenic (137Cs, 239,240 Pu) Radionuclides.” In Handbook of Environmental Isotope Geochemistry, 487–519. Springer. http://link.springer.com/10.1007/978-3-642-10637-8_25.

Mellerowicz, K. T., H. W. Rees, T. L. Chow, and I. Ghanem. 1994. “Soil Conservation Planning at the Watershed Level Using the Universal Soil Loss Equation with GIS and Micorocomputer Technologies: A Case Study.” Journal of Soil and Water Conservation 49 (2): 194–200.

Merritts, Dorothy, Robert Walter, Michael Rahnis, Scott Cox, Jeffrey Hartranft, Chris Scheid, Noel Potter, et al. 2013. “The Rise and Fall of Mid-Atlantic Streams: Millpond Sedimentation, Milldam Breaching, Channel Incision, and Stream Bank Erosion.” Reviews in Engineering Geology 21 (February): 183–203. doi:10.1130/2013.4121(14).

Merritts, Dorothy, Robert Walter, Michael Rahnis, Jeff Hartranft, Scott Cox, Allen Gellis, Noel Potter, et al. 2011. “Anthropocene Streams and Base-Level Controls from Historic Dams in the Unglaciated Mid-Atlantic Region, USA.” Philosophical Transactions of the Royal Society A: Mathematical, Physical and Engineering Sciences 369 (1938): 976–1009. doi:10.1098/rsta.2010.0335.

Nagle, G. N., and J. C. Ritchie. 2004. “Wheat Field Erosion Rates and Channel Bottom Sediment Sources in an Intensively Cropped Northeastern Oregon Drainage Basin.” Land Degradation & Development 15 (1): 15–26.

Olley, Jon, and Ian Prosser. 1999. “Land-Use Impacts on Rivers.” Catchword: Newsletter of the Cooperative Research Centre for Catchment Hydrology, September.

Peart, M. R., and D. E. Walling. 1986. “Fingerprinting Sediment Source: The Example of a Drainage Basin in Devon, UK.” In Drainage Basin Sediment Delivery: Proceedings of a Symposium Held in Albuquerque, NM., 4-8 August 1986. https://hub.hku.hk/handle/10722/157753.

Pionke, Harry B, William J Gburek, and Andrew N Sharpley. 2000. “Critical Source Area Controls on Water Quality in an Agricultural Watershed Located in the Chesapeake Basin.” Ecological Engineering 14 (4): 325–35. doi:10.1016/S0925-8574(99)00059-2.

Quine, T. A., and D. E. Walling. 1993. “Use of Caesium-137 Measurements to Investigate Relationships between Erosion Rates and Topography.” http://agris.fao.org/agris-search/search.do?recordID=GB9403821.

Ritchie, Jerry C., and J. Roger McHenry. 1977. “The Distribution of Cs-137 in Some Watersheds in the Eastern United States.” Health Physics 32 (2): 101–105.

———. 1990. “Application of Radioactive Fallout Cesium-137 for Measuring Soil Erosion and Sediment Accumulation Rates and Patterns: A Review.” Journal of Environmental Quality 19 (2): 215–33. doi:10.2134/jeq1990.00472425001900020006x.

Sawhiney, B. 1972. “Selective Sorption and Fixation of Cations by Clay Minerals: A Review.” Clays Clay Miner 20 (9). http://www.clays.org/journal/archive/volume%2020/20-2-93.pdf.

Shenk, Gary W., and Lewis C. Linker. 2013. “Development and Application of the 2010 Chesapeake Bay Watershed Total Maximum Daily Load Model.” JAWRA Journal of the American Water Resources Association 49 (5): 1042–1056.

Sullivan, Alexandra. 2006. “Geomorphology in the Agricultural Watershed of Big Spring Run, Lancaster, PA: An Integrative Approach to Erosion Research and Remediation.” Bachelor’s Thesis, Franklin & Marshall College.

Swarzenski, Peter W., Mark Baskaran, Robert J. Rosenbauer, and William H. Orem. 2006. "Historical Trace Element Distribution in Sediments from the Mississippi River Delta." Estuaries and Coasts 29 (6): 1094–1107.
Tamura, T. 1964. "Selective Sorption Reactions of Cesium with Soil Minerals." Nucl. Safety 5 (3). https://www.osti.gov/scitech/biblio/4618020.
Taylor, John. 1997. Introduction to Error Analysis, the Study of Uncertainties in Physical Measurements. http://adsabs.harvard.edu/abs/1997ieas.book..
Trimble, Stanley W. 1999. "Decreased Rates of Alluvial Sediment Storage in the Coon Creek Basin, Wisconsin, 1975-93." Science 285 (5431): 1244–46. doi:10.1126/science.285.5431.1244.
Trimble, Stanley W., and Pierre Crosson. 2000. "US Soil Erosion Rates–myth and Reality." Science 289 (5477): 248–250.
United States. Department of Agriculture. 1990. The Second RCA Appraisal: Soil, Water, and Related Resources on Nonfederal Land in the United States : Analysis of Condition and Trends. [Washington, DC] : U.S. Dept. of Agriculture. http://archive.org/details/secondrcaapprais1482unit.
Unterweger, M. P. 2002. "Half-Life Measurements at the National Institute of Standards and Technology." Applied Radiation and Isotopes, Proceedings of the Conference on Radionuclide Metrology and its Applications, ICRM'01, 56 (1): 125–30. doi:10.1016/S0969-8043(01)00177-4.
Unterweger, M. P., and R. Fitzgerald. 2014. "Update of NIST Half-Life Results Corrected for Ionization Chamber Source-Holder Instability." Applied Radiation and Isotopes, Proceedings of the 19th International Conference on Radionuclide Metrology and its Applications 17–21 June 2013, Antwerp, Belgium, 87 (May): 92–94. doi:10.1016/j.apradiso.2013.11.017.
Wallbrink, P. J., J. M. Olley, A. S. Murray, and L. J. Olive. 1996. "The Contribution of Subsoil to Sediment Yield in the Murrumbidgee River Basin, New South Wales, Australia." IAHS Publications-Series of Proceedings and Reports-Intern Assoc Hydrological Sciences 236: 347–356.
Walling, D. E. 1994. "Measuring Sediment Yield from River Basins." Soil Erosion Research Methods, 39–80.
Walling, D. E., and S. B. Bradley. 1988. "The Use of Caesium-137 Measurements to Investigate Sediment Delivery from Cultivated Areas in Devon, UK." Sediment Budgets 174: 325–335.
Walling, D. E., S. B. Bradley, and C. J. Wilkinson. 1986. "A Caesium-137 Budget Approach to the Investigation of Sediment Delivery from a Small Agricultural Drainage Basin in Devon, UK." International Association of Hydrological Sciences Publication 159: 423–435.
Walling, D. E., and T. A. Quine. 1990. "Use of 137Cs Measurements to Investigate Soil Erosion on Arable Fields in the UK: Potential Applications and Limitations." In Soil Erosion on Agricultural Land, edited by J. Boardman, I. D. L. Foster, and J. A. Dearing, 33–53. British Geomorphological Research Group Symposia Series. New York: John Wiley & Sons Inc.
Walter, R. C., and D. J. Merritts. 2008. "Natural Streams and the Legacy of Water-Powered Mills." Science 319 (5861): 299–304.

Walter, R. C., D. J. Merritts, M. Rahnis, M. Langland, D. Galeone, A. Gellis, W. Hilgartner, et al. 2013. “Big Spring Run Floodplain-Wetland Aquatic Resources Restoration Project.” Report of Investigations. Pennsylvania Department of Environmental Protection. http://www.bsr-project.org/uploads/2/6/5/2/26524868/big_spring_run_aquatic_ecosystem_restoration_monitoring_report_2013.pdf.

Wise, S. M. 1980. “Caesium-137 and Lead-210: A Review of the Techniques and Some Applications in Geomorphology.” Timescales in Geomorphology 9: 109–127.

Zaborska, Agata, JoLynn Carroll, Carlo Papucci, and Janusz Pempkowiak. 2007. “Intercomparison of Alpha and Gamma Spectrometry Techniques Used in 210 Pb Geochronology.” Journal of Environmental Radioactivity 93 (1): 38–50.

Zhang, X., T. A. Quine, and D. E. Walling. 1998. “Soil Erosion Rates on Sloping Cultivated Land on the Loess Plateau near Ansai, Shaanxi Province, China: An Investigation Using 137Cs and Rill Measurements.” Hydrological Processes 12 (1): 171–89. doi:10.1002/(SICI)1099-1085(199801)12:1<171::AID-HYP570>3.0.CO;2-L.

F. Deliverable 5: Monitor post-restoration conditions at the BSR restoration site using remote sensing cameras to collect fixed interval time lapsed photography.

Tasks: Install or maintain camera equipment and accessories. Collect post-restoration time sequenced images. Develop a digital image database.

Deliverables: A digital image database with data representing fixed interval time-lapsed site photography.

Staff/Contractor: Telemonitor, Inc. (Robert Johnson and Jim Moore

Time-lapse photos were taken from sunrise to sunset at one minute intervals from two web cameras set up on towers at the downstream and upstream (western tributary) ends of the restoration area at Big Spring Run from 2011-2015, including the time during restoration construction. These images are available and indexed at:

www.bethere.telemonitor.com/BSR/

This site hosts folders for both time-lapse videos and still images, indexed by camera number, year, month, and day. Of particular value is images acquired during high flow events, which show the processes that occur as water rises in small channels, spills over low banks, fills adjacent small channels and low spots, and eventually spreads across the wetland floodplain. During waning stages of high flow events these images illustrate how water remains pooled in low spots, subsidiary channels, and other sinks. They also document the deposition of organic detritus across the wetland-floodplain area.

Deliverable 1

Figure 1.1. Map of the Conestoga River basin showing location of 1948 sampling sites (from Patrick 1949).

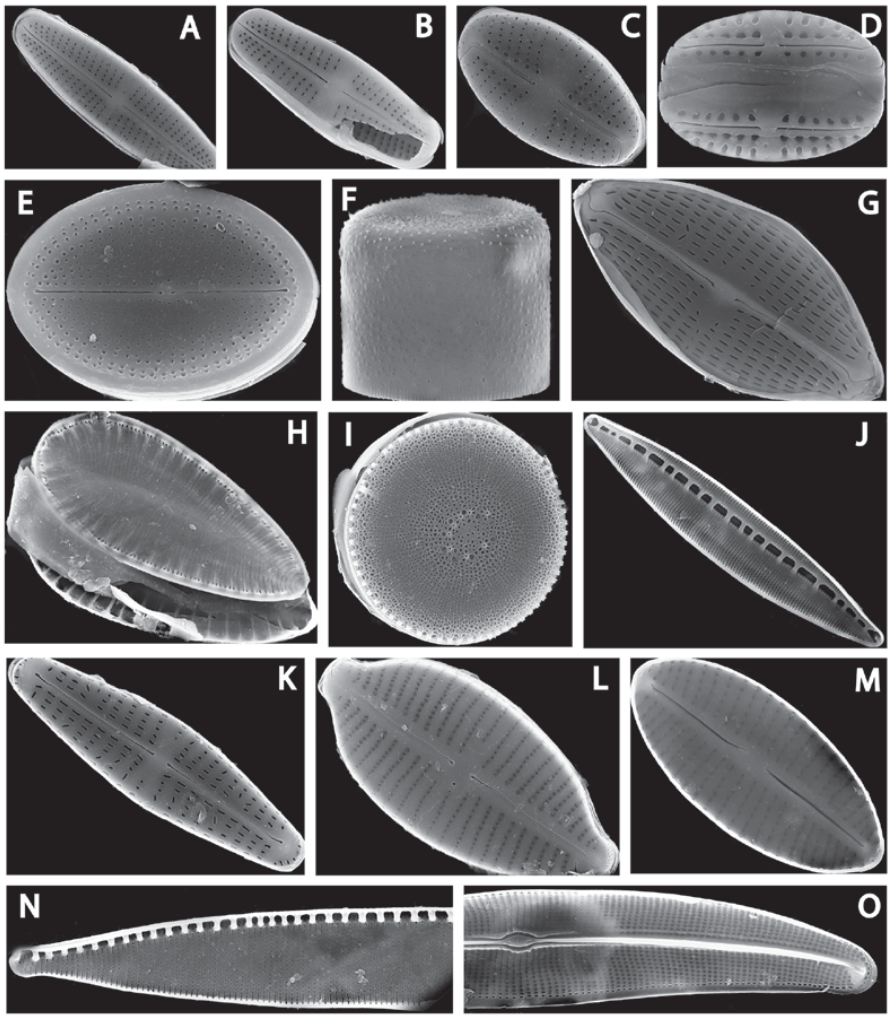

Figure 1.2. Scanning electron microscopy images of the common diatoms from BSR samples. A– *Achnanthidium minutissimum*, B – *A. saprophilum*, C – *Eolimna minima*, D – *Amphora pediculus*, E – *Cocconeis placentula*, F – *Melosira varians*, G- *Navicula antonii*, H – *Surirella lacrimula*, I – *Thalassiosira weissflogii*, J – *Nitzschia dissipata*, K – *Hippodonta pseudacceptata*, L- *Gomphonema parvulum* var. *saprophilum*, M – *Craticula subminuscula*, N- *Nitzschia palea*, O – *Gyrosigma obtusatum*.

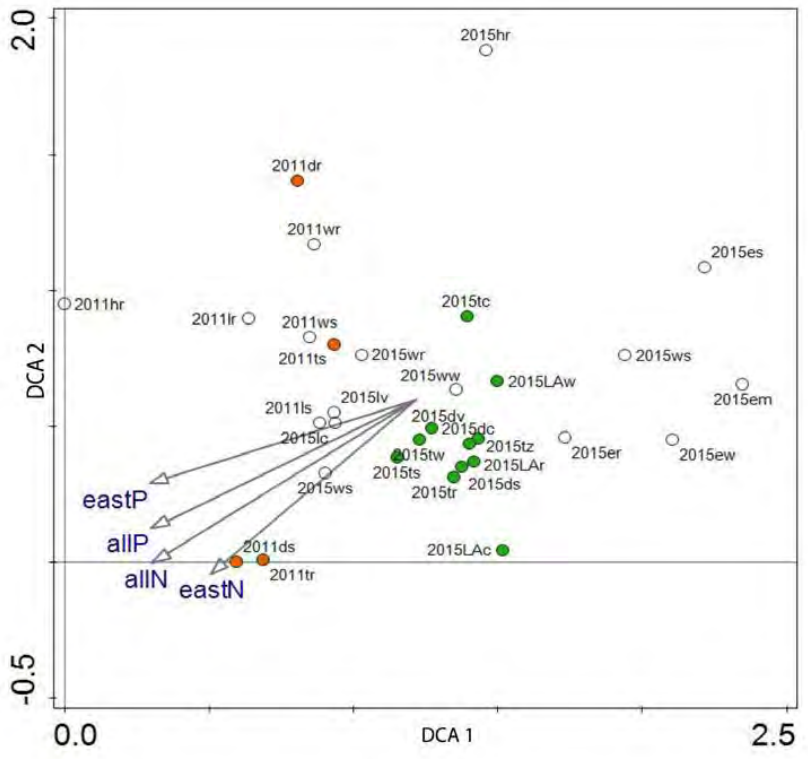

Figure 1.3. Detrended Correspondence Analysis of diatom BSR data. Centroids of 32 samples are shown in the ordination space of the first and second DCA axes. Orange circles - samples collected in 2011 from the main stem BSR, green circles - samples collected in 2015 from the main stem after the restoration. Sample codes consist of the year (2011 or 2015), first one or two letters indicating sampling location (w- West Branch, e – East Branch, h – Houser Grid, l – Long Rifle Rd., t – site 1, LA – site 2, d – site 3) and last letter indicating substrate type (r – rocks, s – silt, v – *Vaucheria*, c – *Cladophora*, z – *Zygnema*, w – watercress, m – moss). Arrows show correlations of DCA axes 1 and 2 with nutrient diatom metrics.

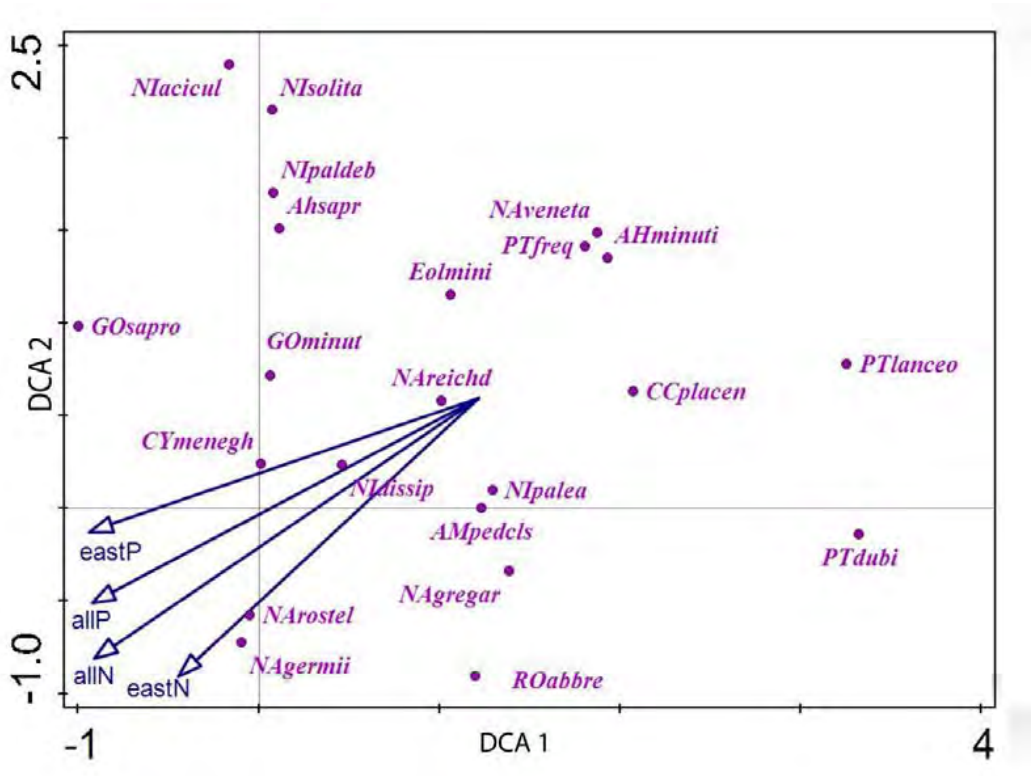

Figure 1.4. Detrended Correspondence Analysis of diatom BSR data: same analysis as shown in Figure 3. Plot showing position of the most common species is shown in the ordination space of the first and second DCA axes. Abbreviations of species names are given in Appendix I. Arrows show correlations of DCA axes 1 and 2 with nutrient diatom metrics.

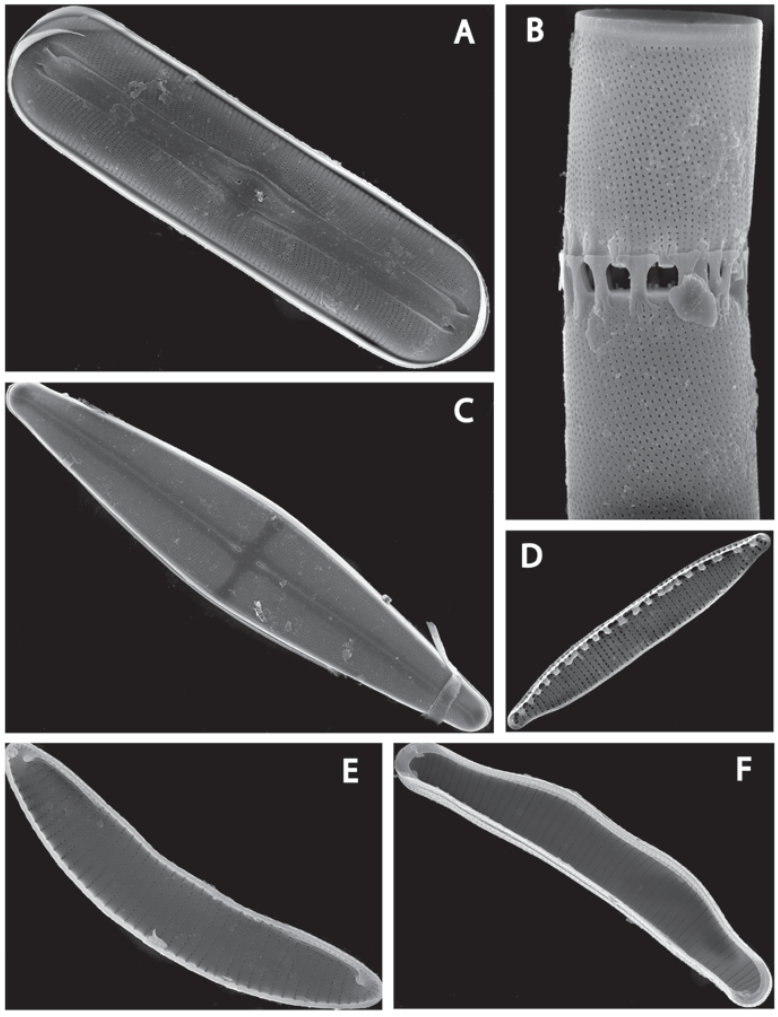

Figure 1.5. Scanning electron microscopy images of the diatoms from Great Marsh wetland. A – *Sellaphora alastos*, B – *Aulacoseira italica*, C – *Stauroneis gracilis*, D – *Nitzschia acidoclinata*, E – *Eunotia bilunaris*, F – *Eunotia minor*.

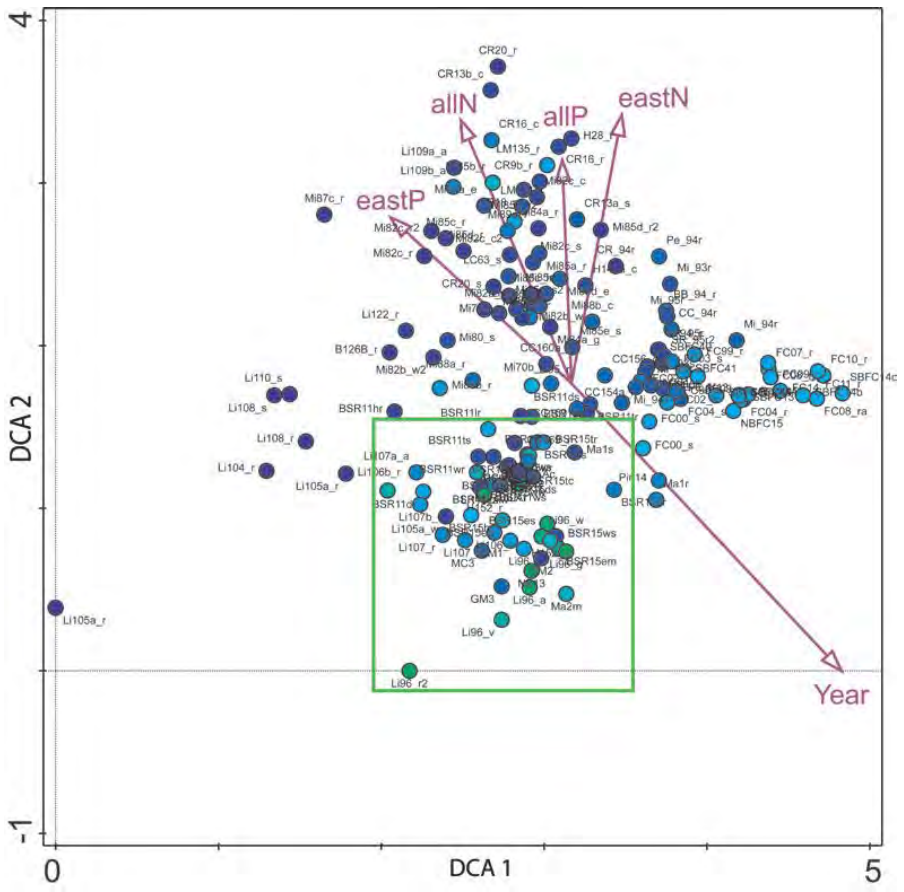

Figure 1.6. Unconstrained ordination (DCA) of diatom relative abundance data from benthic stream samples collected in Lancaster County from 1948 to 2016. Sample centroids are colored according to values of Total Nitrogen nation-wide diatom metric for corresponding samples from green indicating the lowest metric values (<3) to dark blue indicating the highest values (>9). Sample codes are given in the Appendix xx. The first letters indicate water body name (BSR – Big Spring Run, Mi- Mill Creek, LI – Lititz Run, FC – French Creek, CR – Conestoga River, etc.); numbers indicate either collection year (11 – 2011 and 15 – 2015 for Big Spring Run, similarly for other samples collected after 1993) or station number for samples collected in 1948. Green rectangle shows the region containing BSR samples and expanded in Figure 7.

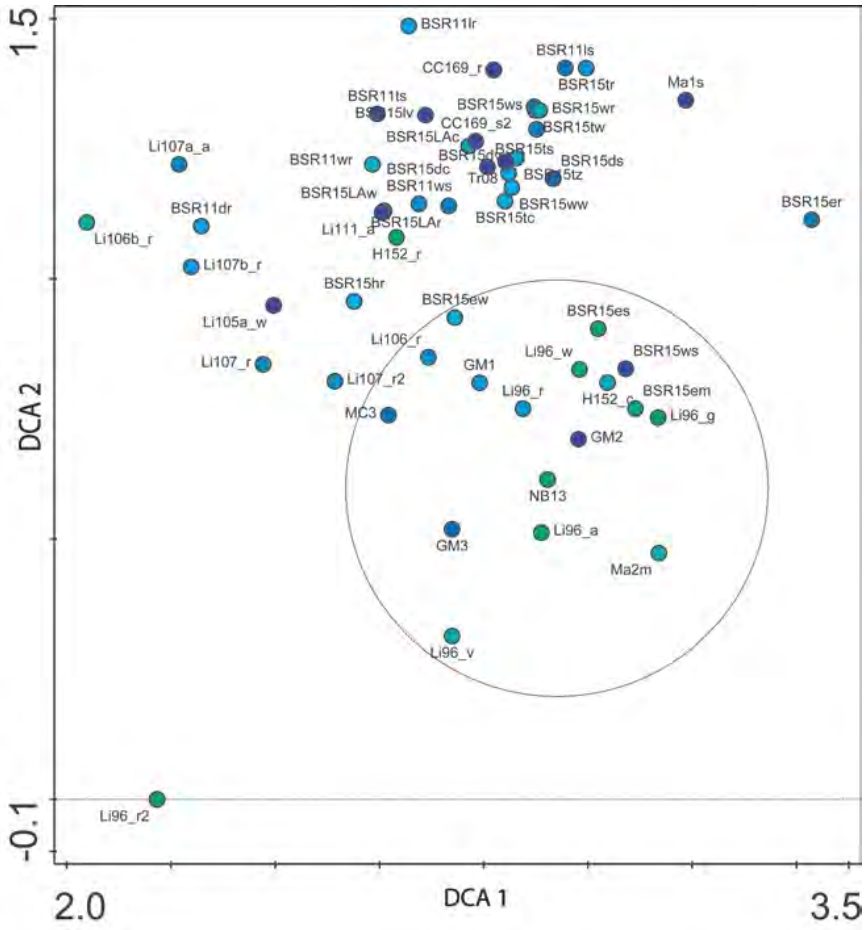

Figure 1.7. Unconstrained ordination (DCA) of diatom relative abundance data from benthic stream samples collected in Lancaster County from 1948 to 2016: expanded section of the plot in Figure 6. Sample centroids are colored according to values of Total Nitrogen nation-wide diatom metric for corresponding samples from green indicating the lowest metric values (<3) to dark blue indicating the highest values (>9). The circle delineates a cluster of sites that include Great Marsh wetland (GM1, GM2, and GM3) and Marsh Creek within the Great Marsh site (MC3), several samples from the headwaters of Lititz Run, Hammer Creek and Big Spring Run.

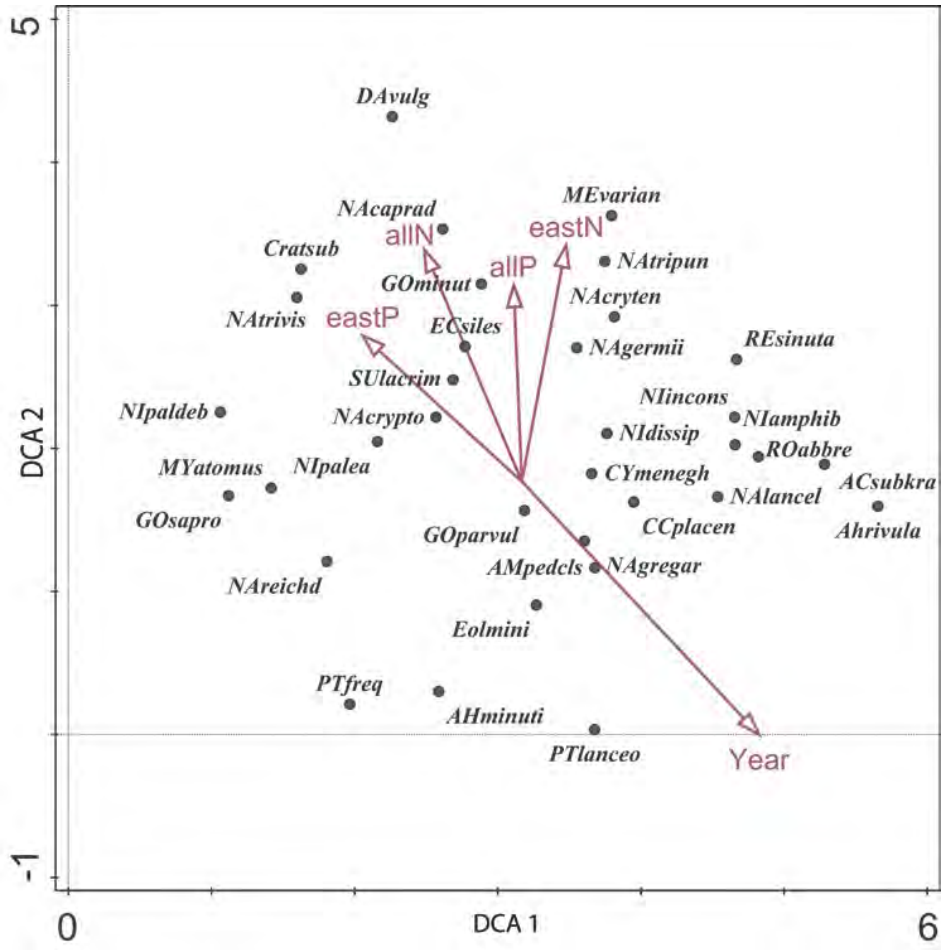

Figure 1.8. Unconstrained ordination (DCA) of diatom relative abundance data from benthic stream samples collected in Lancaster County from 1948 to 2016. Position of the most common species is shown in the ordination space of the first and second DCA axes. Abbreviations of species names are given in Appendix I.

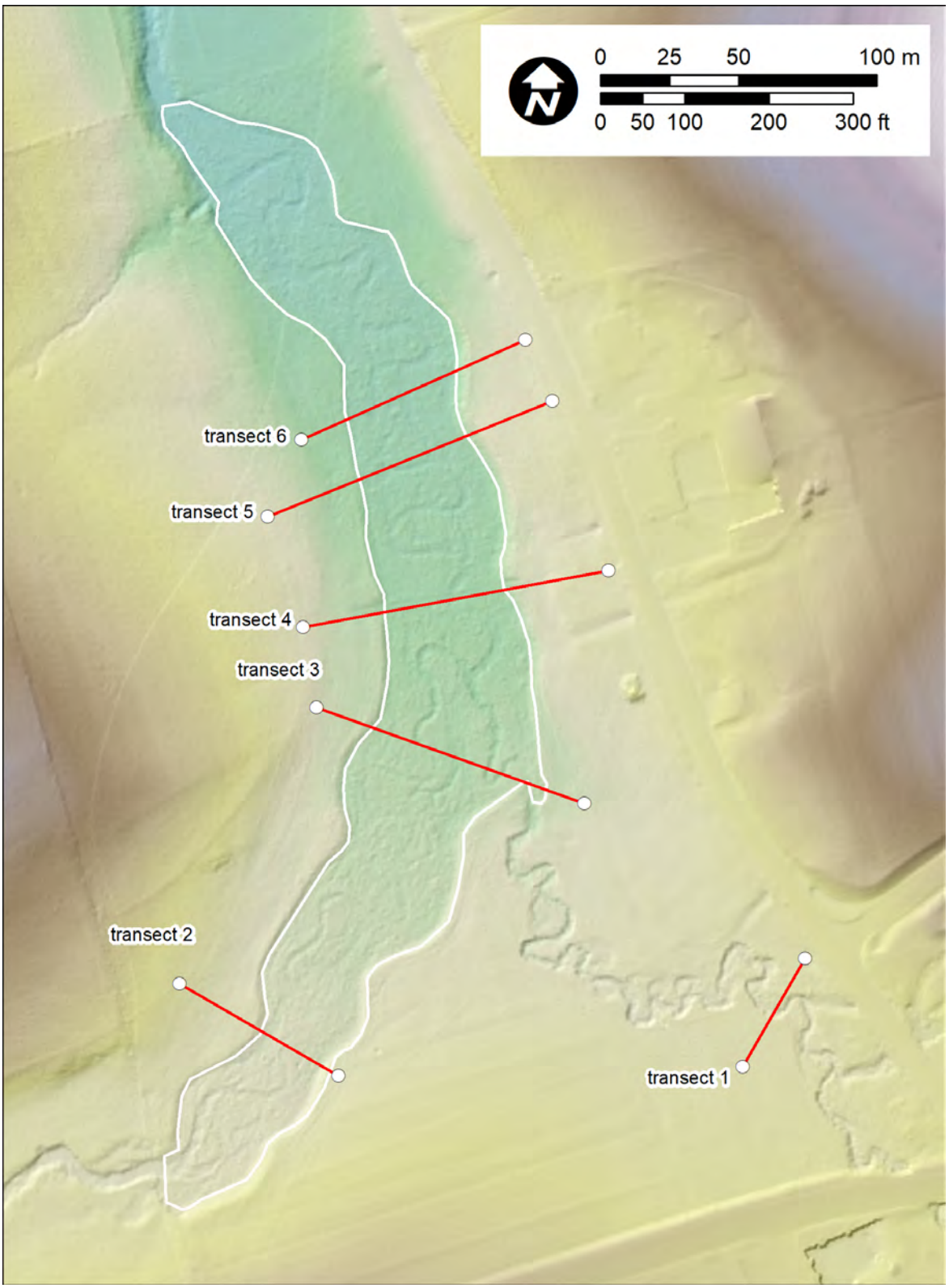

Figure 3.1. Locations of vegetation transects at Big Spring Run.

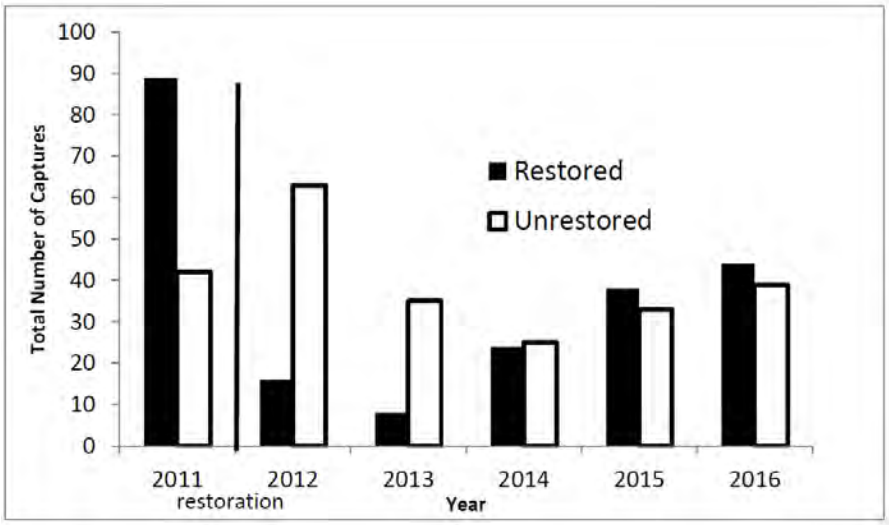

Figure 3.2 Capture records of *Eurycea bislineata* (northern two-lined salamanders) in the restored sections (Main, West, first third of East) and unrestored (remaining two-thirds of East, Kennel). The data are the sum of trapping efforts with litter bags, kick nets, and dip nets. Capture effort was equal for each branch.

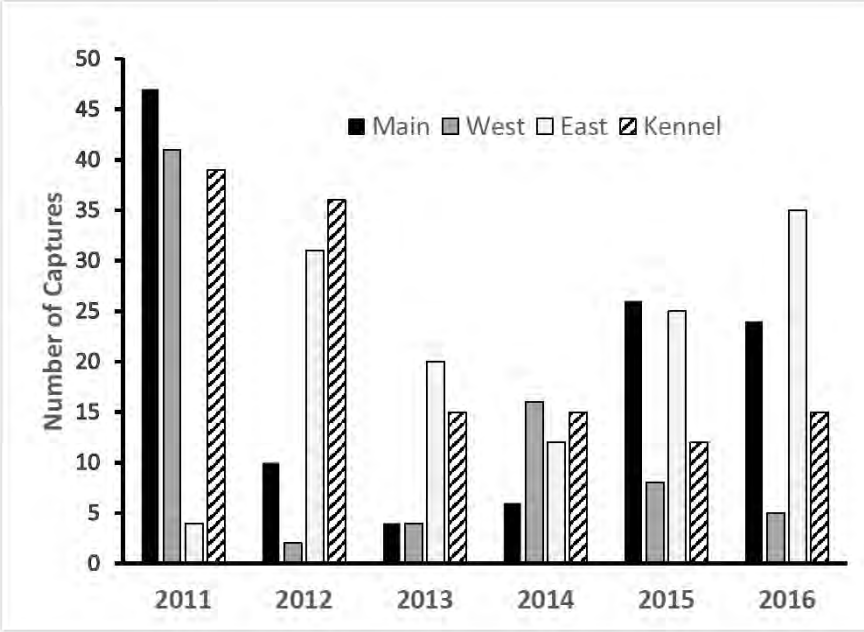

Figure 3.3. Capture records of *Eurycea bislineata* (northern two-lined salamanders) in the three branches of Big Spring Run and Kennel Run, an upstream reference site, before and after the restoration that occurred after the field season in 2011. The data are the sum of trapping efforts with litter bags, dip nets, and kick nets. Capture effort was equal for each branch.

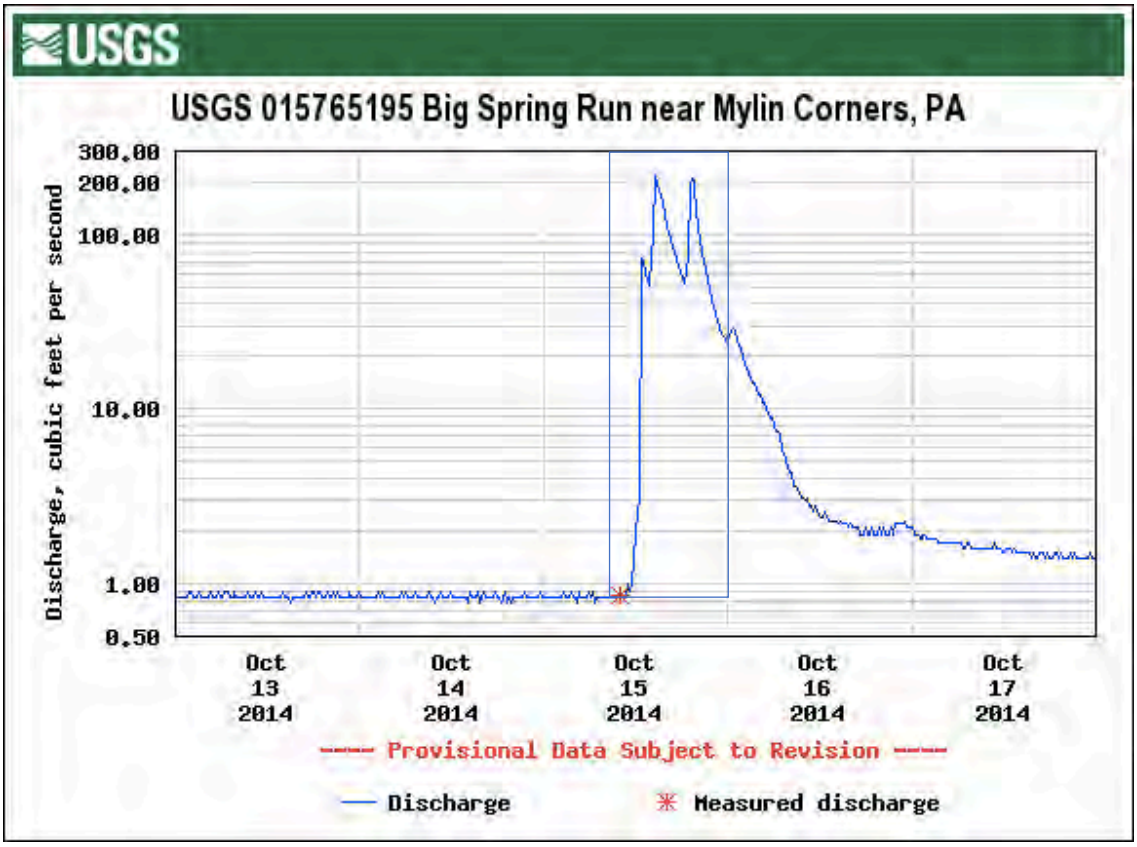

Figure C. 2. 1. October 15, 2014, flow event used in 2D model. Peak discharge 218 cfs, slightly larger than 2-yr peak (198 cfs) estimated from PA StreamStats.

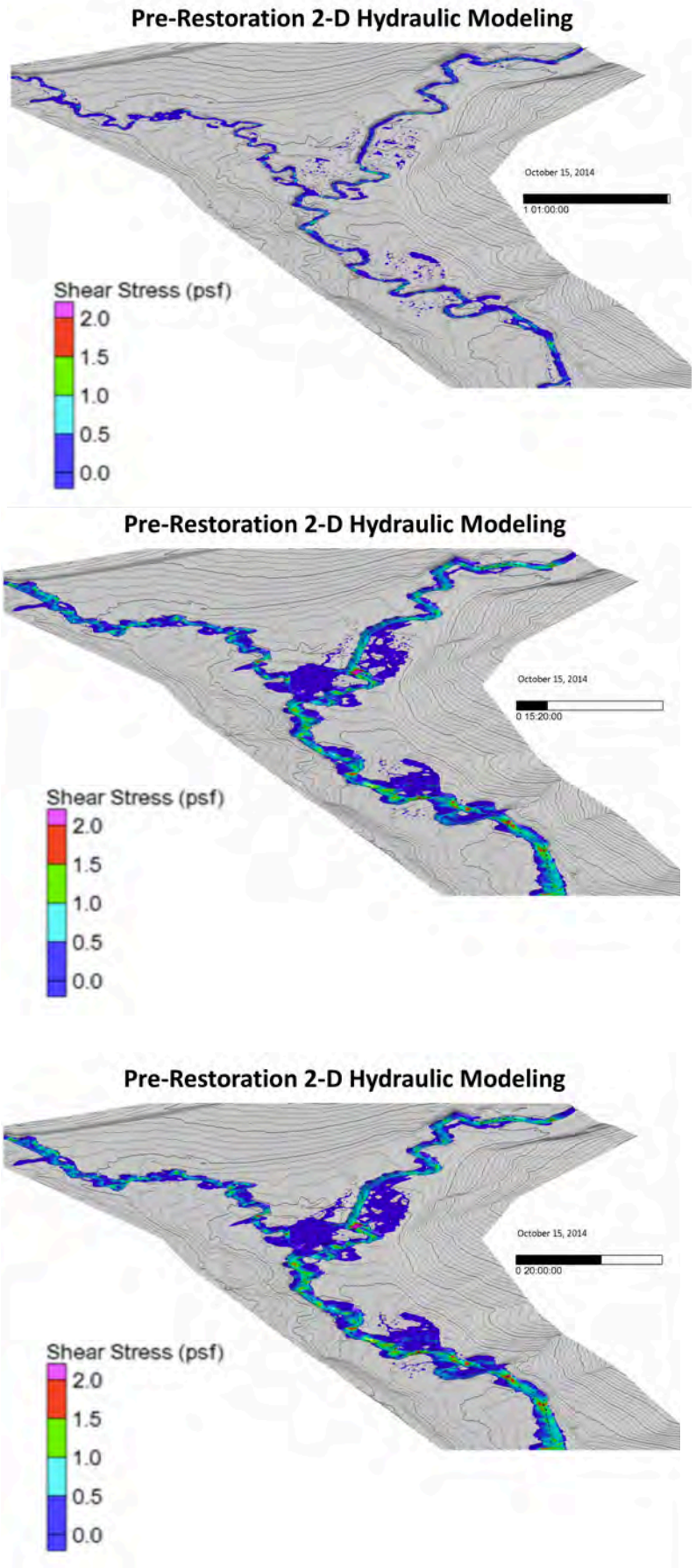

Figure C. 2. 2. Panels show 3 different times during model run of flow event for pre-restoration conditions: Top--beginning (or end) ; middle—at 15:20, or 3 hours and 20 minutes into simulation; bottom—at 20:00, or 5 hours into simulation.

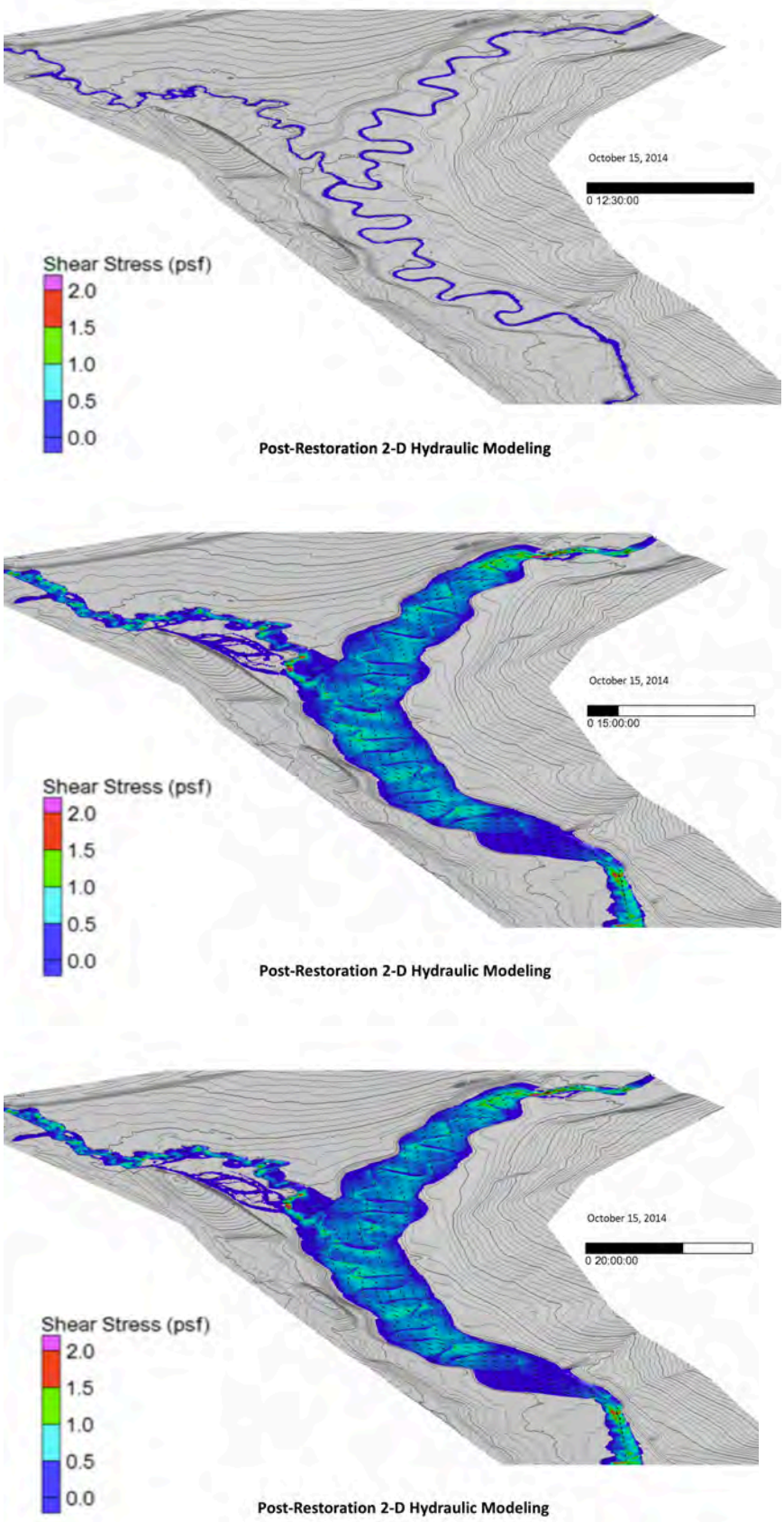

Figure C. 2. 3. Panels show 3 different times during model run of flow event for post-restoration conditions: Top--beginning (or end) ; middle—at 15:20, or 3 hours and 20 minutes into simulation; bottom—at 20:00, or 5 hours into simulation.

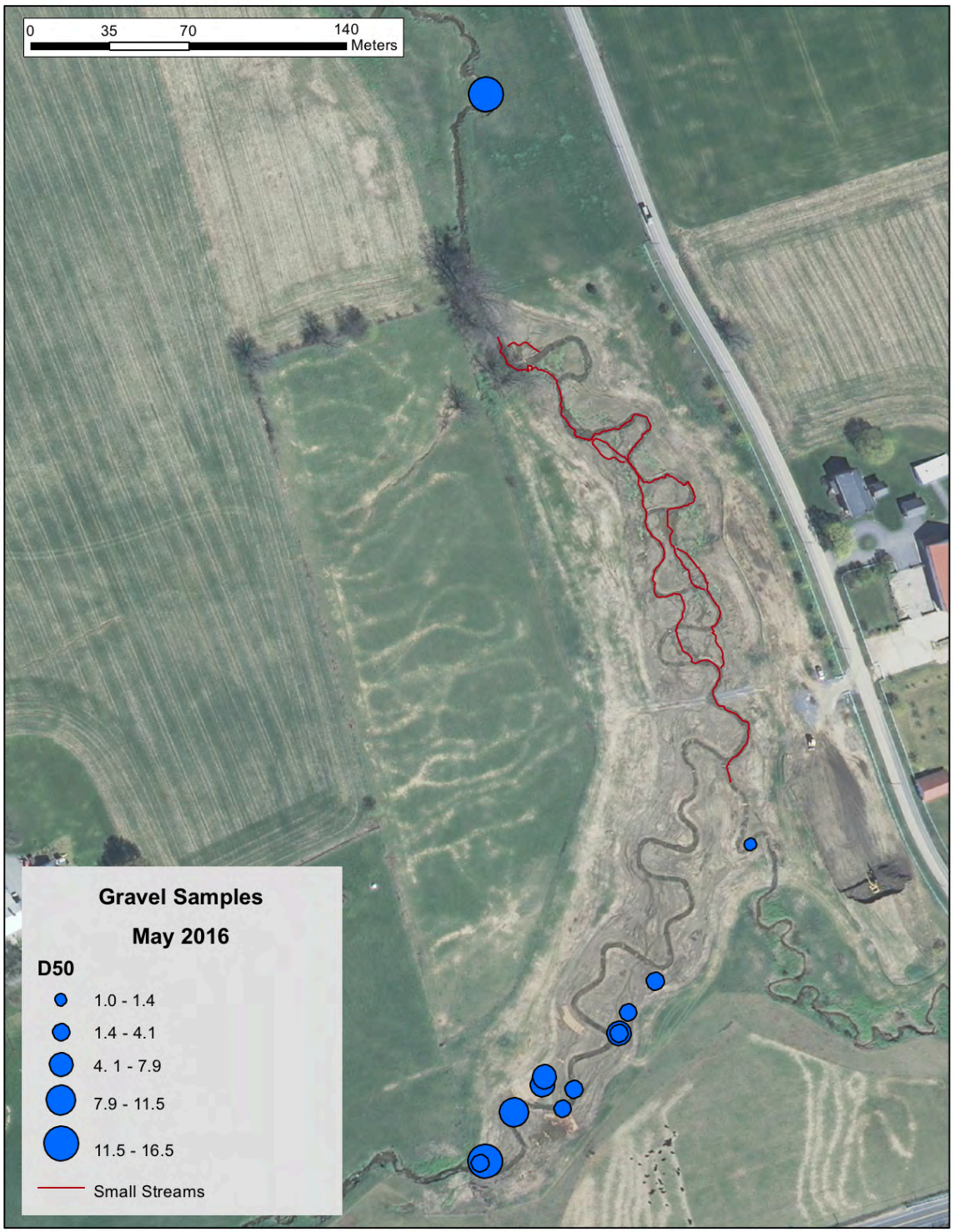

Figure C. 2. 4. Mean gravel size for samples collected after high flow events in April-May 2016. Base orthoimage from 2012. North is at top of image.

Figure 4.1. Aerial photo (2015) from Google Earth of Big Spring Run with locations of USGS gage stations (yellow squares), average annual post-restoration suspended sediment loads (ton) at each gage station (bold italicized white number), approximate boundaries of restoration area (white polyline), distance from gage station to restoration reach (underlined white number), estimated load from reach using lidar dem differencing (bold white number), and estimated range in load (* 1 S. D., from repeat RTK GPS surveying or tile pad deposition data (white numbers inside polyline, with RTK GPS numbers first). Big Spring Run flows northward (top) and has two main tributaries from the west (left) and east (right).

USGS gage station identifier	Location	Distance to restoration reach, ft
01576516 (In)	Eastern tributary	1017
015765185 (In)	Western tributary	131
015765195 (Out)	Main stem	558

USGS Gage Stations		Pre-restoration Period				Post-restoration period				
		2009	2010	2011	Average 2009-11	2012	2013	2014	2015	Average 2012-15
From GCLAS	*In*	103	113	161	126	75	119	127	68	98
	Out	238	309	350	299	176	265	264	108	203
	Out - In	135	196	189	173	101	146	138	40	105
From transport equations	*In*	107	140	185	144	88	127	131	81	107
	Out	241	317	351	303	199	278	278	119	219
	Out-In	134	177	166	159	111	151	147	38	112

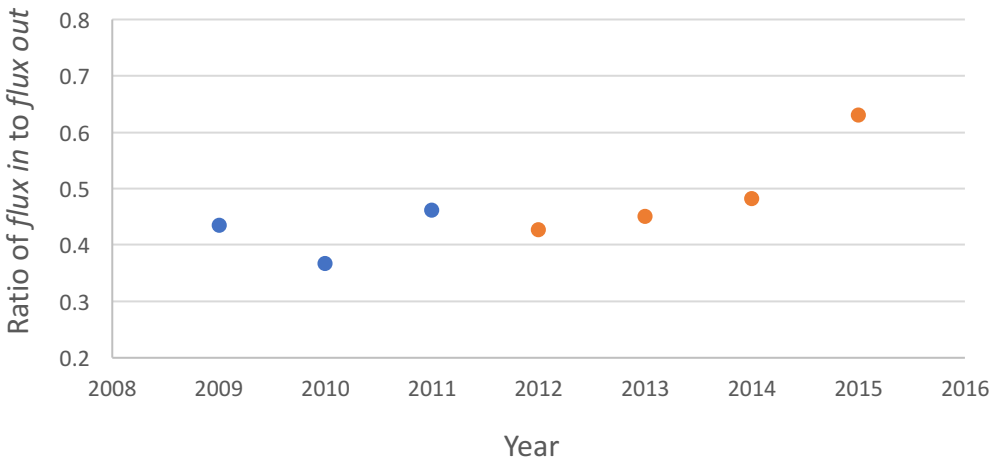

Figure 4.2. Top: Location information for three USGS gage stations along Big Spring Run. Note that gage 01576516 on the eastern tributary was moved downstream in May 2016, to the beginning of the restoration reach. However, all data cited in this report pre-date that location change. Middle: USGS estimates of annual loads from incoming gage stations on eastern and western tributaries (In), and outgoing annual load at downstream gage on main stem (Out). The difference between the two is the amount of sediment derived from the area between the up and downstream stations. Bottom: Ratio of flux in to flux out from pre-restoration (2009 to 2011) and post-restoration (2012 to 2015). Note that the proportion of sediment from the incoming gage stations has increased since restoration.

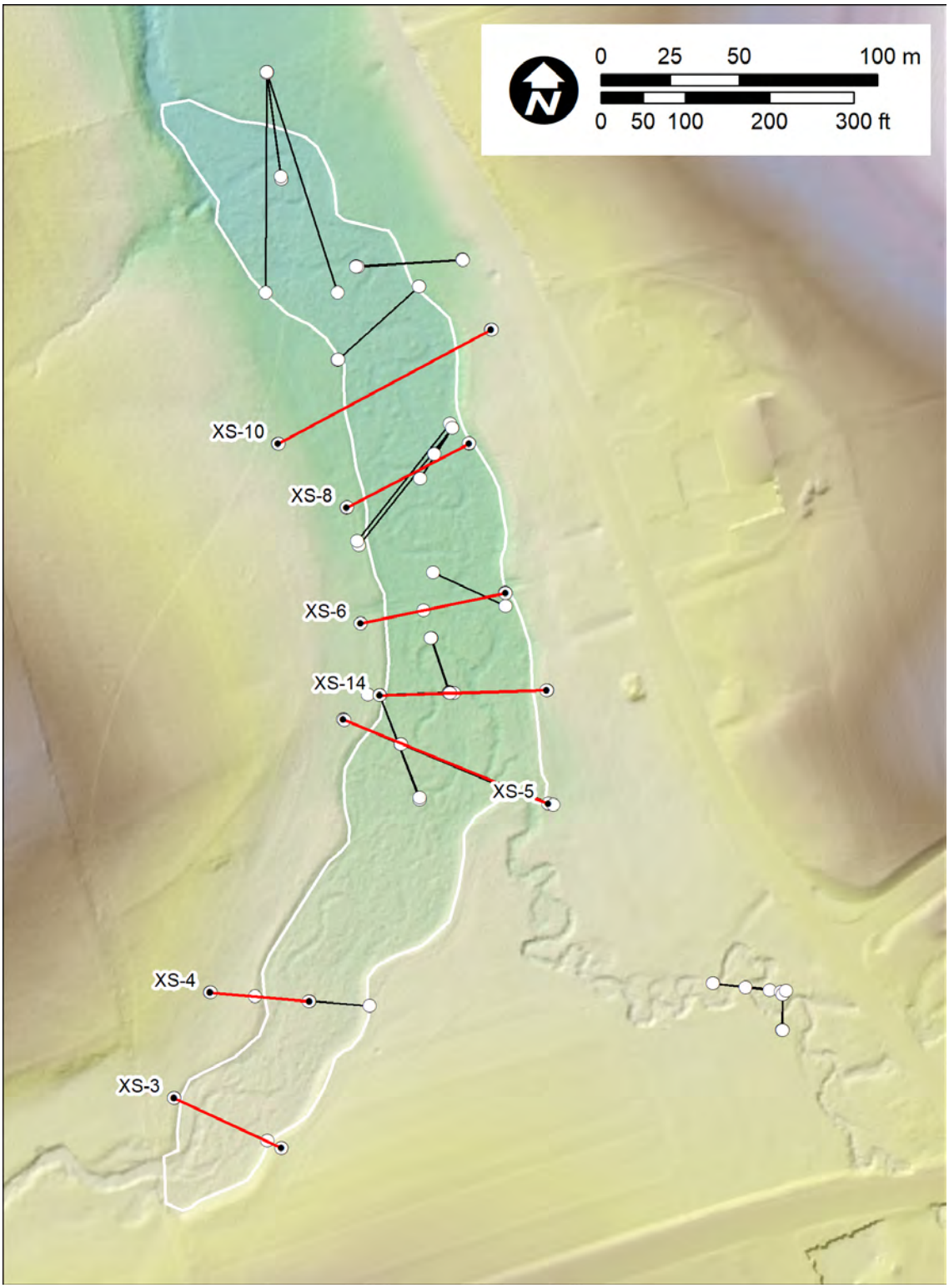

Figure 4.3. Lidar dem hillshade of Big Spring Run restoration area showing locations of cross sections used for repeat RTK GPS surveying. Those highlighted in red were used in this analysis because they cross the entire valley bottom and are close to perpendicular with respect to down valley flow direction.

Section number	Installation date	2nd survey date	Monitoring period yrs	Length ft	Deposition ft^2	Erosion ft^2	Net area change ft^2	Deposition rate ft/yr	Erosion rate ft/yr	Net change rate ft/yr
XS-3	5/14/13	6/9/17	4.07	113.3	43.85	-1.81	42.04	0.10	0.00	0.09
XS-4	5/14/13	6/9/17	4.07	55.4	14.55	-0.32	14.23	0.06	0.00	0.06
XS-5	5/14/13	5/12/15	1.99	210.1	38.80	-2.34	36.47	0.09	-0.01	0.09
XS-14	5/18/13	8/4/15	2.21	172.8	14.02	-10.49	3.54	0.04	-0.03	0.01
XS-6	1/20/14	5/12/15	1.31	145.6	16.04	-1.10	14.94	0.08	-0.01	0.08
XS-8	8/16/13	5/18/15	1.75	163.0	30.78	-8.52	22.26	0.11	-0.03	0.08
XS-10	12/13/12	5/18/15	2.43	244.4	17.23	-6.76	10.47	0.03	-0.01	0.02
Average			2.55	157.8	25.04	-4.48	20.56	0.07	-0.01	0.06
1 S. D.					12.58	4.04	14.03	0.03	0.01	0.03

Figure 4.4. Installation and survey dates for seven cross sections used in this analysis, with data on deposition, erosion, and net change. Note that cross sections are organized by distance downstream, from top to bottom.

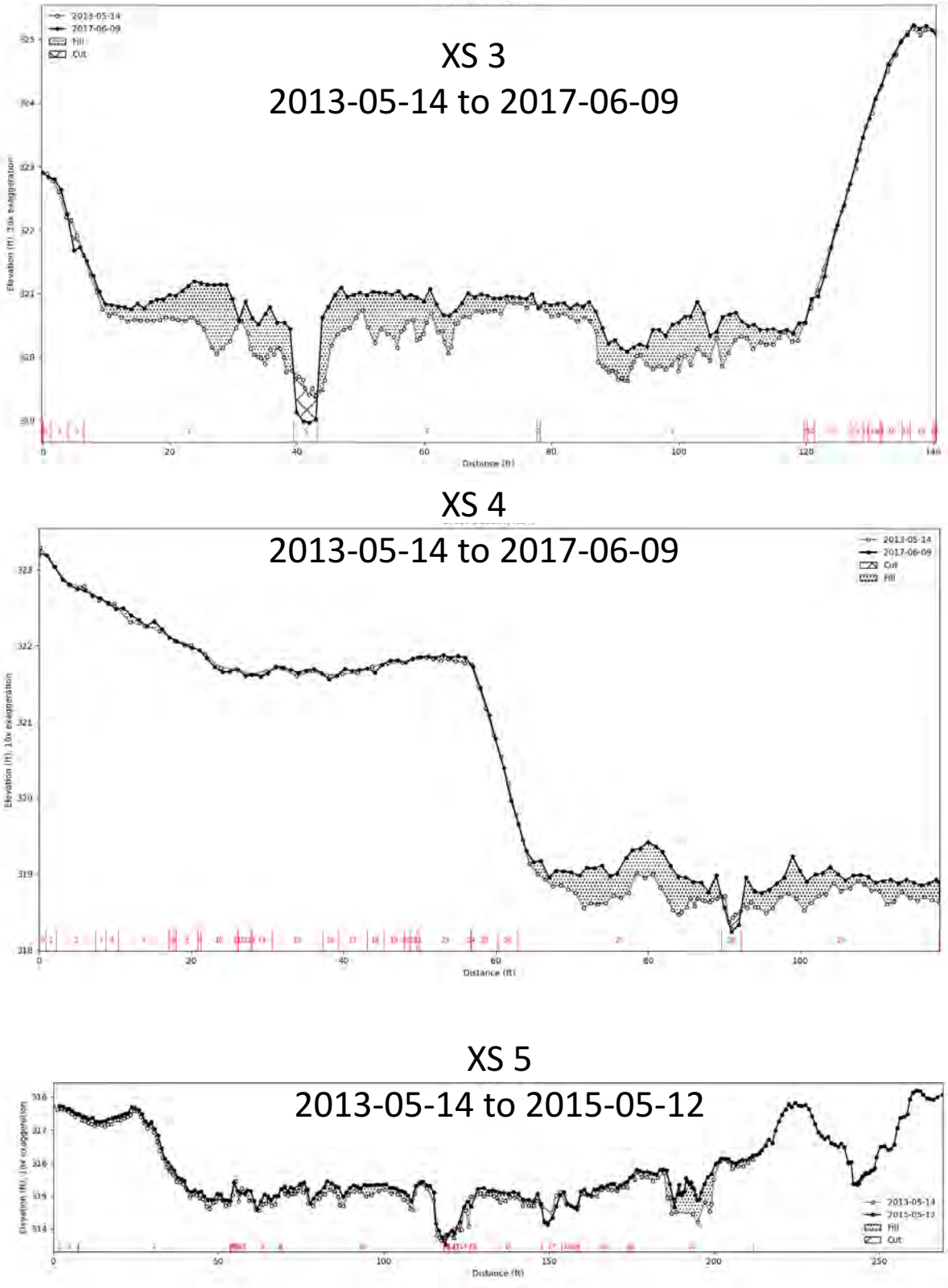

Figure 4.5. RTK GPS survey pairs for two dates for cross sections at Big Spring Run. Dotted areas are positive elevation change (deposition) and hachured areas are negative elevation change (erosion). Low areas, as at 40 ft on XS 3, are small channels. Some channels are filling with sediment, as at ~200 ft on XS 5, whereas others had minor erosion, as at 40 ft on XS 3. Note that cross sections are organized by distance downstream, from top to bottom.

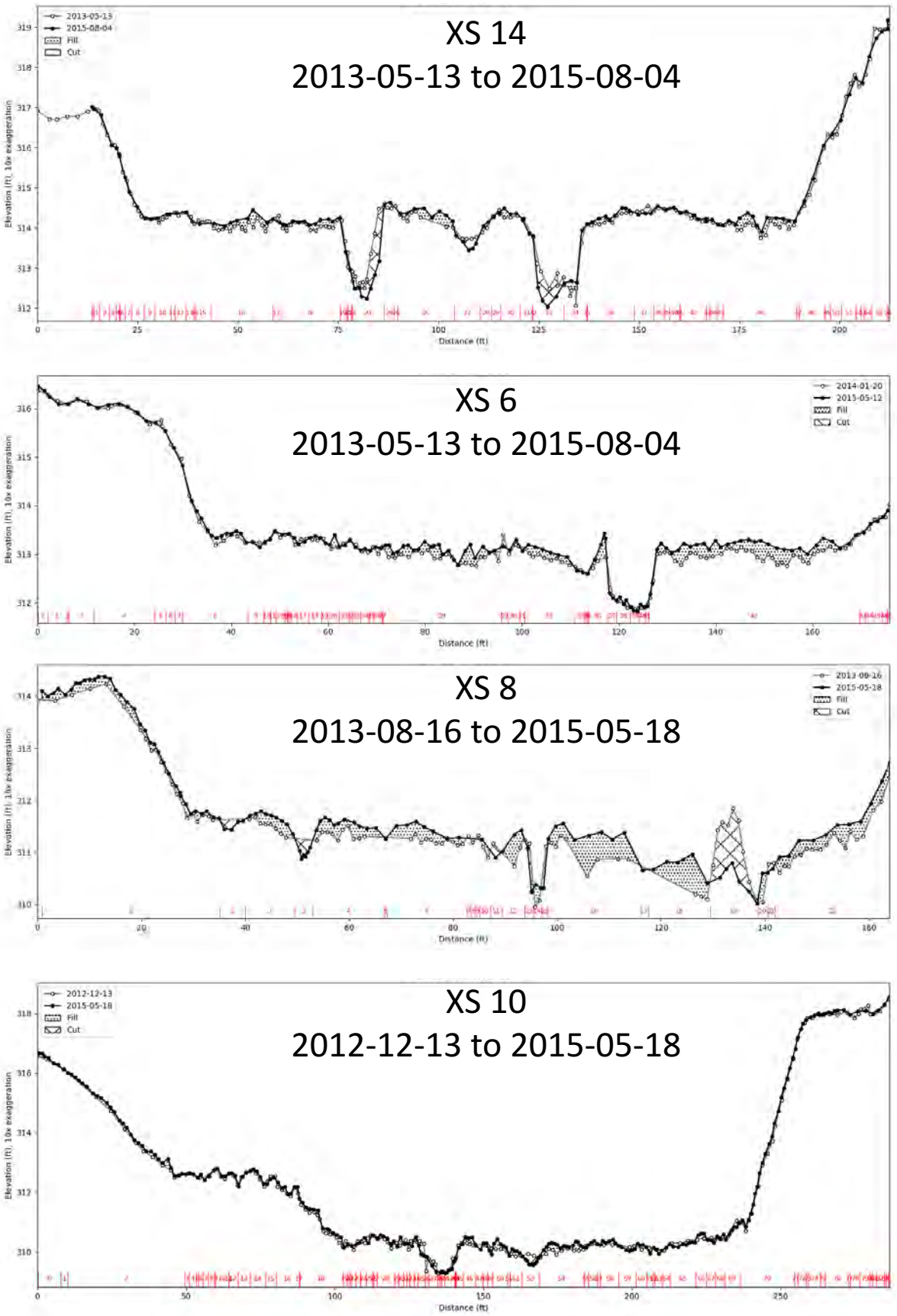

Figure 4.5, continued. RTK GPS survey pairs for two dates for cross sections at Big Spring Run. Dotted areas are positive elevation change (deposition) and hachured areas are negative elevation change (erosion). Low areas, as at 40 ft on XS 3, are small channels. Some channels are filling with sediment, as at ~200 ft on XS 5, whereas others had minor erosion, as at 40 ft on XS 3. Note that cross sections are organized by distance downstream, from top to bottom.

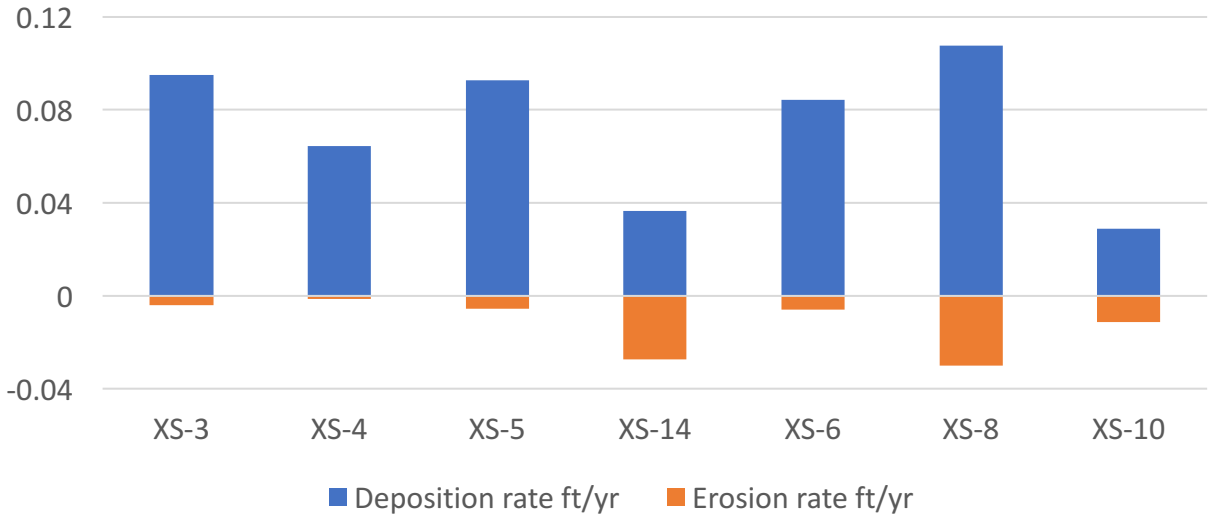

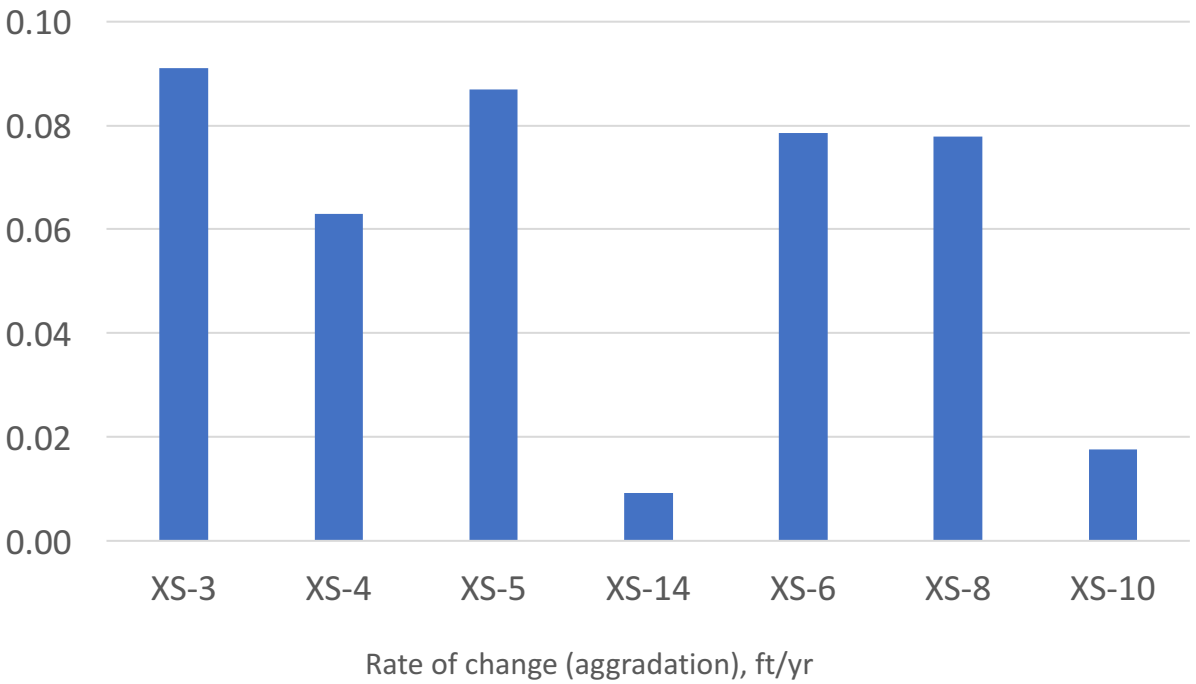

Figure 4.6. Summary of deposition, erosion, and net change (aggradation) data for seven cross sections surveyed with RTK GPS at least twice between 2012-13 and 2015-17. Y-axis values are in ft/yr. Note that cross sections are organized by distance downstream, from left to right.

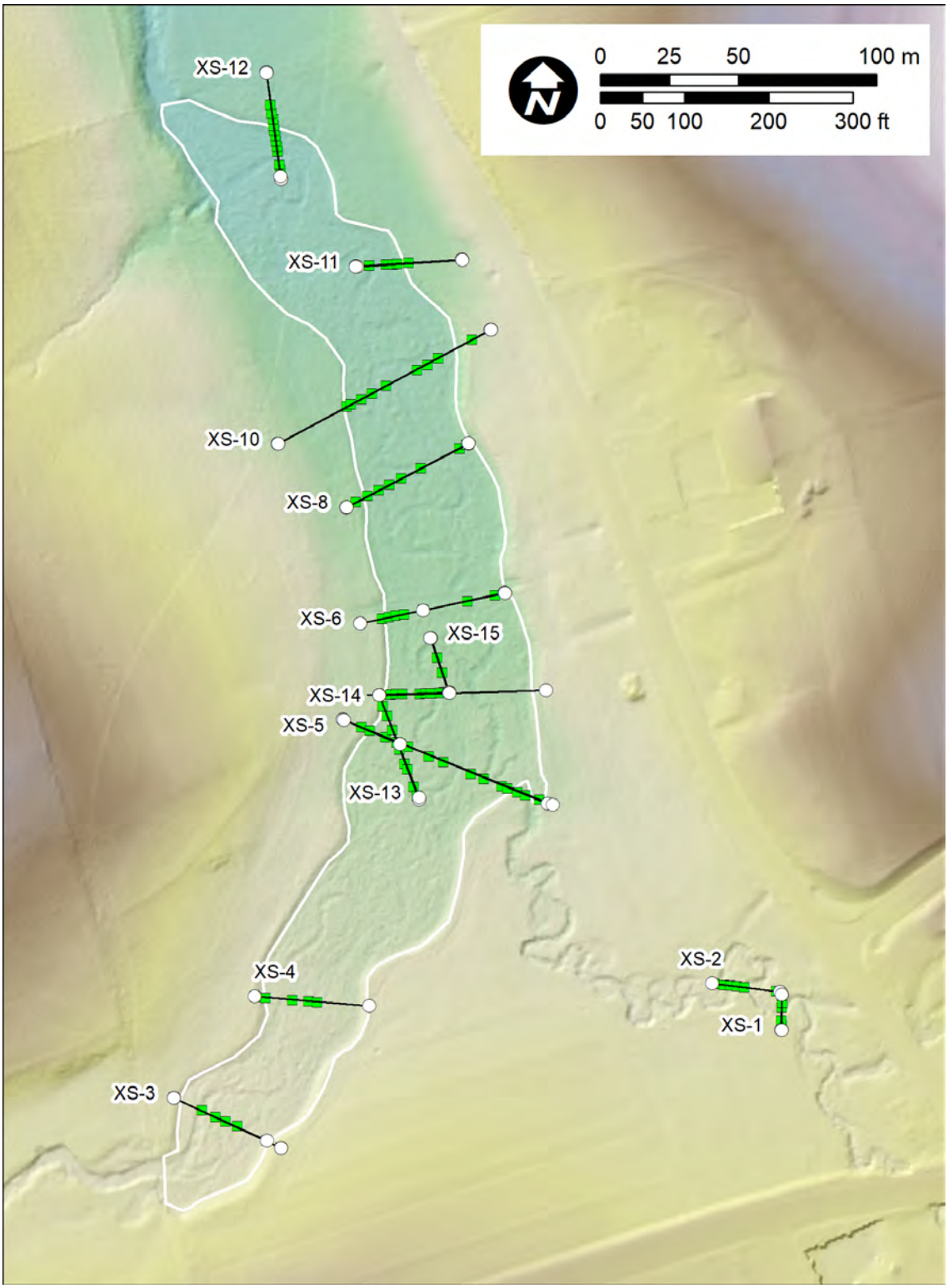

Figure 4.7. Locations of tile pads (green circles) along cross sections at Big Spring Run.

Cross section	Install date	Most recent measurement	Time between measurements, yrs	Distance from end to end, ft	Number of pads	Average deposition rate (weighted by distance), ft/yr	1 S. D. average deposition rate, ft/yr	Deposition rate from RTK GPS surveys, ft/yr
XS-3	1/24/13	4/24/16	3.25	138.8	8	0.02	0.005	0.09
XS-4	1/24/13	4/24/16	3.25	134.8	9	0.04	0.008	0.06
XS-5	1/24/13	6/12/17	4.38	238.7	18	0.01	0.015	0.09
XS-14	12/12/12	6/6/17	4.48	82.5	10	0.02	0.001	0.01
XS-6	12/12/12	6/12/17	4.5	142.7	8	0.08	0.023	0.08
XS-8	12/12/12	6/6/17	4.48	187.3	10	0.02	0.003	0.08
XS-10	12/12/12	4/20/16	3.36	205.3	14	0.04	0.006	0.02
XS-11	12/12/12	4/20/16	3.36	61.7	7	0.03	0.006	
XS-12	12/12/12	4/20/16	3.36	121.6	15	0.03	0.003	
XS-13	12/12/12	5/8/14	1.4	126.5	11	0.02	0.003	
Average			3.58	143.99	11	0.03	0.01	0.06

Figure 4.8. Dates of installation and most recent measurements of deposition on tile pads at Big Spring Run, with average deposition rate and comparison with data from repeat RTK GPS surveys. Note that cross sections are organized by distance downstream, from top to bottom.

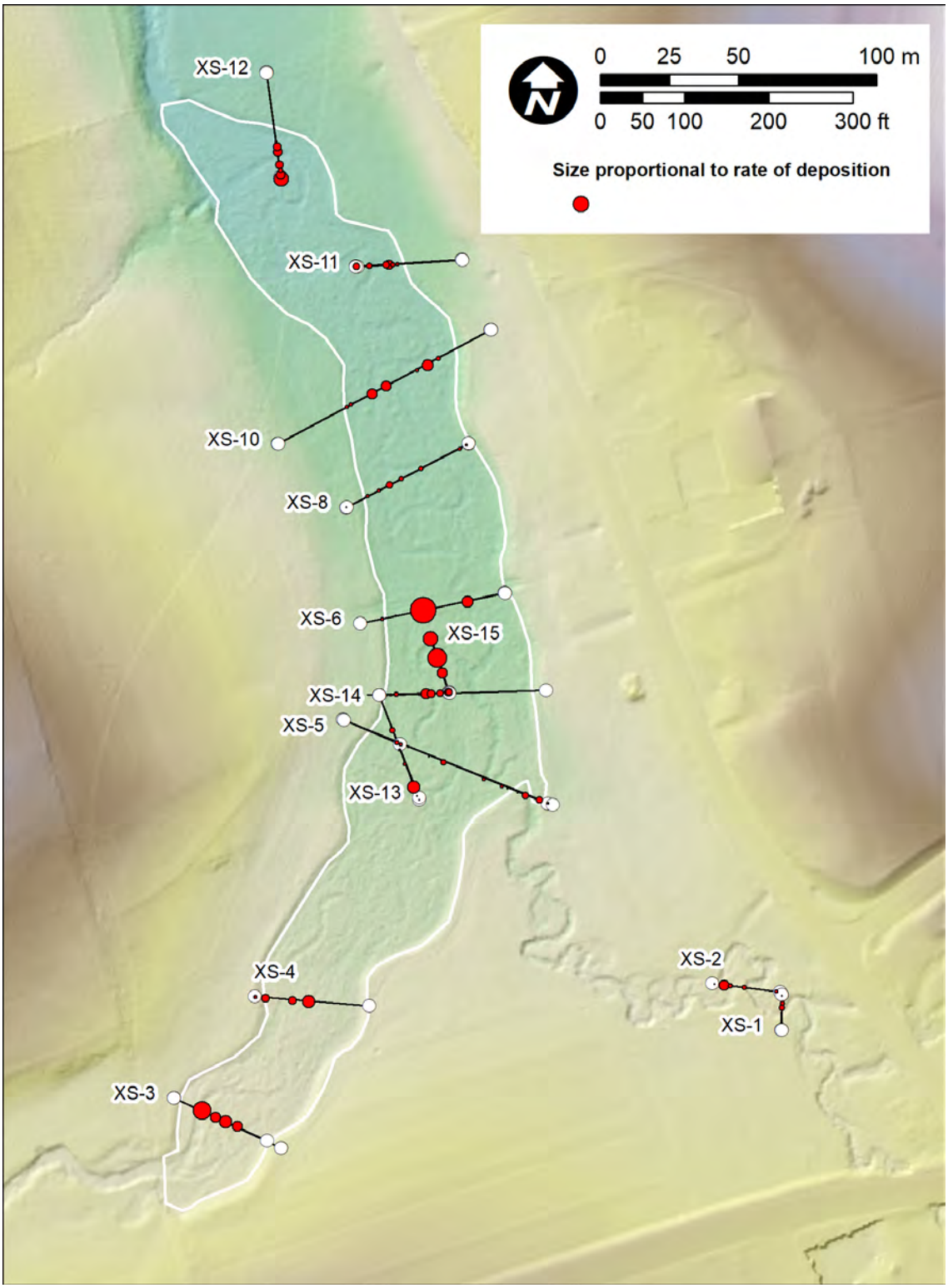

Figure 4.9. Locations of tile pads (red circles) along cross sections at Big Spring Run, with size of circle indicating relative magnitude of rate of deposition.

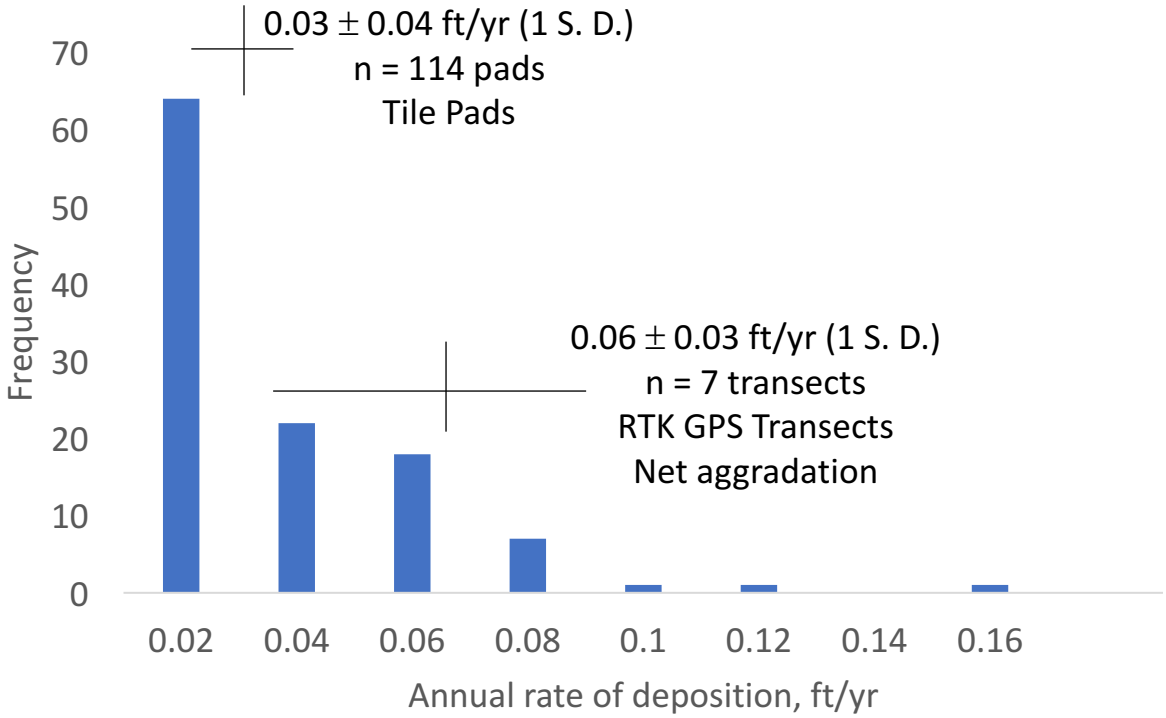

Figure 4.10. Frequency histogram for tile pad deposition rates at Big Spring Run.

Fm lab number	Sample name	Moist bulk density	Dry bulk density
		g/cm^3	g/cm^3
2444	BSR_XS14_TP2	2.2	1.6
2445	BSR_XS14_TP3	1.7	1.1
2446	BSR_XS14_TP4	2.4	1.6
2447	BSR_XS14_TP5	1.2	0.8
2448	BSR_XS14_TP6	1.6	1.0
2449	BSR_XS14_TP7	1.1	0.8
2450	BSR_XS14_TP8	1.4	1.1
2451	BSR_XS14_TP9	1.5	1.1
2452	BSR_XS14_TP10	1.9	1.4
2453	BSR_XS5_TP5	1.31	1.05
2454	BSR_XS5_TP6	2.75	2.37
2455	BSR_XS5_TP7		1.09
2456	BSR_XS5_TP8	0.46	0.38
2457	BSR_XS5_TP9	1.42	0.91
2458	BSR_XS5_TP12	1.19	0.79
2459	BSR_XS5_TP13	0.90	0.62
2460	BSR_XS5_TP14	1.02	0.52
2461	BSR_XS5_TP16	0.94	0.64
2462	BSR_XS5_TP17	1.24	0.77
2463	BSR_XS5_TP18	0.35	0.27
Mean		1.40	0.99
1 S. D.		0.62	0.49

Figure 4.11. Bulk density measurements for 20 samples of sediment collected from deposition on tile pads at cross sections 5 and 14 at Big Spring Run in June 2017.

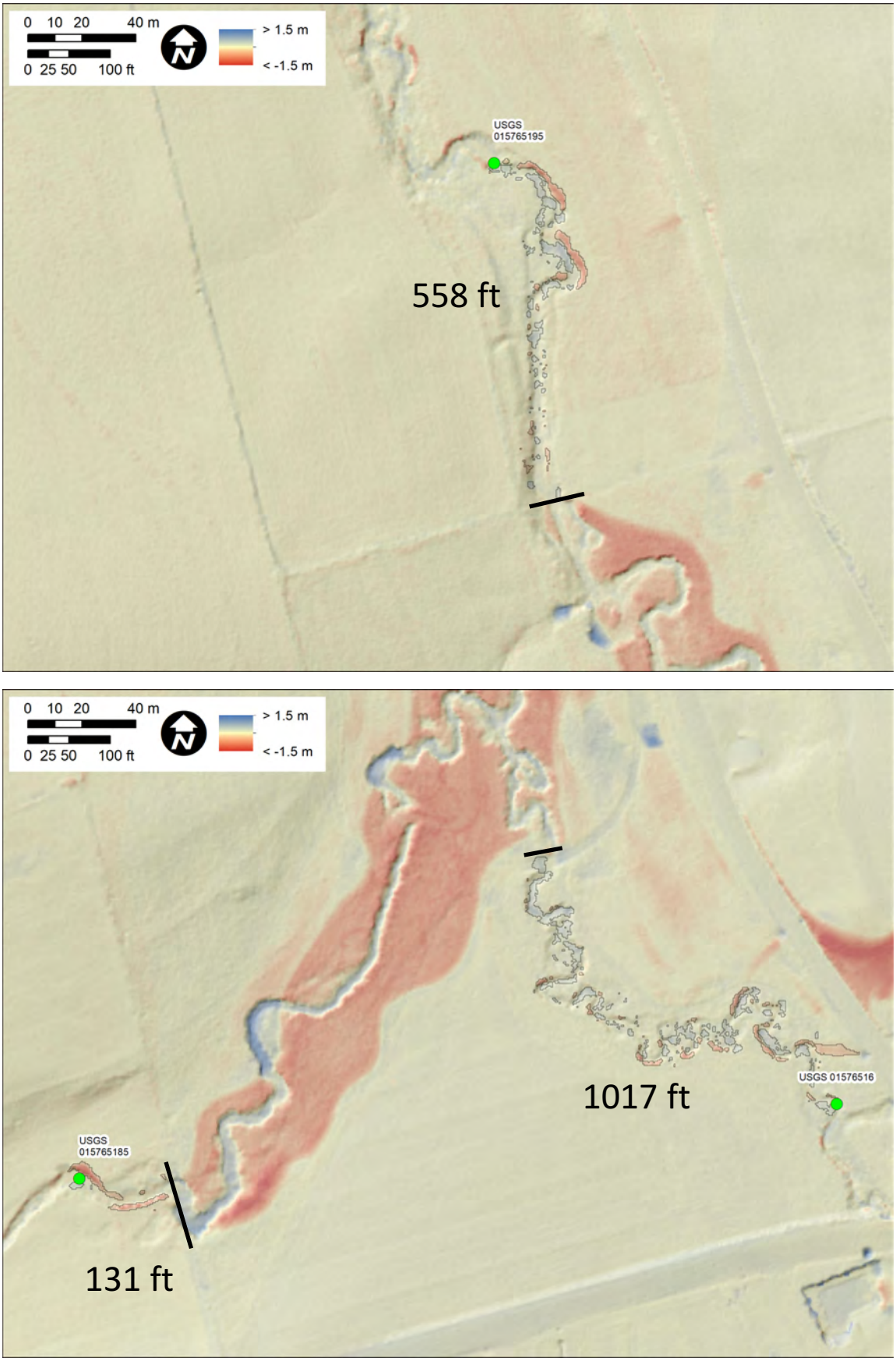

Figure 4.12. Results of lidar dem differencing (2008 to 2014), with erosion shown in red and deposition in blue. Distances between the three gages and the restored reach (131, 1017, and 558 feet) sum to 1706 ft. The overall length of the restoration reach along a mid-line down the center of the valley bottom is 1509 ft. Top: Downstream gage station. Bottom: Upstream gage stations on eastern and western tributaries. Short black lines indicate boundaries of restoration reach. Distances are measured from those boundaries to the gage stations. Note that change within the restoration area includes the removal of legacy sediment in 2011.

Location	Length, ft	Volume eroded, ft^3	Mass eroded, US tons/yr	Fine mass eroded, US tons
Western tributary	131	321 +/- 81	-14 +/-5	-12 +/-4
Eastern tributary	1017	371 +/- 74	-16 +/-5	-14 +/-4
Main stem	558	519 +/- 102	-23 +/-7	-19 +/-6

Location	Length, ft	Volume deposited, ft^3	Mass deposited, US tons	Fine mass deposited, US tons
Western tributary	131	20 +/- 12	1 +/-0.6	0.1 +/-0.06
Eastern tributary	1017	742 +/- 141	38 +/-10	3.8 +/-1.0
Main stem	558	434 +/- 88	22 +/-6	2.2 +/-0.6

Location	Minimum net change, tons/yr	Maximum net change, tons/yr
Western tributary	-7.8	-16.0
Eastern tributary	-5.2	-15.2
Main stem	-10.2	-23.4
Total	-23.2	-54.6

Figure 4.13. Estimates of erosion (top), deposition (middle), and net change for stream reaches between the three USGS gage stations and restoration reach.

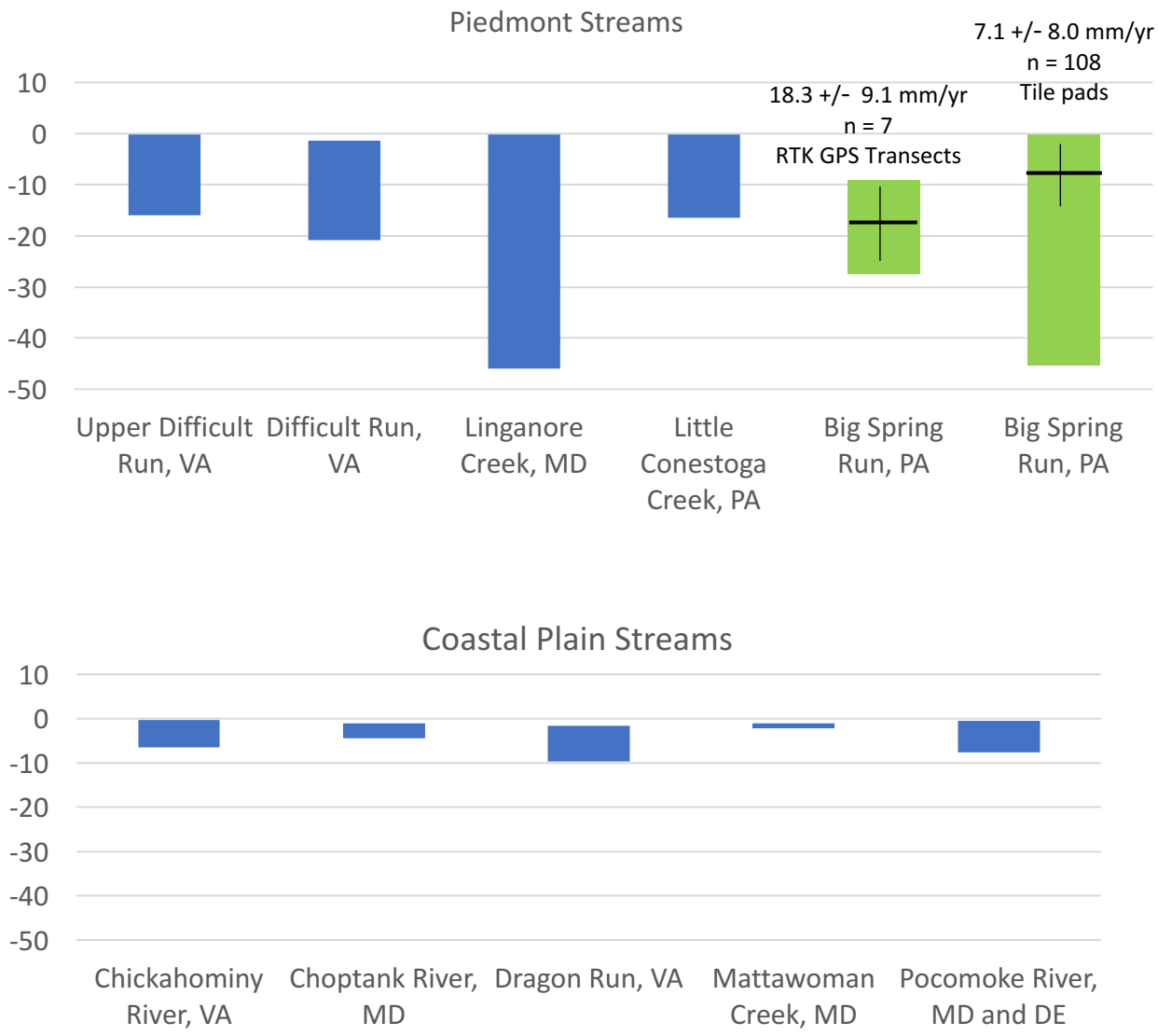

Figure 4.14. Compilation of clay pad deposition rate (in mm/yr) data from other reports, with data from Big Spring Run for comparison. See Figure 4.15 for list of sources of other data. Note that deposition rates are shown here as negative values, consistent with reporting in other source.

	Drainage area, km^2	Floodplain deposition, mm/y			Method	Reference
		Minimum	Maximum	Range		
COASTAL PLAIN STREAMS						
Chickahominy River, VA	650	-0.4	-4.8	-4.4	Clay pads	Noe and Hupp, 2009
Chickahominy River, VA	650	-3.8	-6.48	-2.68	Clay pads	Gellis et al, 2009
Chickahominy River, VA	650	-1.3	-5.7	-4.4	Tree rings	Gellis et al, 2009
Choptank River, MD	293	-1.1	-3	-1.9	Clay pads	Noe and Hupp, 2009
Choptank River, MD	293	-1.2	-4.5	-3.3	Clay pads, tree rings	Gellis et al, 2009
Dragon Run, VA	282	-1.7	-9.7	-8	Clay pads	Gellis et al, 2009
Mattawoman Creek, MD	134	-1.1		-1.1	Clay pads	Gellis et al, 2009
Pocomoke River, MD and DE	8.5	-0.5	-4.2	-3.7	Clay pads	Noe and Hupp, 2009
Pocomoke River, MD and DE	8.5	-0.6	-7.7	-7.1	Clay pads	Gellis et al, 2009
Pocomoke River, MD and DE	8.5	-1.2	-1.8	-0.6	Tree rings	Gellis et al, 2009
PIEDMONT STREAMS						
Upper Difficult Run, VA	14.2	0	-16	-16	Clay pads	Gellis et al, 2017
Difficult Run, VA	151	-1.3	-20.9	-19.6	Clay pads	Schenk et al, 2012
Linganore Creek, MD	147	0	-46	-46	Clay pads	Gellis et al, 2015
Little Conestoga Creek, PA	160	0	-16.4	-16.4	Clay pads	Schenk et al, 2012
Little Conestoga Creek, PA	160	-1.3	-8	-6.7	Clay pads	Gellis et al, 2009
Big Spring Run, PA	4	-9.1	-27.4	-18.3	RTK GPS surveys	This study (mean and S. D.)
Big Spring Run, PA	4	0	-45.3	-45.3	Tile pads	This study

Figure 4.15. Compilation of clay pad deposition rates (in mm/yr) from other reports, with data from Big Spring Run for comparison. Note that deposition rates are shown as negative values, consistent with reporting in other sources.

Deliverable 4
E.2 Figures

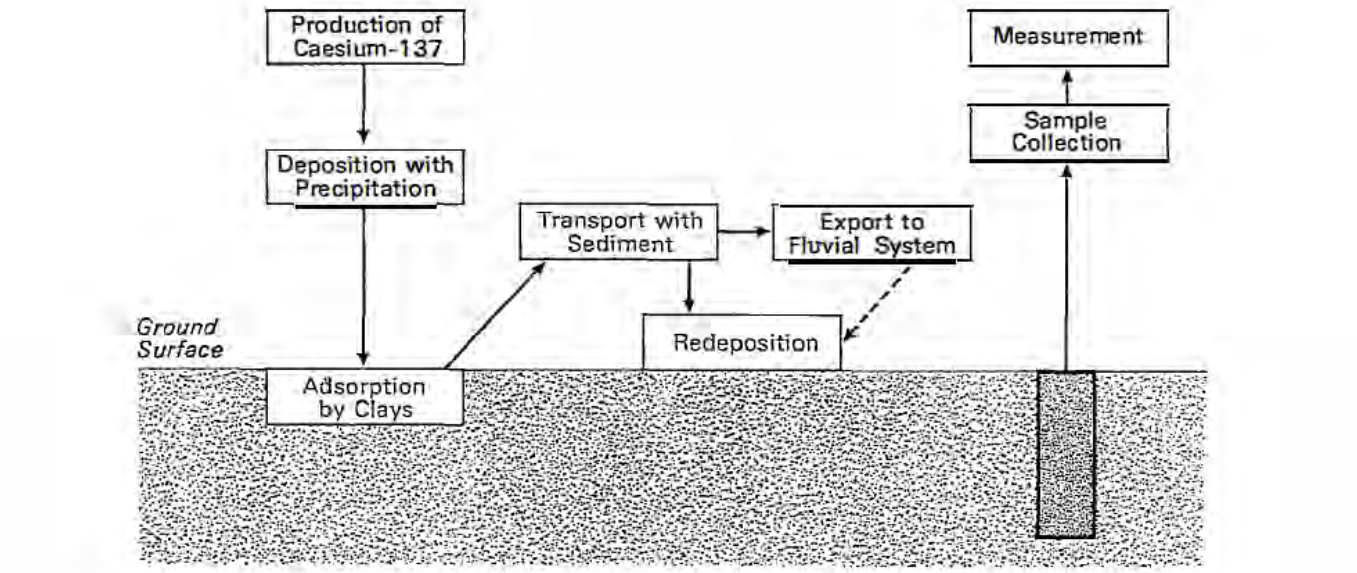

Figure E.2.1 The basis for the ^{137}Cs technique for studying erosion and sediment redistribution (Walling and Quine 1990).

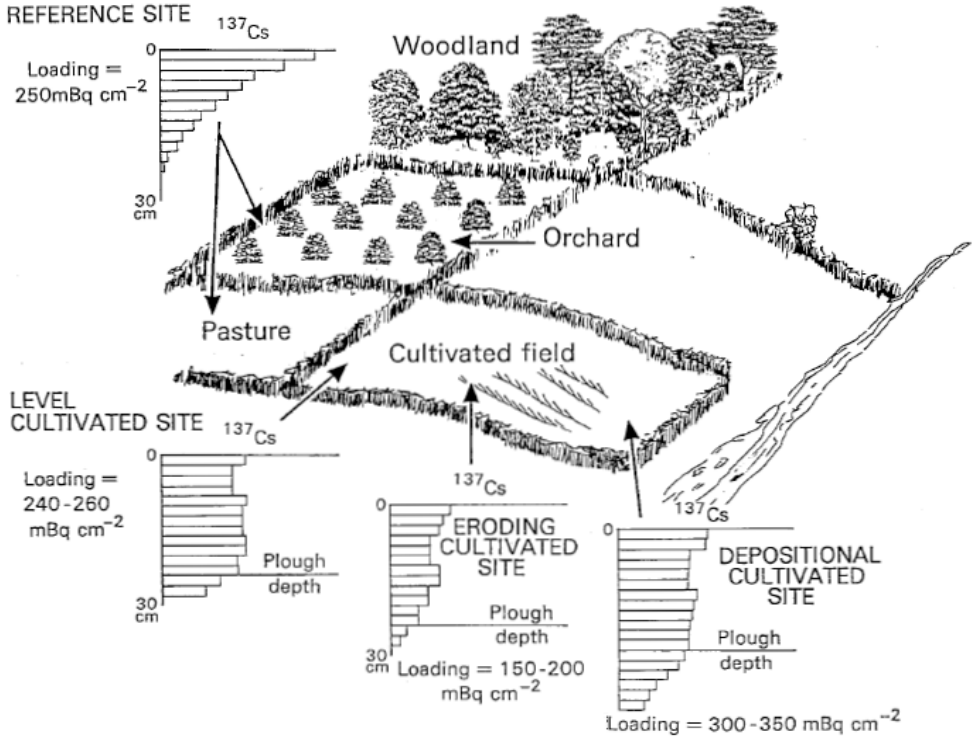

Figure E.2.2 Schematic representation of the impact of various agricultural practices on the loading and profile distribution of 137Cs (Quine and Walling 1993)

Figure E.2.3 Alexandra Sullivan (F&M '06) collects core samples at the BSR reference site, an 18th Century cemetery on a knoll overlooking the BSR watershed. A fence-post driver is used to pound a sharpened PVC tube into the soil, to a depth of 45 cm. This depth is presumed to be below the influence of ^{137}Cs deposition.

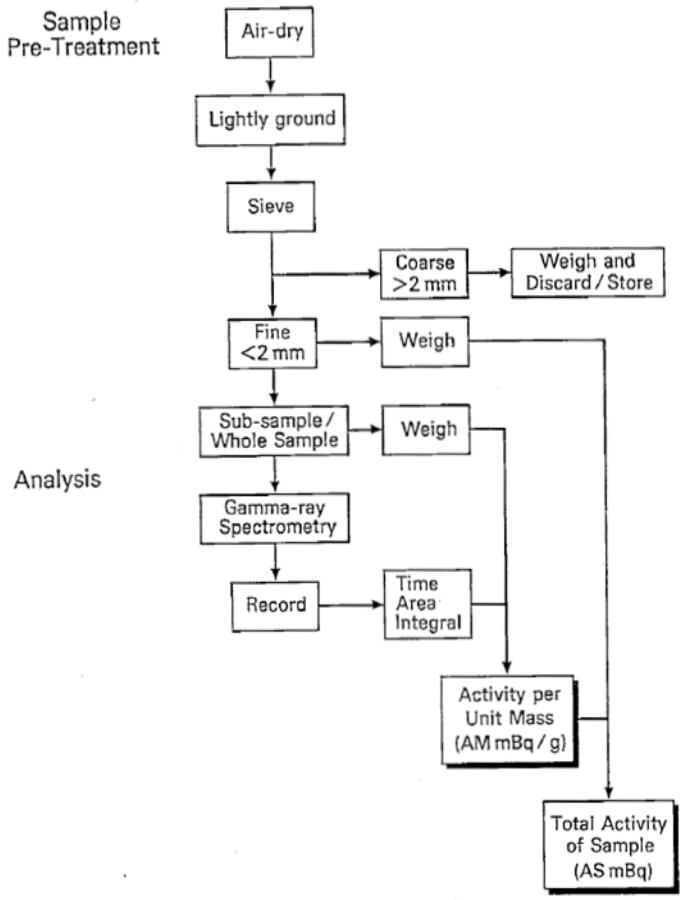

Figure E.2.4 The procedures used for sample preparation and ^{137}Cs gamma analyses (Walling and Quine 1990)

Figure E.2.5 Franklin and Marshall College gamma spectroscopy laboratory, funded by the U.S. National Science Foundation (NSF-MRI NSF-MRI 0923224), with support from PA DEP.: (Left) Two lead-shielded detectors and two liquid nitrogen dewars line the right side of the lab. The multichannel analyzers are on the small table between the detectors; (Right) View into a copper coated, lead-shielded detector with a sample in place for analysis. The sample rests on the base of a 1L plastic Marinelli beaker that fits over the detector window. A PVC spacer prevents the Marinelli beaker from touching the detector.

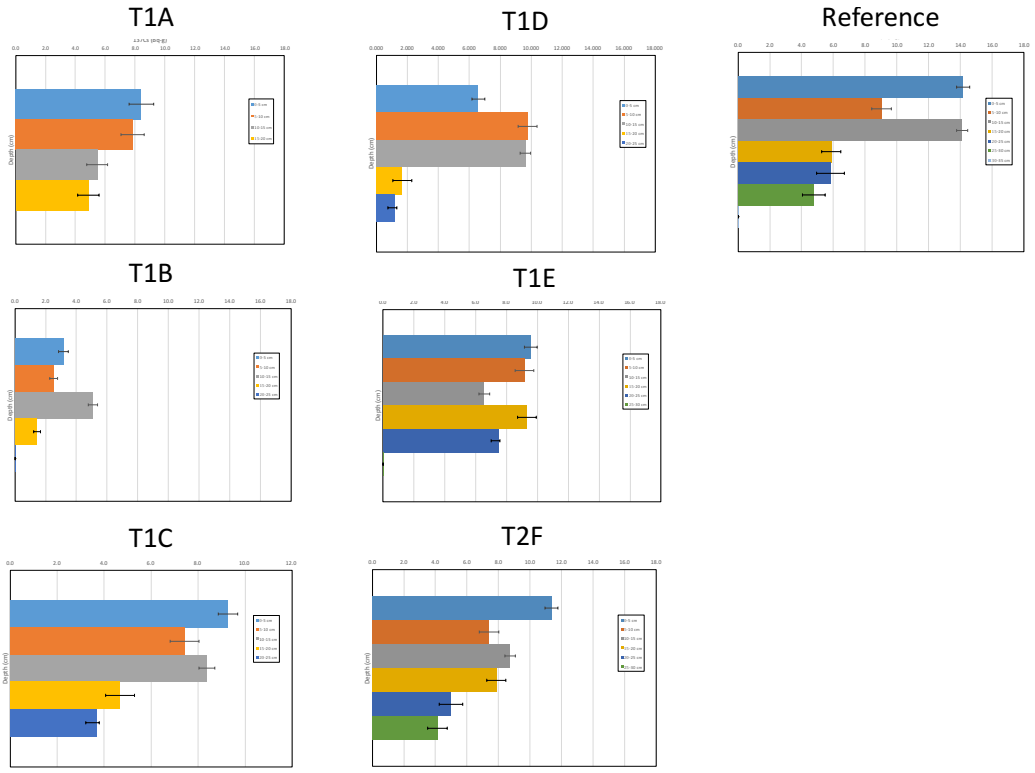

Figure E.2.6a ^{137}Cs profiles for Transect T1 cores. Each box in the bar graph represents 5 cm sampling increments, with the 0-5 cm increment at the top of the graph. Profiles T1A-T1F represent a downslope catena, from T1A at the top of the hill and T1E and F at the foot slope (see Figure E.2.7b). The reference profile is shown on the right (see Figure E.2.6 for locations). From mass balance considerations (Equation 1), T1A, T1B, T1C and T1D indicate net erosion, whereas T1E and T1F indicate net deposition (Table E.2.4). The activities in this graph are in units of Bq-kg.

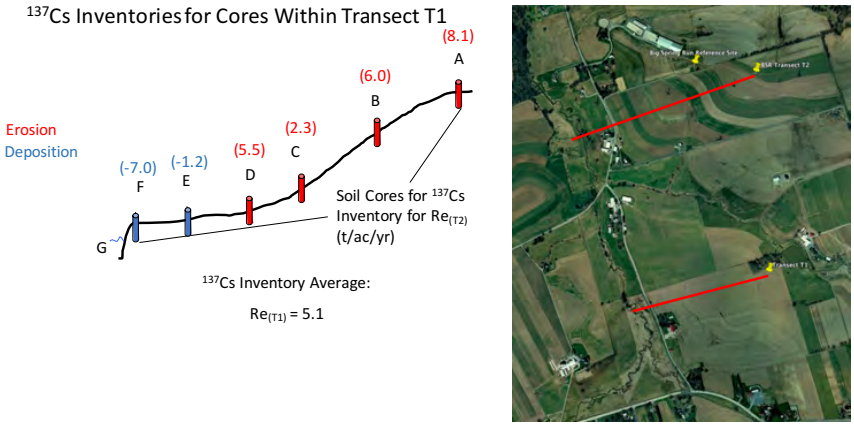

Figure E.2.6b Inventories of ^{137}Cs for cores within Transect T1 at Big Spring Run showing erosion (red, positive) or deposition (negative, blue) at each sample point compared to the reference section. Samples collected by Alexandra Sullivan (Sullivan, 2006); gamma analyses by Ritchie (Walter et al., 2006) and Walter and Merritts (This report). Summary erosion rates (Re) are shown for transect T1 in t/ac/yr.

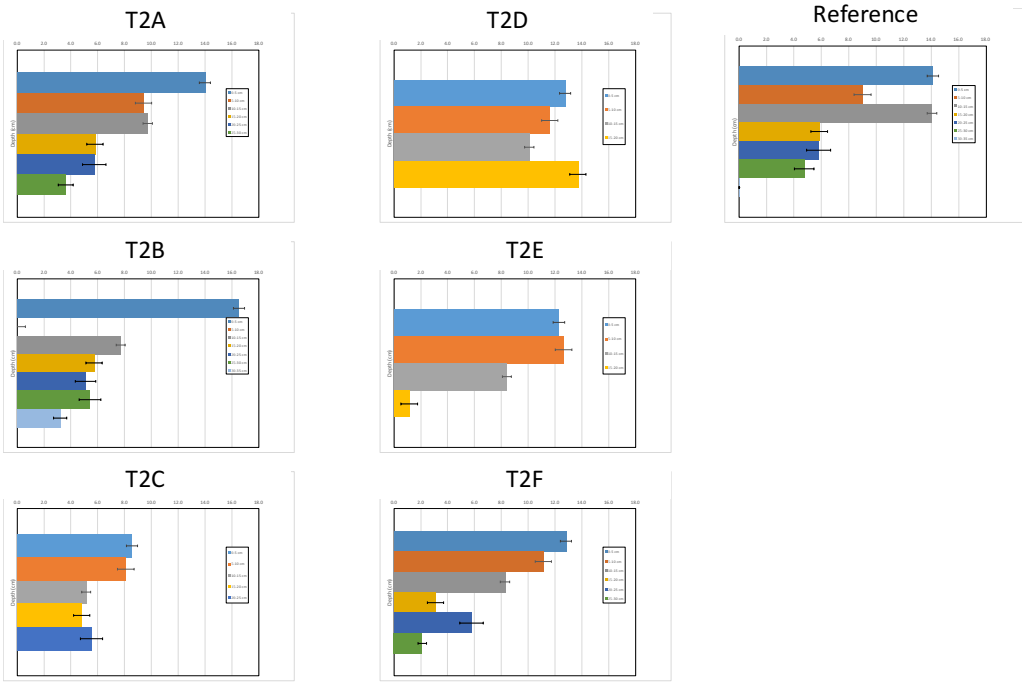

Figure E.2.7a ^{137}Cs profiles for Transect T2 cores. Each box in the bar graph represents 5 cm sampling increments, with the 0-5 cm increment at the top of the graph. Profiles T2A-T2F represent a downslope catena, from T2A at the top of the hill and T2E and F at the foot slope. The reference profile is shown on the right (see Figures E.2.6 and E.2.8.b for locations). From mass balance considerations (Equation 1), profiles profiles T2A, T2B, and T2E indicate net erosion, whereas T2C, T1D and T1F indicate net deposition (Table E.2.4). The activities in this graph are in units of Bq-kg.

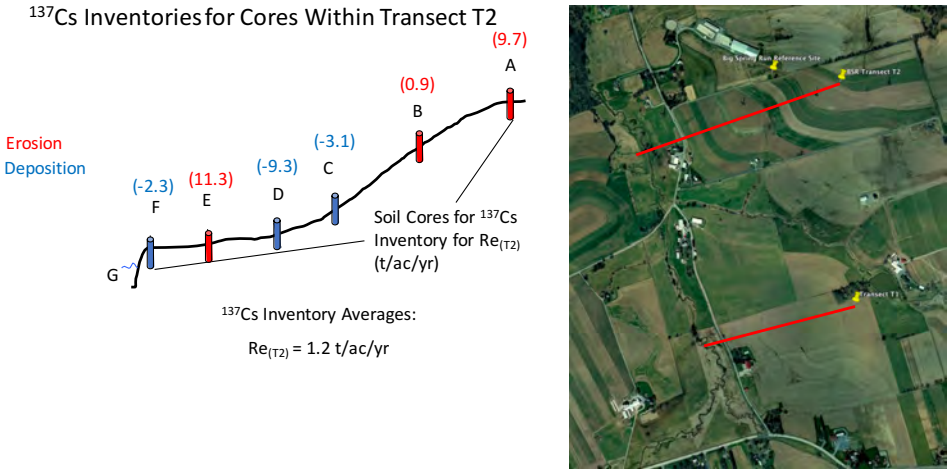

Figure E.2.7b Inventories of ^{137}Cs for cores within Transect T2 at Big Spring Run showing erosion (red, positive) or deposition (negative, blue) at each sample point compared to the reference section. Samples collected by Alexandra Sullivan (Sullivan, 2006); gamma analyses by Ritchie (Walter et al., 2006) and Walter and Merritts (This report). Summary erosion rates (Re) are shown for transect T2 in t/ac/yr.

Figure E.2.8 Sample locations adjacent to and upstream of the BSR restoration study area: (A) Stream Bank sample locations. Site 1 is discussed in this text; (B) Transect T1 (west side of hill); (C) Upland (East) and valley bottom Suspended Sediment sites; (D) Upland sites (South and West).

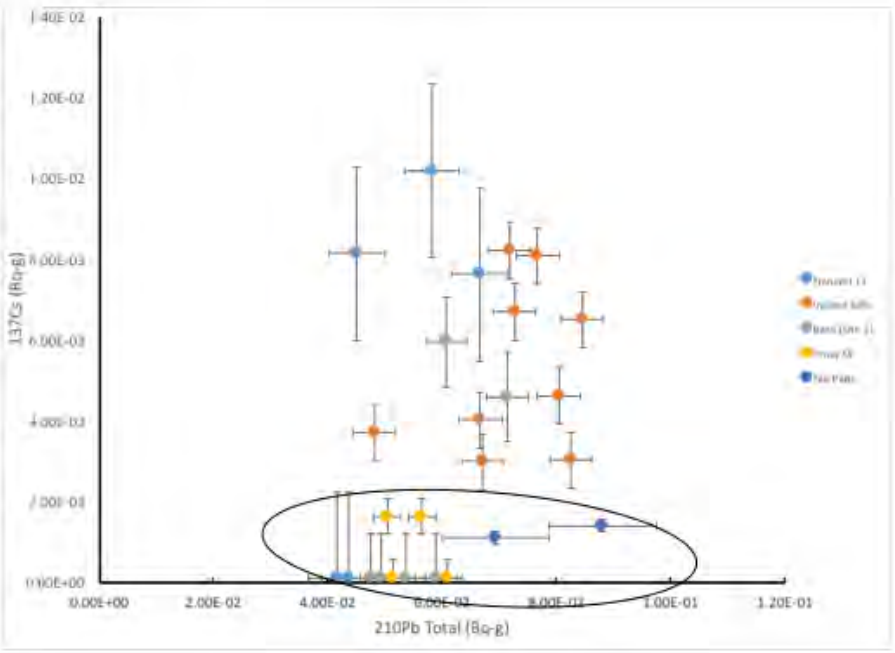

Figure E.2.9a ^{137}Cs vs ^{210}Pb variation diagram for all the samples listed in Table E.2.3.

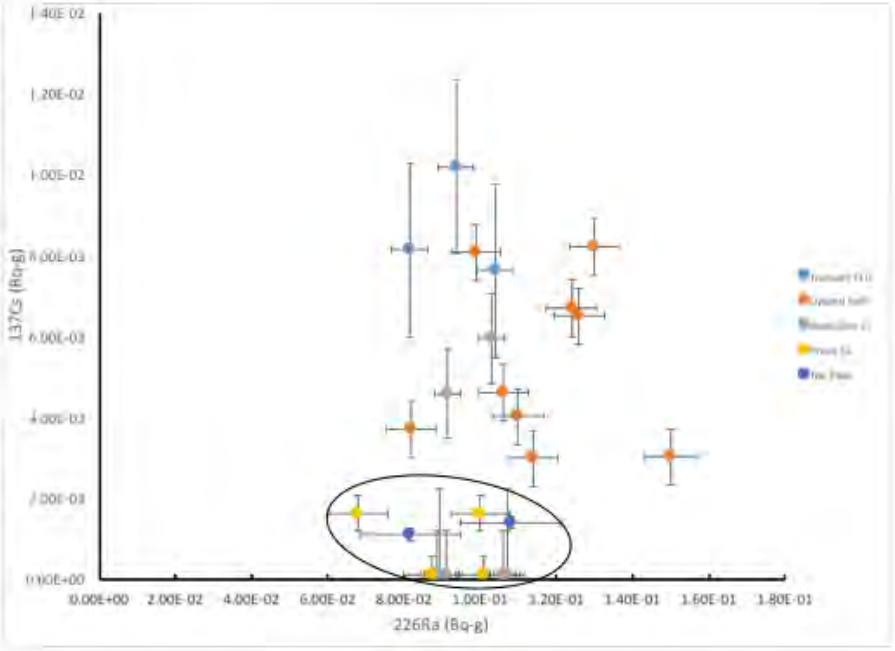

Figure E.2.9b 137Cs vs 226 Ra variation diagram for all samples listed in Table E.2.3.